Technical Review of the Lined Rock Cavern (LRC) Concept and Design Methodology: Mechanical Response of Rock Mass

Prepared for:

U.S. Department of Energy
National Energy Technology Laboratory
Morgantown, West Virginia

Under:
Prime Contract No. DE-AM26-99FT40463
Subcontract No. 735937-30000

Prepared by:

Terje Brandshaug, Mark Christianson and Branko Damjanac

Itasca Consulting Group, Inc.
708 South Third Street, Suite 310
Minneapolis, Minnesota 55415
USA

September 2001

ref: ICG01-2062-1-4

EXECUTIVE SUMMARY

The storage of pressurized natural gas in large steel-lined caverns excavated in crystalline rock has been under development in Sweden for more than 10 years. Unlike the current storage technology, which relies on the existence of large salt caverns, aquifer formations and depleted oil fields, the lined rock cavern (LRC) concept provides the option of greater flexibility in the management of local and regional gas supplies. With the prospect of this technology being used in commercial storage of natural gas in the United States, the U.S. Department of Energy, through the National Energy Technology Laboratory in Morgantown, West Virginia, initiated a technical review of the feasibility of the LRC storage concept and its current design methodology.

The principal idea behind the LRC gas-storage concept is to rely on a rock mass (primarily, crystalline rock) to serve as a pressure vessel in containing stored natural gas at maximum pressures from about 15 MPa to 25 MPa. The concept involves the excavation of relatively large, vertically cylindrical caverns 20 m to 50 m in diameter, 50 m to 115 m tall, with domed roofs and rounded inverts to maximize excavation stability. The caverns are located at depths from 100 m to 200 m below the ground surface, and they are lined with approximately 1-m thick reinforced concrete and thin (12-mm to 15-mm) carbon steel liners. The purpose of the steel liner, which is the innermost liner, is strictly to act as an impermeable barrier to the natural gas. The purpose of the concrete is to provide a uniform transfer of the gas pressure to the rock mass and to distribute any local strain in the rock mass (e.g., from the opening of natural rock fractures) at the concrete/rock interface more evenly across the concrete to the steel liner/concrete interface. To further minimize local circumferential strains in the steel liner, a viscous layer (~ 5 mm thick) made of a bituminous material is placed between the steel and the concrete liners.

The LRC development has included a scaled (approximately 1:9 scale) experiment of the concept conducted at the Grängesberg Test Plant in Sweden, with reported positive results (Stille et al., 1994). A full-scale LRC demonstration facility is currently being constructed at Skallen, a site near the coastal city of Halmstad in southwest Sweden.

The LRC developments have been reflected in a current design methodology. This methodology is a probabilistic, multi-stage approach. Evaluations of the potential for a rock mass to host an LRC facility are made at different stages, with an increasing demand for geophysical information at each stage. The result is an increasingly refined design in terms of probable loads and material response. The methodology is embedded in two models: FLRC1 (Feasibility for Lined Rock Caverns 1), which is an initial procedure for LRC evaluations at an early stage; and FLRC2 (Feasibility for Lined Rock Caverns 2), a more detailed procedure for LRC evaluations and design in later stages of the development, when more site-specific geophysical information becomes available. The FLRC1 and FLRC2 models rely on rock index properties and empirical relations to estimate the rock-mass mechanical parameters (i.e., stiffness and strength); limit-equilibrium, finite-element and analytical (homogeneous and isotropic) models are used to estimate cavern location (i.e., depth), maximum gas pressure, cavern deformations, and steel-liner strain.

The methodology emphasizes two key LRC design criteria associated with (1) safety against ground uplift, and (2) a maximum operating (cyclic) strain range in the steel liner.

The current review of the lined rock-cavern storage concept and design methodology has focused on the feasibility of this technology, and the robustness of its design methodology primarily in the context of the mechanical response of the rock mass during cavern operation (i.e., for a pressurized cavern). The standard of the review has been the demonstrated and established principles of designing large stable underground openings in rock.

The design analyses contained in the FLRC1 and FLRC2 models are somewhat simple, suggesting that verification of the design adequacy be made through analysis using detailed numerical models. Note, however, that "simple design analyses", in this case, does not necessarily mean "inadequate analyses". In this review, independent analyses of the LRC concept were conducted using continuum and discontinuum numerical models. These models show that a soil-anchor analogy embedded in limit equilibrium (LE) models for evaluating ground uplift greatly oversimplifies the conditions of potential uplift. The analogy and the limit equilibrium models may not be well-suited to describe the relatively complex rock-mass response associated with a pressurized LRC. Continuum numerical models used to evaluate the cavern-wall response and steel-liner strain for the Skallen LRC demonstration plant show results in reasonable agreement with those expressed in the review documents using the LRC design methodology. However, the steel-liner response may be affected by the local rock-mass conditions in the vicinity of the cavern wall. This local response results from intersecting fractures occurring naturally in rock masses, creating rock wedges in the cavern wall. Treating the rock mass as a continuum (as is done in the current LRC design methodology) implies global and local averaging of the fracture and intact-rock response and can potentially result in underestimating the steel-liner strain.

While the use of somewhat simple design analyses may be reasonable, it suggests that a confirmation of the design adequacy be made at various intervals in the design process using detailed numerical models, both continuum and discontinuum, for two- and three-dimensional conditions, as appropriate. Although numerical models have been used throughout the development of the LRC design methodology, the methodology does not specify that such models be used in a design confirmation context during the design process. This is a significant concern. However, the problem can be remedied easily by including the use of detailed design evaluations at suitable intervals. Because these are independent, detailed, numerical-model evaluations, they are conducted apart from the design analyses and probabilistic procedures of the FLRC1 and FLRC2 models and, therefore, will not complicate these procedures.

In the current LRC design methodology, the review found finite element models of the fracture evaluation of the concrete liner to use a no-tension fracture propagation criterion. It is noted that fracture propagation depends on the material toughness (or critical energy-release rate). Unless the tensile strength of the concrete is calibrated to the toughness and the element size used in the analysis, the fracture predictions using this approach would

not be appropriate. In lieu of a more sophisticated fracture mechanics analysis, the current method should use consistent values of tensile strength and fracture toughness. An example derivation of consistent values of tensile strength and material toughness is provided in Appendix B.

Although not emphasized in the current LRC design methodology, the methodology is only applicable for the design of a single independent cavern. The design methodology should be used with caution when multiple caverns are involved that have overlapping effects. In such cases, detailed design evaluations will be necessary using numerical models.

The effect of seismic loads is not considered in the LRC design methodology. The potential for seismic loads should be included. The effect of such loads would require detailed design evaluations using numerical models.

The LRC design methodology should include a verification of its probabilistic approach by evaluating the design for a set of credible lower-bound conditions using a detailed numerical model. The minimum result of the model should be a barely acceptable design.

With the noted important exceptions, the review has found the implementation of the LRC concept to be a carefully planned incremental design procedure. Although of considerable proportions, the lined rock cavern size is not unprecedented. There is extensive worldwide rock engineering experience in developing large complex rock caverns. By following established principals, one should expect that stable, large, lined rock caverns can be constructed in different lithology rocks of reasonable quality. During cavern operation, the combination of shallow cavern depth and high gas pressure makes the LRC concept unique in terms of the cavern loads, and the structural integrity of the steel liner must be maintained for these loads. This requires a design methodology that not only relies on the somewhat simple design analyses contained in the FLRC1 and FLRC2 models, but also considers analyses that account for the discontinuum nature of rock masses in detailed two- and three-dimensional numerical models as appropriate. By adopting a careful design methodology that considers the detailed interaction of the rock mass and cavern wall response, and a design implementation that is guided by physical observations during cavern construction, one should expect to develop an LRC storage that will operate successfully for a level of gas pressures as high as 25 MPa in a rock mass of reasonable quality.

Table of Contents

List of Figures

Page

List of Tables

1.0 INTRODUCTION

The U.S. Department of Energy (DOE), through the National Energy Technology Laboratory (NETL) in Morgantown, West Virginia, is participating in the introduction of new technology to the commercial natural-gas-storage market in the United States. For more than 10 years, Sweden has been developing a technology for storing pressurized natural gas in excavated steel-lined caverns in crystalline rock (Larsson et al, 1989; Tengborg, 1989). Although existing underground space (e.g., large salt caverns, aquifer formations, depleted oil fields) is currently being used for the same purpose in the United States and abroad, the flexibility of the lined rock cavern (LRC) concept could contribute to more efficient management of the local and regional supplies of natural gas. This is particularly true for the Northeast and Northwest regions of the United States, where salt caverns and depleted oil fields do not exist. The developers of the technology expect that 50-m to 115-m tall cylindrical caverns, 20 m to 50 m in diameter can be constructed in crystalline rock at depths of 100 m to 200 m. The caverns, which are fitted with an impermeable steel liner, are expected to provide continuous storage of natural gas for maximum gas pressures ranging from 15 MPa to 25 MPa.

A scaled (approximately 1:9 scale) experiment of the concept has been conducted at the Grängesberg Test Plant in Sweden, with reported positive results (Stille et al., 1994). A full-scale LRC demonstration facility is currently being constructed at Skallen, a site near the coastal city of Halmstad in southwest Sweden.

With the prospect of introducing this new gas-storage technology to the U.S., it is timely for DOE/NETL to assess the merits of the LRC concept and examine the details of its design methodology to ensure it is both technically feasible and safe. The following is a technical review that focuses primarily on the rock mechanics aspects of the LRC concept and design methodology. The steel liner/nozzle constructability and structural integrity will be the subjects of a separate technical review.

2.0 TECHNICAL REVIEW: OBJECTIVES, STANDARD AND SCOPE

An earlier DOE-sponsored LRC project (USDOE, 2000) addressed the current state-of-the-art in the LRC concept, market data for conventional alternative storage in the Northeastern United States, identification and selection of two generic geologic sites, conceptual design for the LRC, cost estimate, economic comparison of LRC to alternatives, and environmental impact and permitting issues. The currently sponsored project compliments the previous work by adding an independent review of the LRC storage technology. The objective of the current review was specifically to evaluate:

(1) the general feasibility of the LRC storage concept; and

(2) the proposed LRC design methodology and the adequacy of key design aspects.

An independent technical review was initiated with a meeting between the LRC development group and NETL and Itasca Consulting Group Inc. (the review team) in September 2000. At that time, the LRC group consisted of Energy East Enterprises, Inc. (USA), Gas de France International, S.A., Sydkraft AB (Sweden), and Enron North America Corporation. At this meeting, several presentations were made by the LRC group with regard to the technical aspects of the lined-rock-cavern concept and its design methodology. Key aspects of the LRC design were identified (e.g., safety against ground uplift and maximum steel-liner strain range), and results from a pilot study in Grängesberg, Sweden, were presented.

Subsequent to the September meeting, the review team received a number of review documents from the LRC group. These documents (some of which contain confidential information) provide in-depth technical details of the LRC concept, the design methodology, and test results of the pilot study. A list of the review documents is provided in the next section. The technical review was based on the information in the review documents and on the initial technical presentations made by the LRC group at the September 2000 meeting. Upon request by the review team, additional information was provided by the LRC group during the course of the review.

In addressing the specific review objective, two important components of mechanics are involved:

- *Rock Mechanics* (because a stable rock mass is imperative to the success of the concept during both the cavern-excavation and storage-operation periods, and
- *Structural Mechanics* (because the structural integrity of the steel-liner and nozzle assembly is crucial to the continuous service of the liner as an impermeable barrier to the stored natural gas).

Note that this review is concerned only with rock mechanics aspect of the LRC concept. Review of structural mechanics issues related to the steel liner (e.g., evaluation of liner fatigue) will be the subject of a separate report. The rock-mechanics acceptability standard used was based on demonstrated principles applied in the past and present practice of developing and designing large underground openings in rock in the civil and mining industries. These principles are discussed and advocated in all major textbooks on the subject of rock mechanics and rock engineering (e.g., Stagg and Zienkiewicz, 1968; Hoek and Brown, 1980; Brady and Brown, 1993; Goodman, 1980; Mahtab and Grasso, 1992; Hudson and Harrison, 1997; Harrison and Hudson, 2000). Thus, in evaluating the LRC concept, it was central to the review that the review documents convey an adherence to established and accepted rock mechanics principles of large cavern development, as well as a demonstration of rigor in its design analysis.

While an independent complete LRC design analysis was not performed as part of this review, some analyses were conducted that evaluated key design criteria associated with the rock mass and steel-liner response for LRC conditions. The results of these analyses generally agreed with results expressed in the review documents. However, some results

suggest that the limit equilibrium models used in the ground-uplift design evaluations are too simple to adequately represent the rock-mass load/deformation response for LRC conditions. Results also show potentially important effects from the presence of natural rock fractures on local strains in the steel liner during cavern pressurization. Such effects are not accounted for in the current LRC design methodology, because it regards the rock mass only as a continuum. When a rock mass is represented as a continuum, the deformational effects of natural rock fractures are smeared/averaged throughout the rock mass. Although this is frequently done in rock engineering, the importance of the steel liner strain in the context of the LRC design also warrants evaluation using methods that account for local effects associated with the presence of explicit rock fractures.

The remaining sections of this report contain the following.

- Title list of the review documents (for completeness), with a brief summary of the LRC concept and design methodology expressed in these documents.
- Review of key LRC design aspects:
  - Criterion for Safety Against Ground Uplift;
  - Cavern-Wall Response (Steel Liner/Concrete/Rock Mass Interaction); and
  - Concrete-Liner Fracture Analysis.
- Review of the LRC design methodology:
  - General Comments
  - Probabilistic Approach
- Conclusions
  - Summary and Observations of the Rock Mechanics Review
  - Judgement of the LRC Concept
  - Recommendations

3.0 SUMMARY OF THE LRC CONCEPT AND DESIGN METHODOLOGY

For completeness of documentation, the LRC concept and design methodologies are briefly summarized. This summary is constructed from the review documents supplied by the LRC group. A title list identifying these documents is provided below.

3.1 Title List of Review Documents

The following is a list of the review documents provided to the review team by the LRC group:

- Hard copy of overhead presentation "Commercial Potential of Natural Gas Storage In Lined Rock Caverns (LRC)," presented to the DOE/NETL, September 20 and 21, 2000;
- Hard copy of overhead presentation, with manuscript, "Storage of Gas in Lined Rock Caverns — Conclusions Based on Results from the Grängesberg Pilot Plant";
- Conference paper by Johansson et al. (1994), "Storage of Gas in Lined Shallow Rock Caverns — Conclusions Based on Results from the Grängesberg Test Plant";
- Conference paper by Stille et al. (1994), "High Pressure Storage of Gas in Lined Shallow Rock Caverns — Results From Field Tests";
- Report (confidential), "Thermal Simulation of LRC Storage Operation";
- Report (confidential), "LRC Demo Plant, Safety Against Uplift, Design Procedures and Design Tools";
- Conference paper by Sturk et al. (1996), "Probabilistic Rock Mass Characterization and Deformation Analysis";
- Report (confidential), "LRC Demo Plant, Global Rock Mass Parameters for the Skallen Site";
- Report (confidential), "Cavern Wall, Demo Plant Design"; and
- Report (confidential), "Rock Mechanics Criteria for Location of a LRC Storage".

The review documents identified as conference papers are included in Appendix A.

3.2 Summary of the LRC Concept

The principal idea behind the LRC gas-storage concept is to rely on a rock mass (primarily crystalline rock) to serve as a pressure vessel in containing stored natural gas at maximum pressures from about 15 MPa to 25 MPa. The concept involves the use of relatively large vertically cylindrical caverns 20 m to 50 m in diameter, 50 m to 115 m tall, with domed roofs and rounded inverts to maximize excavation stability. The caverns are located at depths from 100 m to 200 m below the ground surface, and they are lined with approximately 1-m thick reinforced concrete and thin (12-mm to 15-mm) carbon steel liners. The purpose of the steel liner, which is the innermost liner, is strictly to act as an impermeable barrier to the natural gas. The purpose of the concrete is to provide a uniform transfer of the gas pressure to the rock mass and to distribute any local strain in the rock mass (e.g., from the opening of natural rock fractures) at the concrete/rock interface more evenly across the concrete to the steel liner/concrete interface. To further minimize local circumferential strains in the steel liner, a viscous layer (~ 5 mm thick) made of a bituminous material is placed between the steel and the concrete liners.

Pressurization of the gas increases the gas density (i.e., mass per unit volume) and is key to making the storage concept economically viable. An operating cavern is expected to go through pressure cycles from approximately 3 MPa to 25 MPa during periods of gas depletion and recharge, as demand dictates, and may have a nominal design life of 500 cycles. For circumstances in which groundwater is present, the gas pressure also provides structural support to the relatively thin steel liner, which is not designed to withstand external water pressure.

It is expected that the LRC concept can be applied to a variety of different rock types and to rocks of varying quality in terms of strength and deformability.

3.3 Summary of the LRC Design Methodology

The review documents present the LRC design methodology as a stochastic, multi-stage development approach. Evaluations of the potential for a rock mass to host an LRC facility are made at different stages, with an increasing demand for geophysical information in each stage. The result is an increasingly refined design in terms of probable loads and material response. The methodology is embedded in two models: FLRC1 (Feasibility for Lined Rock Caverns 1), which is an initial procedure for LRC evaluations at an early stage; and FLRC2 (Feasibility for Lined Rock Caverns 2), a more detailed procedure for LRC evaluations and design in later stages of the development, when more site-specific geophysical information is available.

Development includes the following stages.

1. *Initial exploration* uses limited, generally available geological information (e.g., from surface observations and any previous underground work in the area) as the basis for estimating rock mass quality, which, in turn, is used in the initial model (FLRC1) to assess the potential for the rock mass to host an LRC facility.
2. Increasingly detailed *site characterization* is specifically aimed at determining the best underground location for the LRC. Details of the rock mass are obtained from core logs and other geophysical investigations. Rock index properties are determined from rock core, and a "better" estimate (in terms of confidence) of rock mass quality is made. Estimates of maximum gas pressure and liner strains are made stochastically, using the procedure in the FLRC2 model. These estimates are used as the basis for the initial LRC design.
3. During the *construction* stage, additional site characterization is conducted, and the Observational Approach is used to provide the "best" estimates of likely cavern response. The new estimates in this phase may affect the final LRC design.

The FLRC1 and FLRC2 models rely on rock index properties and empirical relations to estimate the rock-mass mechanical parameters (i.e., stiffness and strength); limit-equilibrium, finite-element and analytical (homogeneous and isotropic) models are used to estimate cavern location (i.e., depth), maximum gas pressure, cavern deformations, and steel-liner strain. The methodology emphasizes two key LRC design criteria associated with (1) safety against ground uplift, and (2) a maximum operating (cyclic) strain range in the steel liner.

4.0 REVIEW OF KEY LRC DESIGN ASPECTS

According to the review documents, LRCs are expected to operate at maximum gas pressures of 15 MPa to 25 MPa. With the caverns located at a relative shallow depth of 100 m to 200 m, this generally means the rock mass could be subjected to pressures 4 to 8 times higher than the in-situ rock-mass stresses. Because the LRC concept relies on the rock (not the steel or concrete liners) to serve as the pressure vessel, an adequate cavern depth (or rock overburden) is important. The overburden rock mass must resist the maximum cavern pressure in a stable manner. This key aspect of the LRC design is evaluated in this section.

For a given cavern geometry, the mechanical response of the cavern wall to the LRC pressure depends on the site-specific character of the rock mass and on the structural interaction between the rock mass, concrete liner, viscous bituminous layer, and the steel liner. In general, the gas pressure will displace the cavern wall radially outward, result-

ing in extensional strains in the tangential horizontal and vertical directions in the steel liner, concrete liner, and in the rock at the cavern wall. For a given pressure, the amount of extensional strain depends mostly on the rock mass strength and deformability, which become important attributes of the LRC design. The cavern wall response and its affect on the steel liner strain are also evaluated in this section.

Note that the parts of this review requiring evaluation using numerical models have been considered for LRC conditions similar to the Skallen demonstration plant, which is currently being constructed near the coastal city of Halmstad in southwest Sweden.

4.1 Criterion for Safety Against Ground Uplift

The design analysis of Safety Against Ground Uplift is described in the LRC review document "LRC Demo Plant, Safety Against Uplift, Design Procedures and Design Tools". The determination of a "safe" LRC depth combines the results of either of two limit-equilibrium (LE) models: a "rigid-cone" or a "log-spiral" model in addition to a finite-element numerical model. The principle of Limit Equilibrium (LE) in this case compares the LRC load (from the gas pressure) to the resistance provided by the weight of the overburden rock mass. The results from the models are used to determine the thickness of a "Non Robust (rock mass) Zone" below which large deformations of the rock mass will not influence LRC failure. The LE models are used to determine the safe LRC depth to prevent rock mass failure, while the finite-element numerical model is used to determine the depth at which the steel liner strain is no longer influenced by the proximity of the ground surface. The difference in these depths is defined as the thickness of the Non Robust Zone. Presumably, if the LRC is located inside the Non Robust Zone "a small variation in depth can lead to an unwanted behavior of the storage" — hence the name "Non Robust Zone".

The rigid-cone and log-spiral models differ primarily in the volumetric shapes of the resisting rock mass. The log-spiral model also accounts for the frictional resistance along the log-spiral failure surface. Both models implicitly regard the naturally fractured rock mass as a continuum. In the context of assessing potential uplift, this is a reasonable assumption, as the volume of the potentially affected rock mass above the LRC is very large relative to the size of distinct blocks generally created by a natural fracture system. However, it is important to assess the reasonableness of this assumption for site-specific LRC conditions, paying particular attention to any large continuous structures such as faults or shear zones in the near vicinity of the LRC site.

As part of the LRC design methodology development, the rigid-cone and log-spiral LE models have been calibrated to match experimental data of soil anchor pull-out tests. These calibrations have produced a model correction factor "M", which is used as an integral part of the rigid-cone and log-spiral models in predictions of ground uplift. The correction factor is defined as the ratio of the observed (experimental) resistance to the predicted resistance, with approximate mean values of 3 and 2 determined for the rigid-cone and log-spiral, respectively. The following sections examine the reasonableness of

using the LE models to evaluate ground uplift associated with pressurized caverns in rock. Because it is important to understand the basic capacity of these models in predicting uplift, a model-correction factor has not been applied in this evaluation. To provide additional perspective, the LE models are compared to a numerical model of ground uplift using conditions similar to the Skallen demonstration plant.

4.1.1 Rigid-Cone Limit-Equilibrium Model

The rigid-cone model assumes the resisting rock mass to be the weight of a cone above the cavern, as shown in Figure 4-1. According to Littlejohn and Bruce (1975), the cone angle, α, is taken as 30^o or 45^o degrees, with the lower angle used for a soft, heavily fissured or weathered rock mass. Other than the cone angle, this model does not account for any rock mass strength; thus, relative to the rock mass response that can be expected for an LRC system, the rigid-cone concept is very simplistic.

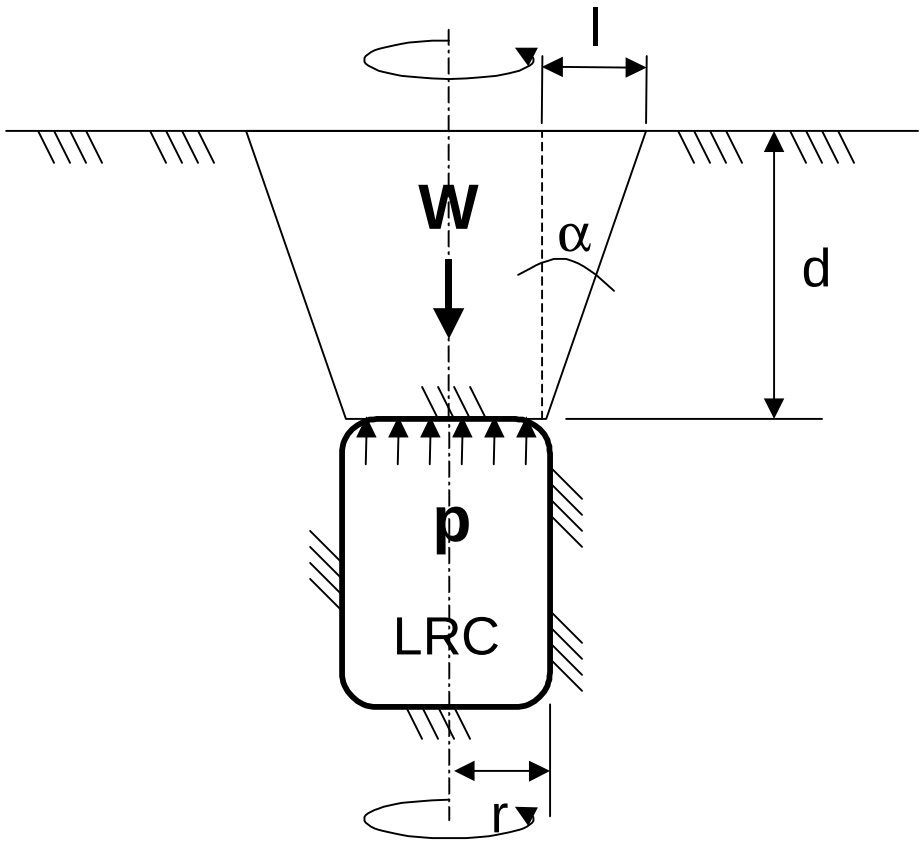

Figure 4-1 LRC Rigid-Cone Concept

Because the model neglects the inherent strength (cohesive and frictional) of the rock mass, it is most likely conservative in its estimate of resistance.

A simple check of the rigid-cone model can be done by expressing it in terms of the cone angle versus LRC depth and applying it to conditions at the Skallen demonstration site. Using the dimensions defined in Figure 4-1, the resisting force, *W*, can be expressed by Equation (4-1), and the LRC load by Equation (4-2):

$$W = \rho g \pi \left\{ r^2 d + \left[r d^2 \tan(\alpha) \right] + \frac{\left[d^3 \tan^2(\alpha) \right]}{3} \right\} \tag{4-1}$$

where W = total vertical force from the weight of the rigid cone (acting downward);

ρ = rock mass density;

g = gravitational acceleration;

r = LRC radius;

d = depth of LRC (or rock mass overburden); and

α = cone angle = atan*(l/d)*.

$$F_{LRC} = \pi r^2 p \tag{4-2}$$

where F_{LRC} = total vertical force from the cavern gas pressure (acting upward); and

p = gas pressure.

A factor-of-safety (FS) against ground-surface uplift can be defined as in Equation (4-3):

$$FS = W / F_{LRC} \tag{4-3}$$

Solving Equation (4-3) for *l*, and noting that $l = d \tan(\alpha)$, the cone angle, α, can be expressed as in Equation (4-4):

$$\alpha = \text{atan}\left(\left(r \left(9 - 12 \left(1 - \frac{pFS}{\rho g d} \right) \right)^{1/2} - 3r \right) \left(\frac{1}{2d} \right) \right) \tag{4-4}$$

The cone angle is shown as a function of depth in Figure 4-2 for Skallen conditions of 17.5-m cavern radius, 20-MPa gas pressure, and 2500-kg/m^3 rock mass density. An FS of 2 was chosen in Figure 4-2; this is a common FS for slope stability design using limit equilibrium (e.g., Hoek and Bray, 1977) and in tunnel design (e.g., Hoek and Brown, 1980) to ensure safety against potentially falling ground. Figure 4-2 shows that, for a depth of 110 m (i.e., Skallen conditions), a cone angle of 39^o is required to achieve an FS of 2 against uplift. Thus, this simple check shows that the angle is within the expressed limits (i.e., 30^o to 45^o) of the rigid-cone model.

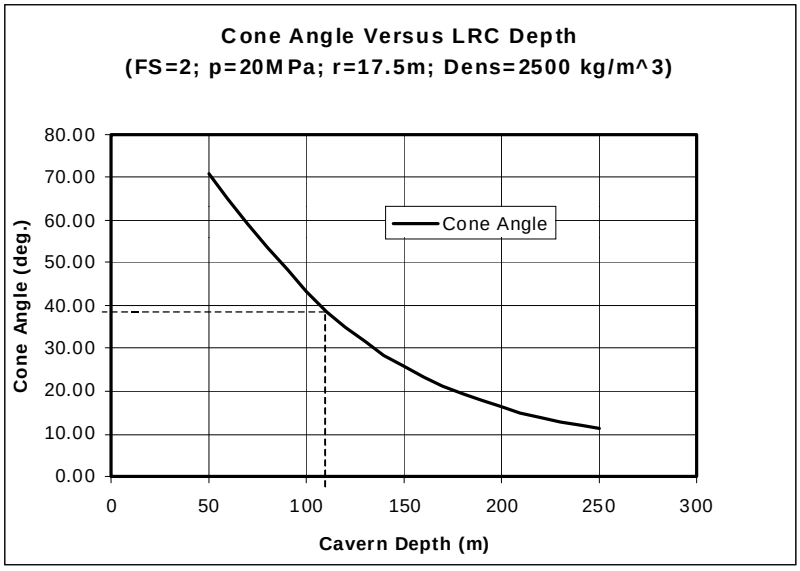

Figure 4-2 Cone Angle versus Depth for Skallen Conditions

4.1.2 Log-Spiral Limit Equilibrium Model

The log-spiral model used in estimating resistance against ground uplift is illustrated conceptually in Figure 4-3; it is based on the response of soils in resisting pull-out of soil anchors at shallow depth (Ghaly and Hanna, 1994). The spiral shape is a function of the friction angle as defined by Equation (4-5). In addition to the rock-mass weight, the model also includes resistance from friction along the log-spiral failure surface.

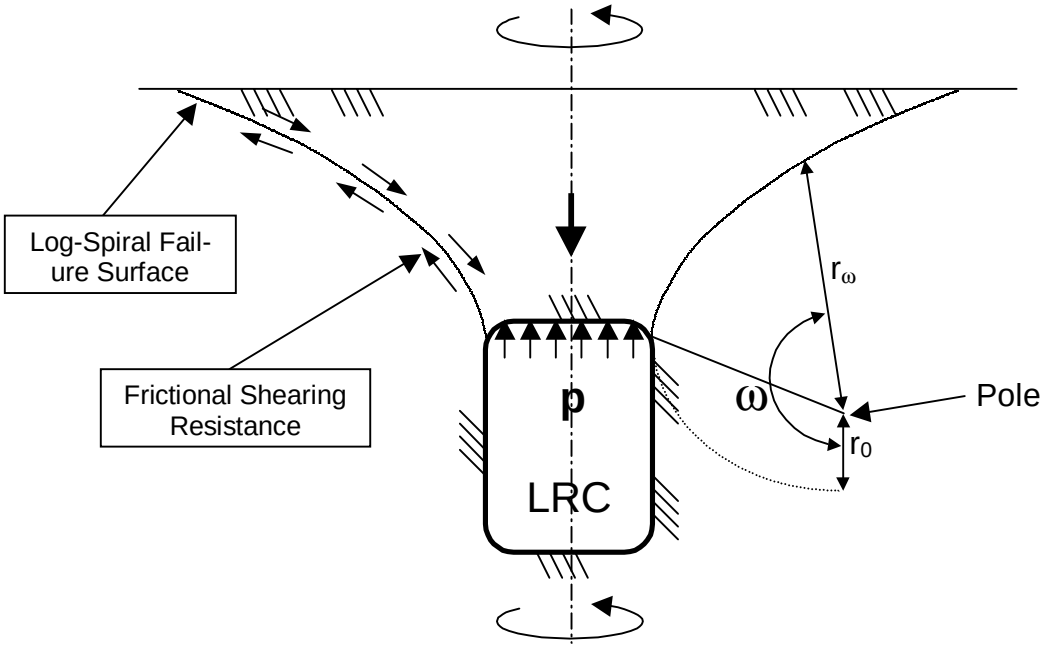

Figure 4-3 Conceptual View of the Log-Spiral Criterion

$$r_\omega = r_0 \, e^{(\omega)\tan(\phi)} \tag{4-5}$$

where r_ω = radius of log-spiral at angle ω,

r_0 = initial radius of log-spiral at $\omega = 0$,

ω = angle of revolution, and

ϕ = material friction angle.

As expressed in Equation (4-5), the log-spiral criterion remains constant for a rock mass of a given friction angle. However, Mandl (1988), in his discussion of faulting, shows results of sandbox experiments in which wide spiral-shaped precursor faults from differential uplift occur — but subsequently develop into steeper dipping spirals, as in Figure 4-4. More significantly, Mandl (1988) finds the width and dip of the spirals to be sensitive to the amount of horizontal stress, with narrower, steeper dipping spirals occurring for lower horizontal stresses. This implies that the log-spiral criterion as defined in the LRC design could overestimate the safety against ground uplift for ground conditions of low in-situ horizontal stresses (e.g., $K_o = 1$, where K_o is the ratio of the average horizontal-to-vertical in-situ ground stress). The vertical stress in the ground usually results only from the weight of the overburden rock mass, while the horizontal components are most often affected by tectonics in addition to purely gravitational effects. Local topography and rock mass structure can also affect the horizontal stress levels. Major ground structures such as faults and shear zones can influence the direction and magnitude of the local in-situ horizontal stresses. Thus, there can be large variations in stress on a relatively

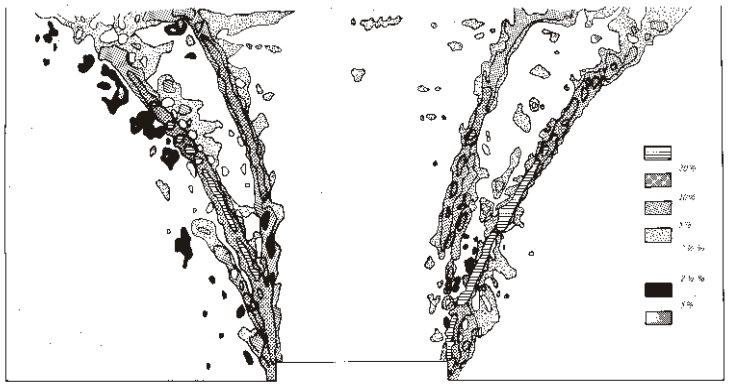

Plot of accumulated dilation during 1 cm uplift of a 10 cm wide basement block bounded by vertical faults. The plot was made using a stereophotogrammetric technique (Butterfield et al., 1970.) Numbers give volume change in percents of original specific volume. Negative numbers indicate zones of compaction. Zones of positive dilation are closely associated with the curved precursor shears.

Figure 4-4 Sand Dilation Along Shear Zones in the Uplift Experiment [after Mandl, 1988, pp. 71-75]

local scale. Although at shallow depths (less than 500 m), K_o is generally greater than 1.0, it is not always so. In many regions of the world, including the U.S., normal faulting stress regimes exist where K_o would be close to or less than 1.0 (e.g., Mueller et al., 2000).

As verification of the effects implied by Mandl (1988), the computer code FLAC (Itasca, 2000) was used to evaluate the soil-anchor analogy with a numerical model. FLAC simulates materials as a continuum, and the code has been specialized to analyze soil and rock-mechanics problems. An axisymmetric FLAC model of a soil anchor was prepared, as shown conceptually in Figure 4-5. The model was verified by first comparing it to experimental results of soil anchor pullout, and subsequently used to evaluate effects of lateral pressure on such pullout. The effects of different anchor depths were analyzed for the soil conditions listed in Table 4-1. The soil was represented as a Mohr-Coulomb material with frictional strength only. While the high bulk and shear moduli values listed in Table 4-1 are more representative of a rock mass than a soil, these values have an in-significant effect on the anchor-pullout results. The results of the analysis are shown in Figure 4-6, along with published experimental results (Vesi• , 1971). Note that the FLAC model results in Figure 4-6 reflect the use of $K_o = 1$; the results fall well within the experimental data and validate the FLAC soil-anchor model to some extent.

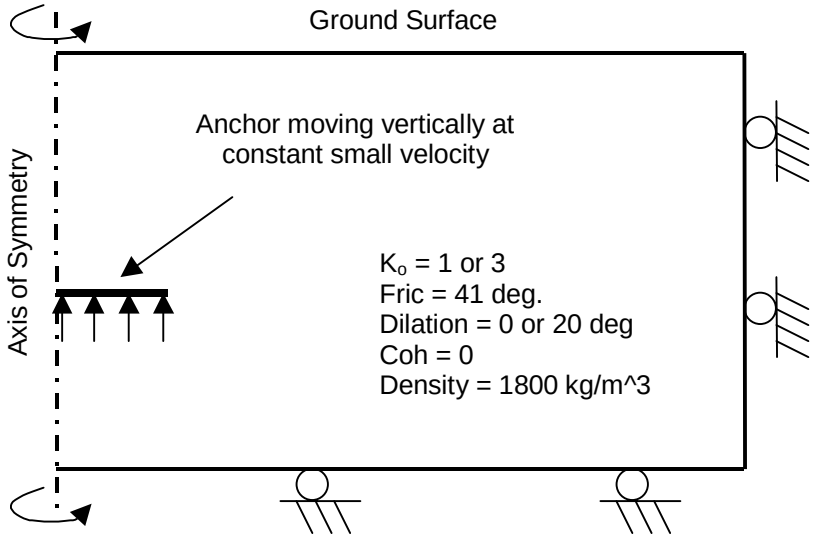

Figure 4-5 Conceptual View of the FLAC Soil-Anchor Model

Table 4-1 Parameters Used in the FLAC Soil-Anchor Model

Bulk Modulus (GPa)	20
Shear Modulus (GPa)	15
Friction Angle (degrees)	41
Dilation Angle (degrees)	0 or 20
Cohesion (MPa)	0
Tensile Strength (MPa)	0
Density (kg/m^3)	1800
K_o [(a)]	1 or 3

(a) K_o is the ratio of the average initial horizontal stress to the vertical stress

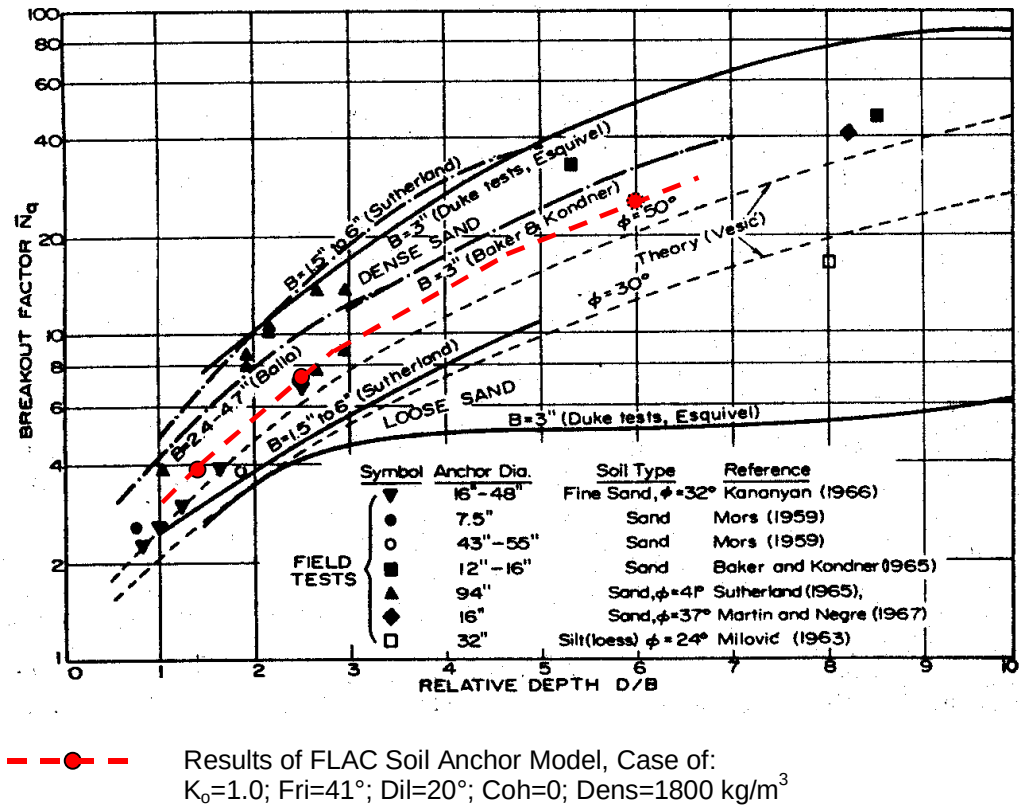

Figure 4-6 Experimental Results of Soil-Anchor Pullout [after Vesi• , 1971] and Results of the FLAC Soil-Anchor Model

Figure 4-7 shows the results of the soil-anchor model when the initial horizontal stress is 3 times higher than the vertical stress (i.e., K_o = 3); the dilation angle is 0 for these results. Because we use an axisymmetric model, results are only shown for the right-half of the model. The location of the anchor plate is indicated. Note that the results in Figure 4-7(a) reflect an earlier state of the anchor pull (i.e., less total anchor movement) than in than in Figure 4-7(b). As the anchor plate is being pulled out (i.e., upward), the surrounding soil (particularly above the plate) is set in motion, as indicated by the black velocity vectors in the figure. After sufficient motion, the soil starts to yield in shear. Actively yielding soil (shear failure) is indicated by red symbols. The green color appearing in portions of the soil indicates that the soil was previously subjected to yield but, as a result of load transfer, has now obtained a stress state that is below the Mohr-Coulomb yield criterion.

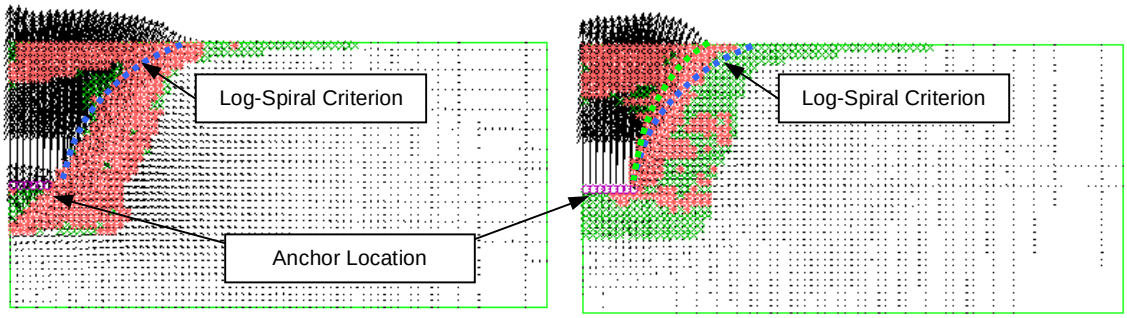

Figure 4-7 Results of the FLAC Soil-Anchor Model for K_o = 3 and Dilation Angle = 0°

The light-blue dashed line in Figure 4-7(a) shows the approximate location of the log-spiral failure surface. For this state, there appears to be a good match between the log-spiral model and the numerical predictions (indicated primarily by the velocity vectors). However, at the later state in Figure 4-7(b), failure occurs along a narrower cone with a steeper-dipping log-spiral surface, indicated in dashed light-green color. This material response is consistent with that discussed by Mandl (1988).

When the model in Figure 4-7 is repeated for K_o = 1, results as shown in Figure 4-8 are obtained. The velocity vectors and the column of shear yielding (i.e., red symbols) indicate a vertical cylindrical failure surface above the soil anchor. This response seems also to agree with the discussion by Mandl (1988) on the effect of lateral stress on precursor faulting. The log-spiral location is also shown in Figure 4-8 (in dashed light blue), which suggests a significant overestimation of the safety against uplift in this case. Using a dilation angle of 20^o had very little effect on the results in Figure 4-7 and only slightly changed the results in Figure 4-8.

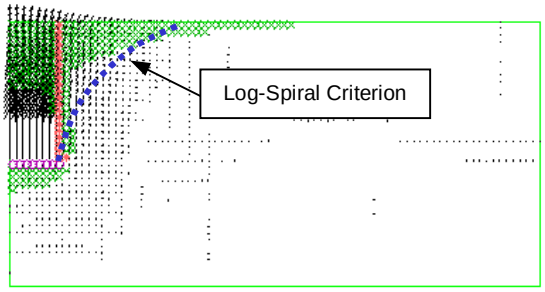

Figure 4-8 Results of the FLAC Soil-Anchor Model for K_o = 1 and Dilation Angle = 0°

The results of the soil-anchor model, therefore, point out that the use of the log-spiral LE model is not necessarily appropriate when in-situ stress conditions are such that K_o is close to 1. A numerical model that has been validated to some extent should be used to check that the log-spiral criterion is reasonable for the local LRC site conditions. When applying the log-spiral criterion to the Skallen conditions in the same manner as for the rigid cone, an FS of 2.6 against ground uplift is estimated. Note that the resisting force in this case includes frictional forces along the log-spiral surface in addition to the force from the weight of the failed rock mass.

4.1.3 Ground-Uplift Evaluation of the Skallen Demonstration Plant Using a Numerical Model

A numerical model brings much more mechanistic detail to the evaluation of the potential for ground uplift associated with the LRC pressure. At any stage in the design process, the numerical model can be used to check the LRC design in terms of its potential for affecting ground uplift. Such analyses add assurance to a design procedure that bases a significant portion of its design analysis on simple LE models. Assessment of a factor-of-safety can also be gathered from a numerical model, allowing direct comparisons to LE models.

Itasca's computer code FLAC (Itasca, 2000) was used to analyze the uplift potential for rock mass conditions at the Skallen demonstration plant. An axisymmetric model was used as shown conceptually in Figure 4-9. The rock mass was modeled as an elasto-plastic material using a Mohr-Coulomb failure criterion and the properties listed in Table 4-2. In assessing an uplift factor-of-safety, the model was analyzed repeatedly, with the rock mass strength reduced by a constant factor ($C_f < 1.0$) each time (i.e., C_f* cohesion and C_f*tan(friction angle)). The uplift factor-of-safety was defined as C_f^{-n} , where n is the number of repeated analyses necessary to cause large incremental vertical displacements in the rock mass. C_f^{-n} is, therefore, equivalent to the ratio of the "actual" rock-mass shear strength to the minimum shear strength required to prevent failure. This procedure for obtaining a factor-of-safety has been used in geomechanics for a long time (e.g., Zienkiewicz et al., (1975), Naylor (1982), Donald and Giam (1988), Matsui and San (1992), Ugai (1989), Ugai and Leshchinsky (1995)) and is consistent with the traditional method of determining the factor-of-safety for slope stability (Bishop, 1955). During the analyses, the vertical displacement in the center of the cavern roof and at the ground surface was monitored. After sufficient rock-mass strength reduction, significant vertical displacements occurred at these monitoring locations. Figure 4-10 shows a plot of C_f^{-n} versus vertical displacement for the two monitoring locations, as well as the final failure state in the rock mass surrounding the LRC. A significant increase in the incremental vertical displacement is seen for C_f^{-n} beyond about 9. Thus, using a numerical model, an uplift factor-of-safety of 9 can be estimated for the Skallen conditions. When comparing this estimate to those obtained for the rigid-cone and log-spiral LE models (FS of 2 and 2.6, respectively), the simpler LE models are found to be very conservative for the Skallen site conditions and not well-suited to describe the resistance to uplift associated with a pressurized cavern in a rock mass.

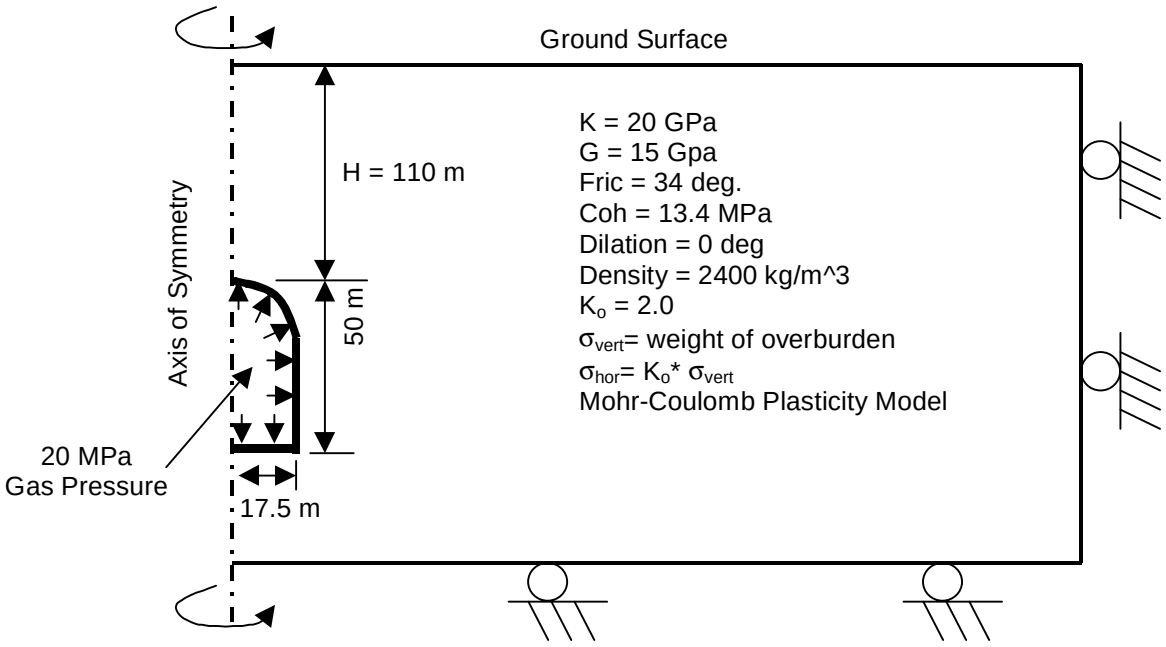

Figure 4-9 Conceptual FLAC Model for Evaluation of Ground Uplift

Table 4-2 Parameters Used in the FLAC Model for Evaluation of Ground Uplift

Bulk Modulus (GPa)	20
Shear Modulus (GPa)	15
Friction Angle (degrees)	34
Dilation Angle (degrees)	0
Cohesion (MPa)	13.4
Tensile Strength (MPa)	0
Density (kg/m^3)	2400
K_o[(a)]	2

(a) K_o is the ratio of the average initial horizontal stress to the vertical stress

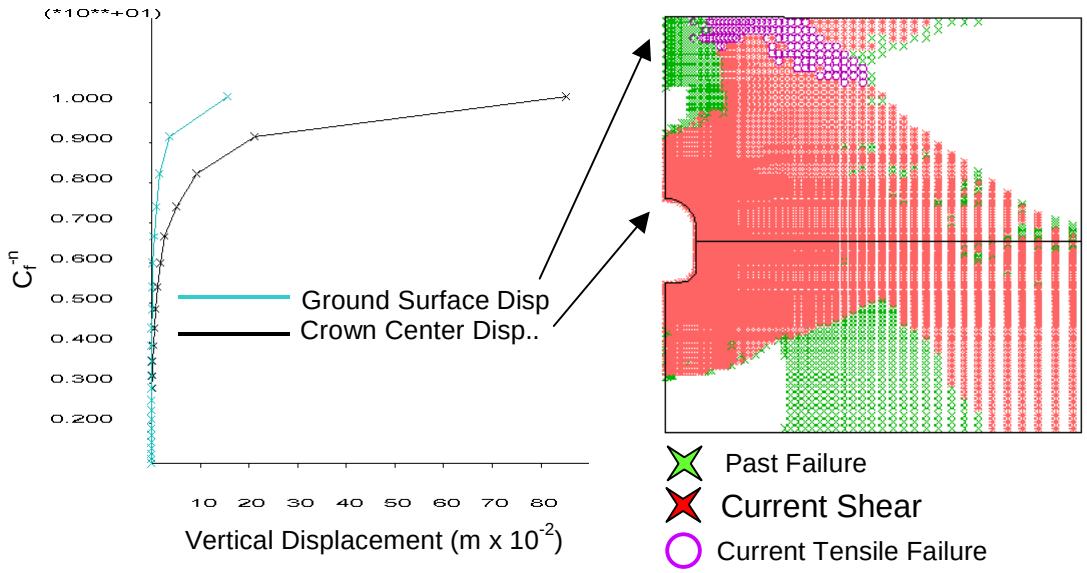

Figure 4-10 C_f^{-n} versus Vertical Displacement of the Cavern Roof and Ground Surface Indicating an Uplift Factor-Of-Safety of 9 (The final failure state in the rock mass is also illustrated.)

It is noted that the LRC uplift-design methodology also uses results of a finite-element numerical model. The numerical model is used to determine the LRC depth that ensures no influence from the proximity of the ground surface on strains in the cavern steel liner. This is a relatively strict design criterion that should eliminate the need for using the rigid-cone or log-spiral LE models.

4.2 Cavern-Wall Response (Steel-Liner/Concrete/Rock-Mass Interaction)

The thin steel liner behaves essentially as an impermeable membrane. The maximum, operating, liner strain range (i.e., membrane strain), therefore, is another key aspect of the LRC design. While, for a given cavern geometry, this strain depends on the maximum gas pressure, it is also closely tied to the structural interaction between the steel liner, the viscous (bituminous) layer, the reinforced concrete liner, and the rock mass. Hence, accurate estimates of the steel-liner response require analyses that include sufficient physical detail of these wall elements.

The rock mass, which serves as the pressure vessel, affects most of the cavern wall deformations and therefore has the most influence on the average steel-liner strain. Rock mass conditions are often anisotropic, and this can impose additional effects on the amount, as well as the distribution, of the strain in the steel liner. The anisotropy can result from the rock mass itself having directional material properties (material

anisotropy, often influenced by oriented structure) or by the two in-situ horizontal stresses being of different magnitude (stress anisotropy). The effect of anisotropy on the cavern-wall response is evaluated in the next sections.

During LRC operations, the steel liner is subject to cyclic loading from periodic gas injection (increasing cavern pressure) and depletion (decreasing cavern pressure). Excessive steel-liner strain during these cycles may lead to liner fatigue failure. Therefore, structural fatigue in the liner is of concern. In the context of the Skallen demonstration plant, the steel used has yield strength of 355 MPa at 0.17% strain. It is expressed in the review documents that, if the strain range is kept below 0.34% (i.e., twice the yield strain), the cyclic strain in the steel liner will remain elastic, with an expected fatigue life of more than 100,000 cycles. However, for a strain range of 0.5%, for example (i.e., more than twice the yield strain), the steel liner will yield in tension and compression on every gas injection/depletion cycle. This will reduce the fatigue life of the steel liner. The review documents express that for smooth specimens of structural steel, failure generally will occur after approximately1000 cycles for a strain range of about 2%. Therefore, the number of cycles to failure would be larger for a 0.5% strain range. The nominal number of cycles expected for a commercial LRC plant during its service life is expressed as 500. The steel-liner strain for the Skallen demonstration plant is evaluated in the following sections.

An adequate evaluation of these LRC design aspects requires numerical analyses that incorporate sufficient physical detail of the cavern wall and the local rock mass conditions, including the natural rock fractures. The following sections describe two such evaluations in which the rock mass is first considered to behave as a continuum with average rock mass properties and, subsequently, as a discontinuum containing multiple discrete fractures that can induce locally high deformations and strains.

4.2.1 Independent Analysis of the Cavern Wall Using a Continuum Approach

A continuum approach is a relatively simple and computationally efficient method of analyzing stresses and deformations in rock masses. A rock mass, however, is generally a naturally fractured material made up of a system of individual interlocking wedges and rock blocks and, therefore, does not conform strictly to the notion of a continuum. Depending on scale, however, it may still be reasonable to characterize the mechanical response of a blocky rock mass as a continuum in which details of distinct local deformations between blocks are smeared into an average response. If detailed local response is unimportant to a particular underground design, the continuum approach may serve well in a design analysis.

4.2.1.1 Horizontal Cavern Section

The response of the cavern wall was evaluated for conditions similar to the Skallen demonstration plant. A horizontal section, which distinctly includes the steel liner, the viscous bituminous layer, the concrete liner and the rock mass, was analyzed in a 2D FLAC model for plane-strain conditions. This model is somewhat conservative, because the plane-strain conditions imply the cavern is an infinitely long cylinder, which neglects the constraining effects of the rock mass above and below the cavern. The conceptual FLAC model is shown in Figure 4-11 and is taken to represent a horizontal section at the cavern mid-height. Note that, because of symmetry, only a quarter of the cavern needs to be analyzed. The model parameters used are listed in Table 4-3, with the rock mass defined as an elasto-plastic material using a Mohr-Coulomb failure criterion.

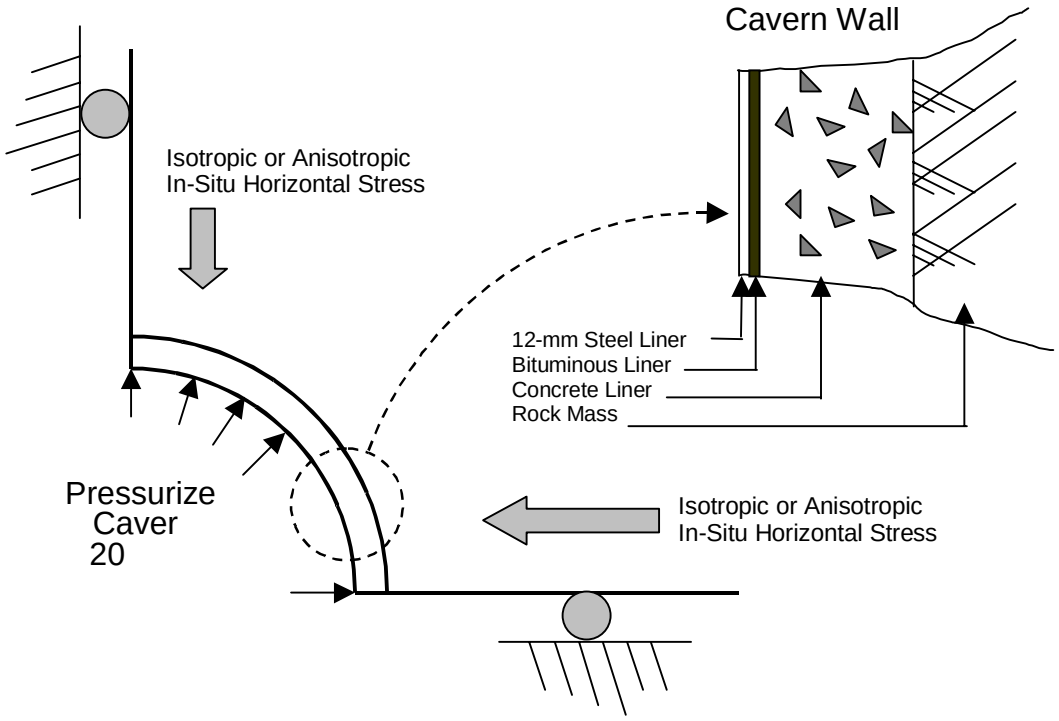

Figure 4-11 Conceptual FLAC Model of a Horizontal Section Through the Mid-Height of the LRC

Table 4-3 Parameters Used in FLAC Model to Evaluate Cavern Wall Response

Parameters	*Rock Mass*	*Concrete Liner*	*Steel Liner*	*Sliding Interface*[(a)]
Bulk Modulus (GPa)	20	16.7	167	—
Shear Modulus (GPa)	15	12.5	77	—
Friction Angle (degrees)	34	35	—	5
Dilation Angle (degrees)	0	0	—	—
Cohesion (MPa)	13.4	9.6	—	—
Tensile Strength (MPa)	0	2.7	—	—
Density (kg/m^3)	2400	2400	7870	—
Normal Stiffness (MPa/m)	—	—	—	113e9[(b)]
Shear Stiffness (MPa/m)	—	—	—	113e9[(b)]

(a) i.e., bituminous layer
(b) assumed values

The material properties in Table 4-3 were taken from the LRC review documents and are intended to reflect average conditions. The steel-liner thickness was 12 mm, and the concrete liner was approximately 1 m. The viscous bituminous layer between the steel and the concrete liners was included as a sliding interface with zero cohesion and a low friction coefficient. Note that the structural element logic in FLAC was used to simulate the steel liner assuming an elastic response of the steel.

The model in Figure 4-11 was evaluated for isotropic and anisotropic in-situ horizontal stress conditions. According to the review documents, the in-situ horizontal stresses at Skallen are anisotropic, with estimated minimum and maximum stresses of about 4 MPa and 8 MPa, respectively, in the principal directions.

The model was analyzed first for isotropic horizontal stresses of 4 MPa and a cavern gas pressure of 20 MPa. The predicted results are shown in Figure 4-12, with an average radial wall displacement of about 14 mm and an average steel-liner strain of about 0.09%. This strain is considerably less than twice the steel yield limit of 0.34%, ensuring a cyclic steel-liner strain that operates only in the elastic range. When accounting for a static pore pressure of 1.25 MPa associated with the groundwater, the results change only slightly, to a maximum strain of 0.1% and a wall radial displacement of 15 mm. These results suggest the design is adequate for conditions of an isotropic, initial horizontal-stress state.

When evaluating the model for an anisotropic horizontal stresses state of 4 MPa and 8 MPa, the results obtained are shown in Figure 4-13. The maximum radial wall displacement is 15 mm in the direction of the minimum in-situ stress and 11 mm in the maximum stress direction. The highest predicted steel liner strain is 0.18% percent — which is at the yield limit and double that of the isotropic conditions, but still well below twice the yield limit of 0.34%. As in the isotropic case, the effect of pore pressure from the groundwater only slightly changes the results. The analyses demonstrate that the

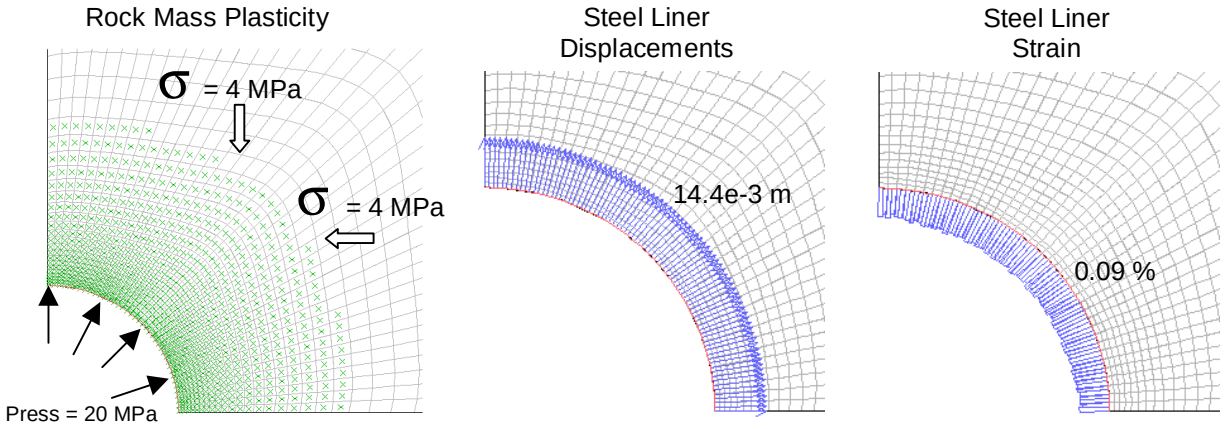

Figure 4-12 Predicted Rock-Mass Failure, Radial Wall Displacement, and Steel-Liner Strain for Isotropic In-Situ Stress Conditions of 4 MPa (steel liner shown in red)

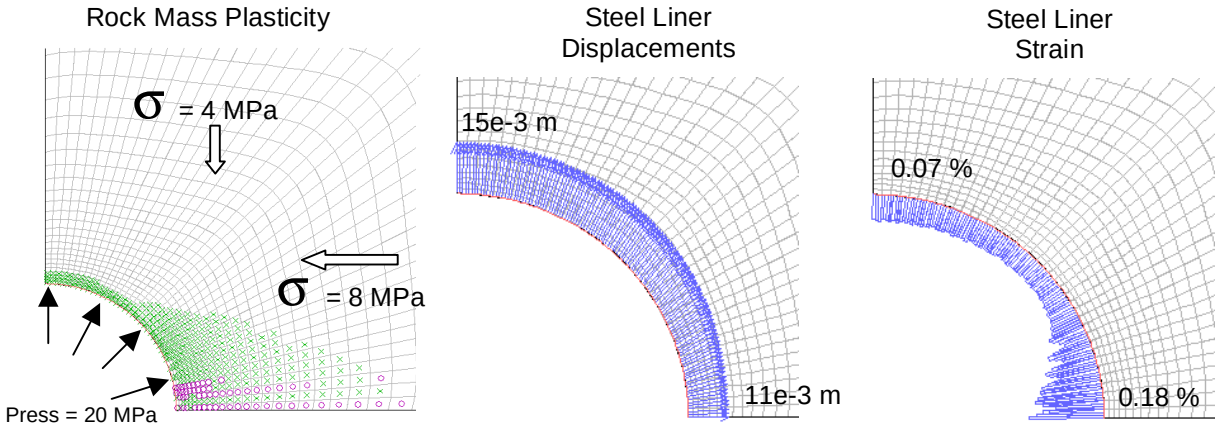

Figure 4-13 Predicted Rock-Mass Failure, Radial Wall Displacement, and Steel-Liner Strain for Anisotropic In-Situ Horizontal Stress Conditions of 4 MPa and 8 MPa (steel liner shown in red)

effect of anisotropy can be significant and underscore the importance of understanding local site conditions in designing the LRC. Note that the steel-liner strain in Figure 4-13 does not show a smooth transition from the minimum to the maximum value. This is a consequence of local tensile failures (i.e., implied tensile cracks) that occur along the concrete liner. As expected, the tensile failure in the concrete liner is associated with higher local strain in the steel liner. While the interface used to simulate the bituminous layer allows slip to occur between the steel and the concrete, enough shear strength is mobilized to cause significant local strain in the steel liner. Considering that average

rock-mass conditions are used, these results suggest the design is also adequate for conditions of an anisotropic, initial horizontal-stress state.

The systems of natural fractures in a rock mass can form rock blocks and wedges that are free to move individually under sufficient force. In many instances in underground excavations, these rock wedges and blocks represent a potential problem in terms of keeping the excavation stable simply under the force of gravity and the in-situ ground stresses. Because the forces associated with the gas pressure in an LRC are substantial, a real potential exists for displacing any precariously located blocks or wedges in the cavern wall relative to the surrounding rock mass. This relative rock displacement at the cavern wall can lead to high local strains in the steel liner. While the continuum representation of the rock mass as used in the above analyses cannot address the potential for block motion, estimates of its effect can be explored. The results of motion of an assumed rock wedge are shown in Figure 4-14. The final state for the case of isotropic in-situ stress analyzed previously was selected, and the assumed rock wedge was forced to move about 0.05 m relative to the surrounding rock mass in the direction shown in the figure. Because of the high gas pressure, the concrete and steel liners conform to the wedge motion, resulting in a maximum local strain in the steel of 0.54% during the first pressurization cycle.

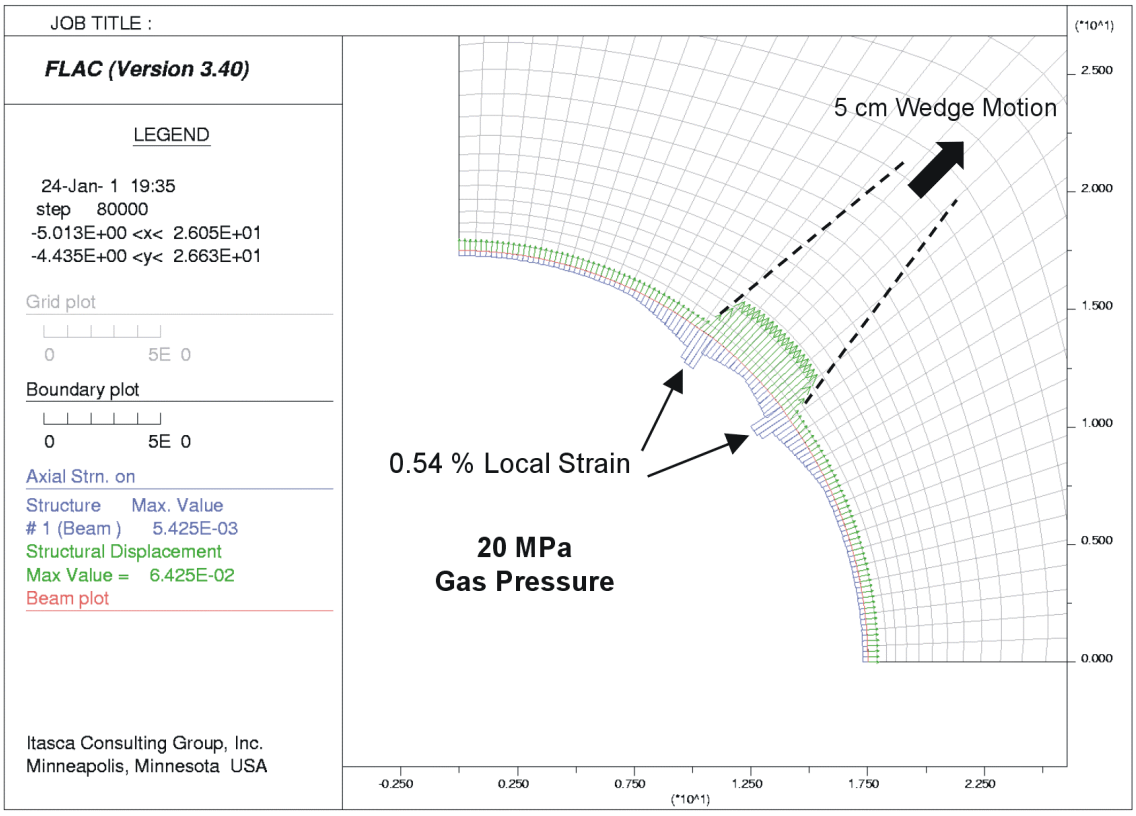

Figure 4-14 Predicted Radial Wall Displacement (Green) and Steel-Liner Strain (Blue) As a Result of Deformations of an Assumed Rock Wedge (4-MPa isotropic in-situ stresses conditions; steel liner shown in red)

Since the liner response is elastic in these analyses, the actual local strain (sum of elastic and plastic strain) may be larger. Because the relative motion of rock wedges and blocks can be expected to decrease significantly after the initial cavern pressurization (i.e., the blocks have become "seated"), the strain range in subsequent cycles can be expected to be smaller than 0.54%. Because the possibility of encountering rock wedges is real at any likely LRC site, the simple analysis above is a reminder of the need to understand the rock mass well enough to identify and immobilize such wedges and blocks, if necessary. Further evaluation of this potential problem is presented in Section 4.2.2, which discusses the discontinuum aspect of rock mass deformations.

4.2.1.2 Vertical Cavern Section

The response of the cavern wall was also evaluated in a vertical section using the same axisymmetric FLAC model shown in Figure 4-9. While $K_o = 2$ was used in this model for the ratio of in-situ horizontal-to-vertical stress, the in-situ horizontal stresses were isotropic (a limitation of the axisymmetric assumption). To include anisotropy of the in-situ horizontal stresses in this case would require a fully three-dimensional model. The axisymmetric model accounts for much of the three-dimensional effects associated with an LRC response, and is valid for reasonably homogeneous and isotropic rock-mass conditions. The steel and concrete liners are not expressed explicitly in this model; thus, the predicted strains are that of the rock. In the vertical plane, it is the average tangential strain across the finite-difference zone dimension that is reported. In the horizontal plane, the tangential strain represents the average based on the full circumference of the cavern wall. Thus, the local strain in the steel liner could be higher than that predicted in this model.

Results for rock mass conditions similar to Skallen are illustrated in Figure 4-15. The tangential strains in the cavern wall in the vertical and horizontal planes are plotted starting from the middle of the dome to the middle of the invert. The tangential strain along the wall in the vertical plane shows peaks (1) in the corners between the dome and the vertical wall, and (2) between the wall and the invert. Stresses tend to concentrate at corners, resulting in more local failure of the rock mass. The green and purple symbols in the cavern sketch in Figure 4-15 show the local rock-mass failure that has taken place along the cavern wall.

Current tensile failure is indicated in purple, while previous shear or tensile failure is indicated in green. Local concentration of failure is observed in the corner regions of the cavern wall. The highest tangential strain of 0.2% occurs in the vertical plane at the relatively sharp corner between the vertical wall and the invert. As expected, hardly any tangential strain is induced along the straight vertical portion of the cavern wall where the effect of the pressure is primarily in the horizontal direction.

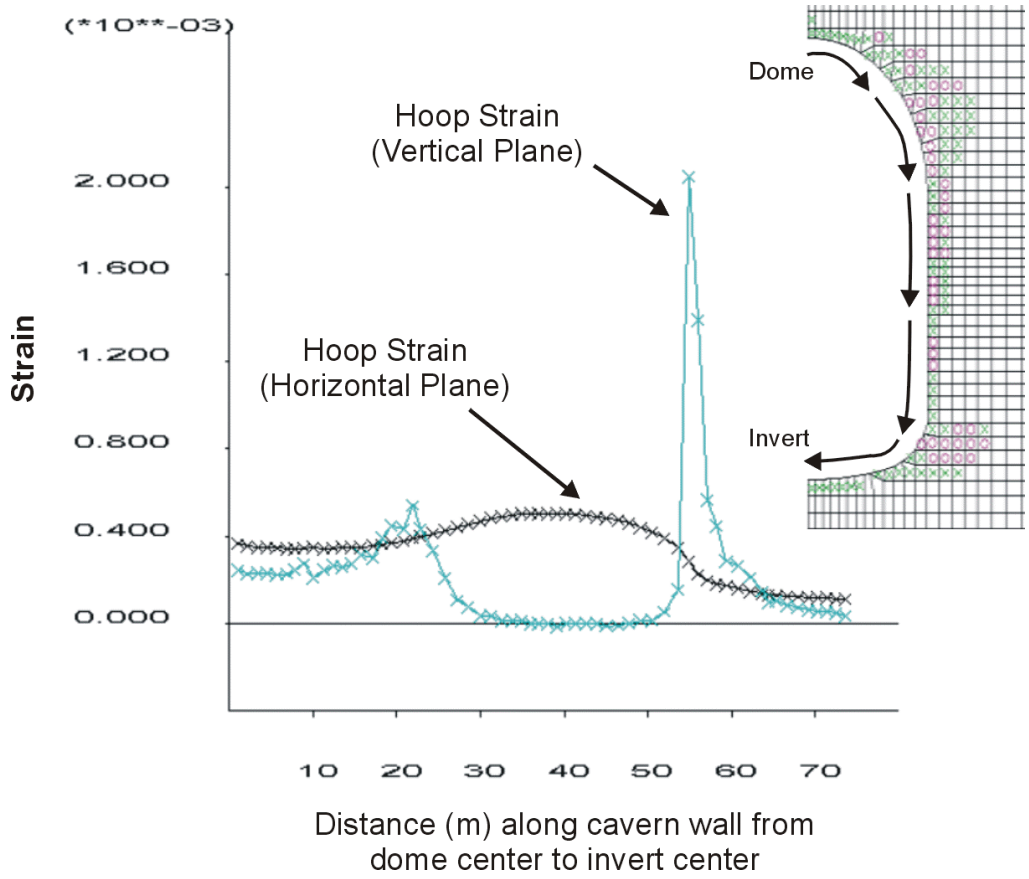

Figure 4-15 Predicted Vertical and Horizontal Tangential Strains Along the Cavern Wall

The predicted tangential strain in the horizontal plane of the axisymmetric model shows a maximum of 0.05% approximately at the mid-height of the wall, corresponding to a horizontal wall displacement of about 9 mm. These predictions can be compared to the results obtained previously in the plane-strain model for the conditions of isotropic in-situ horizontal stress, where the average strain was about 0.09% and the radial wall displacement 14 mm. Much of the difference between these results can be attributed to the conservatism associated with the plane-strain assumption in the model of the horizontal cavern section.

The results of these FLAC models of the response of the cavern wall generally fall well within the guidelines expressed by the LRC design criterion. However, the results rely on the assumption that the mechanical response of a naturally fractured rock mass can be represented by the smeared response of a continuum material. Rock blocks, particularly wedges, created by the intersection of the cavern with the natural rock fractures can effect local deformations of the cavern surface in ways that may be important to the structural integrity of the steel liner. Therefore, the use of continuum models in estimating the response of the LRC wall must be evaluated very carefully.

4.2.2 Independent Analysis of the Cavern Wall Using a Discontinuum Approach

All rock masses are more-or-less naturally fractured; hence, an important consideration when designing underground openings is the extent to which these fractures may influence the design. For openings in crystalline rock at shallow depths (i.e., < 500 m), such as an LRC, opening deformations and stability are primarily associated with the mechanics and kinematics of the interlocking blocks and wedges created by the natural fractures. The type of analysis to use in assessing the stability/deformations for these conditions generally depends on the block geometry and size relative to the size of the underground opening. Treating the rock mass as a continuum normally means that the blocky system responds in a homogeneous and isotropic manner, while explicitly including the natural fractures means that a distinction of relative block deformations can be made.

General guidelines (e.g., Hoek and Brown, 1980) exist for determining whether it is reasonable to represent the rock mass as a continuum or discontinuum. The keyword is *guideline*, and the choice of a continuum or discontinuum approach must be decided based on the specific conditions and intended purpose of the cavern. Of course, this requires that sufficient information exists about the site-specific nature of the natural fractures, which must come from local geophysical data. For LRC storage, the high gas pressure and shallow depth puts it in an unconventional category in terms of design load. The maximum cavern gas pressure is considerable, from 4 to 8 times that of the in-situ ground stresses. Maintaining the structural integrity of the thin steel liner for the design load is imperative to the LRC objective. This means that accurate assessment of the local cavern wall deformations is exceedingly important and strongly suggests that an evaluation of the wall response should include a discontinuum analysis.

A discontinuum approach, such as the distinct element method (Cundall, 1971), has become routine in the design analyses of underground openings, and it is applied in this review (in a simplified manner) as an example for conditions similar to the Skallen demonstrations plant. The two-dimensional Universal Distinct Element Code (Itasca, 1999) was used for this purpose. UDEC simulates the two-dimensional mechanics of an interlocked system of blocks of arbitrary shape and allows for individual block-to-block sliding, separation, and rotation.

In the context of the LRC, the discontinuum model is used to estimate the extent of fracture opening in the wall as a result of the high internal cavern pressure. It is also used to explore the formation and differential displacement of rock wedges in the wall. Both fracture opening and wedge displacement can result in high local strains in the steel liner.

To evaluate these effects, UDEC was applied to horizontal and vertical sections of the LRC. The conceptual models are shown in Figures 4-16(a) and (b). These are plane-strain models and are, therefore, conservative in terms of the predicted deformations. Note, however, that the only purpose in this case is to illustrate the qualitative aspects of a discontinuum analysis in the context of LRC conditions. When applied in a careful and detailed manner, discontinuum analyses can also provide a useful quantitative perspective

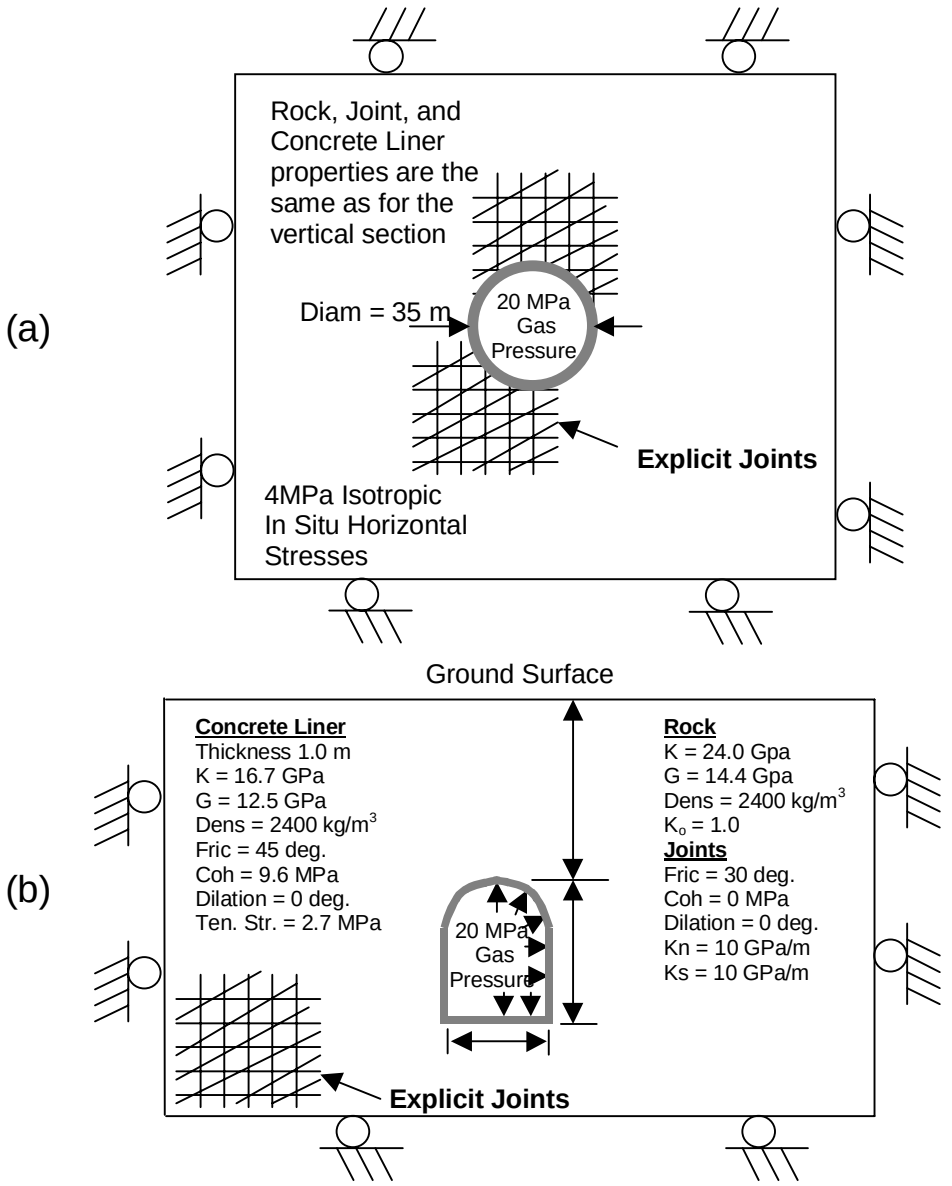

Figure 4-16 Conceptual UDEC Model of LRC conditions: (a) horizontal section; (b) vertical section

of fracture opening and relative shear displacement in the vicinity of the cavern wall. The steel liner was not included in these models, but the concrete liner was present and was simulated as an elasto-plastic material using a Mohr-Coulomb failure criterion. The model parameters used are listed in Table 4-4. The natural fractures have stiffness both in the normal and shear directions and shear strength characterized by an initial cohesion and constant friction coefficient. The rock blocks were taken to respond elastically.

Table 4-4 Parameters Used in the UDEC Model

Parameters	*Blocks*	*Joints*	*Concrete Liner*
Bulk Modulus (GPa)	24	—	16.7
Shear Modulus (GPa)	14.4	—	12.5
Normal Stiffness (GPa/m)	—	10	—
Shear Stiffness (GPa/m)	—	10	—
Friction Angle (degrees)	—	30	45
Dilation Angle (degrees)	—	0	0
Cohesion (MPa)	—	0	9.6
Tensile Strength (MPa)	—	0	2.7
Density (kg/m^3)	2400	—	2400

The horizontal section was analyzed only for conditions of isotropic in-situ horizontal stresses of 4 MPa; in the vertical section, $K_o = 2$ was used for the ratio of in-situ horizontal-to-vertical stress. The models were cut by an assumed system of natural fractures consisting of three separate sets, each with a different — but constant — orientation and fracture spacing. Fracture orientation and spacing could be assigned statistically or from detailed mapping, when such information is available. The effect of continuous and finite-length fractures was evaluated. Although natural fractures in crystalline rock can be persistent over considerable distances, they are rarely continuous.

Figure 4-17 shows results of the UDEC model for the vertical LRC section for the cases of continuous and finite-length fracture systems. The red-colored lines identify locations of relative shear displacements in the fracture systems. The thicker the line appears, the higher the shear displacement. It is apparent from these results that rock wedges develop and are being forced into the rock mass by the gas pressure. More important is the observation that the wedge itself consists of many smaller blocks, which could have been used initially to justify a continuum approach according to the general guidelines by, for example, Hoek and Brown (1980). Thus, this result points out the importance of including discontinuum analysis among the tools used in LRC design. Note that, even for less-organized fracture systems than those shown in Figure 4-17, the block kinematics can be such that significant rock wedges develop.

It should be emphasized that the pressure-induced rock wedge movements are inelastic, which precludes most of the movements from reversing upon cavern depressurization. This implies a cavern wall load-displacement response that is hysteretic, but with diminishing hysteresis during repeated cavern pressurization/depressurization cycles. The diminishing aspect of the hysteresis is important in estimating the maximum induced steel-liner strain, as the cyclic strain (i.e., strain range) potentially will be high only during the first few cavern pressure cycles.

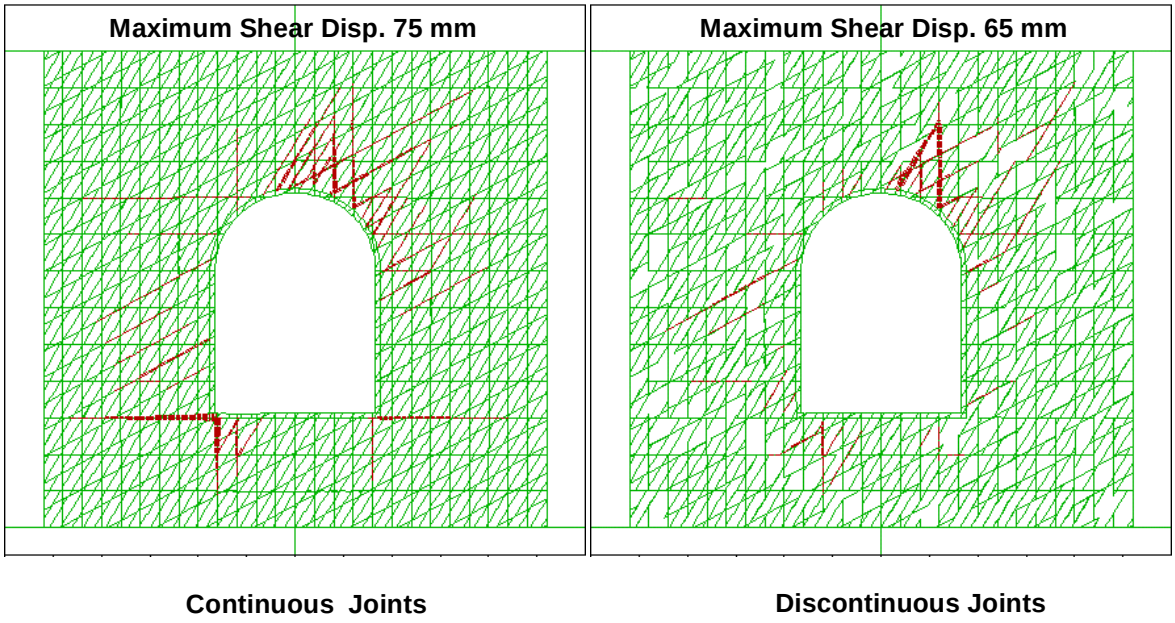

Figure 4-17 Formation of Rock Wedges in the Cavern Wall Identified by the Predicted Shear Displacements Along the Natural Rock Fractures (indicated in red) As a Result of Cavern Pressurization

In Figure 4-18, the prediction of fracture separation is shown in the same manner as for the previous shear displacements. Opening of rock fractures in the cavern wall occurs in the same general location as where the significant wedges formed. While the finite-length fractures tend to reduce wedge formations, it has a lesser effect on fracture opening and maximum wedge displacements.

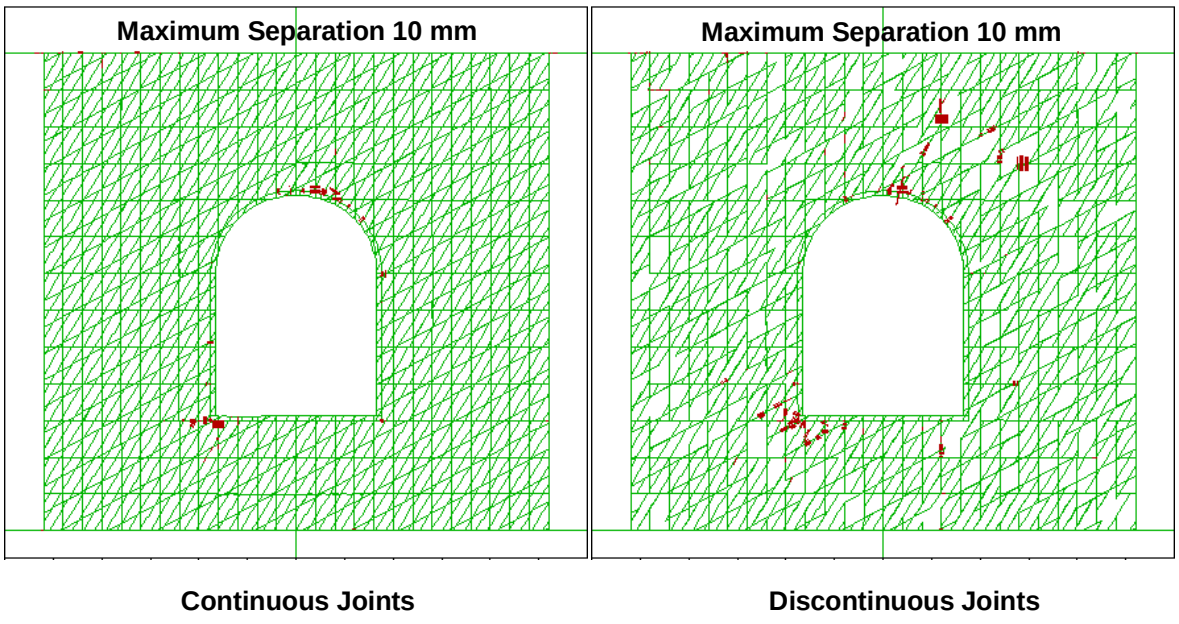

Figure 4-18 Predicted Separation (i.e., Opening) of the Natural Rock Fractures (indicated in red color) As a Result of Cavern Pressurization

Figure 4-19 illustrates the results of the UDEC model for the horizontal section in terms of cavern deformation, fracture shear displacement, and fracture separation. Although the in-situ horizontal stresses and material properties are isotropic, a non-uniform cavern displacement indicates anisotropic conditions. The apparent effect of anisotropy is a result of the fracture system and, more importantly, the fracture orientation — thus, it is an effect of material anisotropy. The direction of the largest wall displacement is indicated in Figure 4-19; it falls along the line of most wedge formation and fracture separation.

Note that the purpose of these UDEC models was not to predict accurate deformations of the cavern, but to illustrate qualitatively the richness of the rock mass response embedded in these models. At any given LRC site, rock wedges are likely to appear, and fracture separation will occur during cavern pressurization. Discontinuum analysis is an approach that considers the local aspect of these issues in the context of predicting the steel liner strain.

4.3 Concrete-Liner Fracture Analysis

The development of cracks in the reinforced concrete liner can be expected as a result of local deformations in the adjacent rock mass during cavern pressurization. An accurate evaluation of the size of these cracks is important to the prediction of the associated local strain in the steel liner. In this context, the review documents present, in some detail, an approach for analyzing induced fractures in the concrete liner. The approach uses a finite element model to predict the local crack development in the concrete as induced by the separation of a vertical fracture in the rock mass. The model characterizes the concrete as a Mohr-Coulomb material with a tension cut-off (i.e., finite tensile strength). Unless the tensile strength in each element of this model reflects the critical fracture toughness (or critical energy-release rate) of the reinforced concrete, the solution becomes mesh-dependent (Detournay et al., 2001). This can affect both the predicted crack separation and distribution.

In lieu of a more sophisticated fracture propagation analysis, the finite element approach described in the review documents should use a tensile strength that reflects the material toughness of the concrete liner. An example of the derivation of this tensile strength is provided in Appendix B.

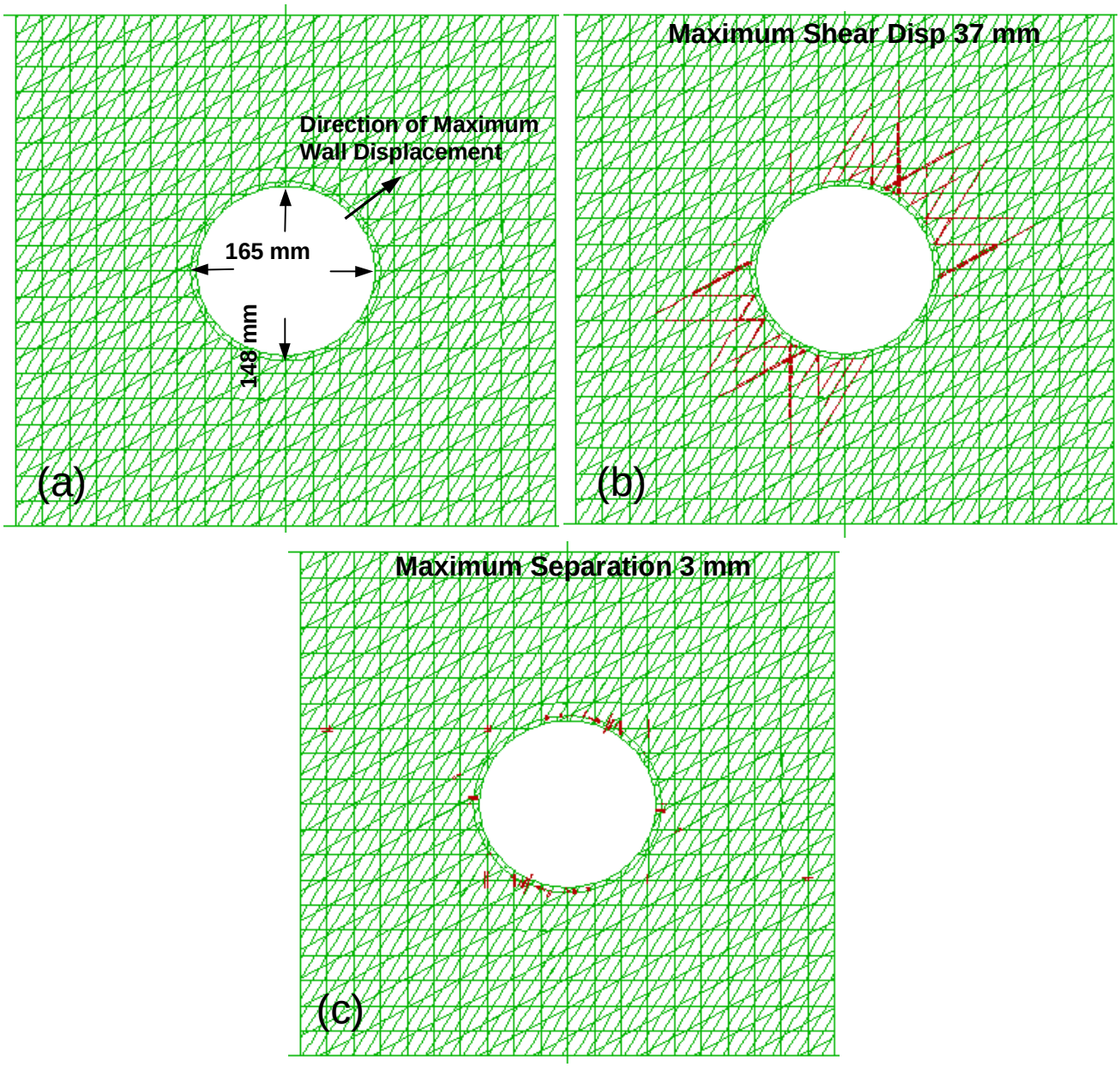

Figure 4-19 (a) Cavern Wall Displacements, (b) Predicted Shear Displacements, and (c) Separation (i.e., Opening) of the Natural Rock Fractures (indicated in red) As a Result of Cavern Pressurization

5.0 REVIEW OF THE LRC DESIGN METHODOLOGY

5.1 General Comments

A brief summary of the LRC design methodology was given in Section 3.3. In general, the review documents convey a methodology that seems to recognize the need for, and value of, a phased design approach that builds site-specific geophysical understanding through incremental site characterization and analysis. Also reflected in the methodology is the use of the Observational Approach during cavern excavation to treat unexpected conditions that may require changes to the final LRC design. Thus, the methodology shows recognition of the unique and uncertain characteristics of a rock mass. This is further reflected, in a seemingly disciplined manner, through the use of a probabilistic design approach.

Two key LRC design criteria are expressed in the review documents: (1) safety against ground uplift; and (2) maximum induced strain range in the steel liner. Both criteria, which are closely tied to the mechanical response of the rock mass, address the essential LRC design aspect of limiting the strain induced in the steel liner — that is, the rock mass overburden must be sufficient to provide effective resistance to the maximum cavern pressure.

The LRC design methodology oversimplifies the evaluation of ground uplift by its use of the rigid-cone and log-spiral limit-equilibrium models. Independent calculations using a numerical model (refer to Sections 4.1.2 and 4.1.3) show that the soil-anchor analogy used in the development of the rigid-cone and log-spiral models is not well-suited to describe the more complex loading and material response of LRC conditions. Both the rigid-cone and log-spiral models are exceedingly conservative, primarily because they oversimplify the mechanistic aspects of ground uplift associated with a pressurized, lined rock cavern. While uplift response can be evaluated mechanistically with relative ease using a numerical model, there seems to be an objection in the review documents to using a numerical model for this purpose. The documents suggest that such models are unable to provide a reliability measure and have difficulties in handling large deformations. For most available finite-element or finite-difference numerical codes in rock mechanics (e.g., FLAC, in these analyses), neither of these arguments is accurate.

The two key LRC design criteria mentioned are central to the FLRC1 and FLRC2 models used as part of the design methodology to evaluate the feasibility and the design of lined rock caverns. These models represent streamlined calculation procedures that rely on rock index properties and empirical relations to estimate the rock-mass mechanical properties (i.e., stiffness and strength), and limit-equilibrium, finite-element and analytical (homogeneous and isotropic) models to estimate cavern location (i.e., depth), maximum gas pressure, cavern deformations, and steel-liner strain. Thus, these models represent knowledge-based expert systems for LRC siting and design.

The simplification in material response and rock mass conditions reflected in the FLRC1 and FLRC2 models is in contrast to what, elsewhere in the review documents, seems to be recognition that each rock mass is a unique material with uncertain characteristics. Most notably, these models do not account for possible local effects associated with the explicit nature of a naturally fractured rock mass. In most strong igneous and metamorphic rocks like dolerites, basalts, granites, gneisses and quartzites, the stability of caverns of LRC size and depth (about 200 m) will depend almost entirely upon structurally controlled rock wedges and blocks exposed as a result of the cavern excavation. While, arguably, such stability can sometimes be evaluated using the average rock-mass response accounted for in the FLRC1 and FLRC2 models, the requirement to limit the steel-liner strain will most certainly depend on the local rock-mass response at the cavern wall. However, by definition, average rock-mass conditions cannot differentiate such a local response. Independent calculations using average rock-mass conditions (in the continuum FLAC model) and accounting for explicit, natural rock fractures (in the distinct element model, UDEC) illustrate the possibility of local effects along the cavern wall from fracture separation and shear (associated with rock wedge or block deformations). With a distinct element approach, the effect of realistic fracture patterns on the cavern-wall response can be incorporated and analyzed. Depending on the conditions, the local steel-liner strain range could be found to exceed 0.34% (i.e., twice the yield limit) using these models, which potentially would affect the fatigue life of the liner. It is important, therefore, to gather information during site characterization that describes the natural rock fractures (dip, strike, roughness, weathering, alteration, etc.) and to investigate the characteristic fracture stiffness and strength through laboratory testing. Careful use of this and other site information in distinct element models can warn of possible local problems in cavern-wall/steel-liner response. Detailed fracture mapping, which is possible during cavern excavation, should be considered for use in distinct element models to provide additional assurance of adequate design.

The review documents presenting experimental results from the Grängesberg Test Plant show that separation and differential slip along fractures occur as a result of cavern pressurization. Although it is encouraging that rock fracture deformations did not cause structural difficulties with the steel liner in this case, it must be noted that this observation cannot be extrapolated to other sites, where rock mass conditions will be different. Rock masses are unique and uncertain in their characteristics, and they must be evaluated on this premise. Because the current LRC design methodology is based on an integrated procedure of relatively simple analyses contained in the FLRC1 and FLRC2 models, it is important that the methodology also includes the use of detailed numerical models for the purpose of confirming the adequacy of the design. The detailed analyses should be conducted at various stages in the design process using both continuum and discontinuum 2D and 3D numerical models as appropriate.

The LRC design methodology as presented by the review documents applies to the conditions for which a single cavern is designed. However, an LRC facility may contain multiple caverns. If overlapping effects are expected between caverns, the LRC design methodology must be used with great caution. In this case, the design should rely on detailed numerical models that can account for cavern interactions.

The methodology does not consider the possibility or the effects of seismic load. The possibility of significant seismic load is great in many parts of the world and should be considered in the LRC design methodology. Statistically realistic seismic records can be determined (e.g., from an equal-probability seismic hazard spectrum). When such records are used in detailed 3D numerical models, the response of the operating LRC can be evaluated for the dynamic load associated with a possible earthquake.

From the review documents, it appears that much was learned about the basic rock mass response from the Grängesberg small-scale experiment. However, the scale of the experiment was too small to serve as proof-of-concept. Operation of the large-scale Skallen demonstration plant, currently being constructed, will be very important in this context. While the need for refinement of the design methodology have been pointed out, the extensive experimental efforts behind the methodology (i.e., the small-scale Grängesberg test and, currently, the large-scale Skallen demonstration plant) are extremely encouraging and provide real understanding that no amount of numerical modeling alone can contribute.

5.2 Probabilistic Design Approach

All rock masses are inherently heterogeneous in their mechanical characteristics, and this attribute is a substantial reason behind the challenges of building stable structures in rock. Traditionally, uncertainties in a rock mass response are treated by conducting systematic design analyses — e.g., analyzing detailed deterministic numerical models for a range in conditions and rock mass properties. Such ranges are often estimated from experience using sparse data of lithology, rock structure, in-situ stress, and basic rock-mass index properties, and would represent a maximum credible range. When analyzed for a set of lower-bound properties and conditions, the results must indicate, as a minimum, a barely adequate design. If little inelastic response is expected, measurements of rock mass deformations during excavation can be used to verify initial estimates of rock mass stiffness. Detailed numerical models are used for this purpose in so-called “back-analyses”, where the rock mass stiffness is adjusted to match the measured deformations. In combination with careful observations during construction, the traditional approach generally leads to the design of stable and economical underground structures.

The LRC design methodology uses a probabilistic approach. The use of such an approach in rock engineering in the United States is not common. While there may be many reasons for this, they are not necessarily all good— for example, the unfamiliar concept among many rock engineers of the probability of failure, or even accepting failure. The many choices of methods include Monte Carlo simulation, Latin Hypercube sampling technique (Iman et al., 1980), Fast Probability Integration method (e.g., Wirsching and Wu, 1987), First-Order Second-Moment methods (e.g., Ang and Tang, 1975), Point Estimate method (Rosenblueth, 1981). The differences between these methods can make the topic confusing. More legitimate reasons are supported by the often-sparse geophysical data available to the rock engineer, which hardly justifies a probabilistic design approach.

The probabilistic approach in the LRC design methodology is imbedded in the FLRC1 and FLRC2 models, which make use of Monte Carlo simulations to generate, for example, a probabilistic distribution of rock-mass strength properties from a distribution of rock index properties. Subsequently, a probabilistic distribution of steel-liner strain is generated from simple models that use the stochastic input of rock mass properties and conditions. The Monte Carlo method requires the entire probability density function of each independent variable to be known initially. This is seldom the case. If assumed functions are used, as the review documents indicate, the outcome (e.g., rock mass properties or steel-liner strain) will be affected by the assumption!

One positive aspect of a probabilistic approach is that it provides an organized and disciplined way of considering uncertainty (e.g., in the basic rock-mass properties) and its affect on the response (e.g., steel-liner strain). However, in cases of sparse geophysical data, it does not necessarily lead to a technically better or more economical design than that obtained from traditional methods.

A reasonable check of the probabilistic prediction would be to perform a detailed design analysis using a deterministic numerical model for credible lower-bound rock-mass properties and conditions. The minimum acceptable result of this check would be a barely adequate design.

6.0 CONCLUSIONS

The rock mechanics review of the Lined Rock-Cavern Storage Concept and Design Methodology has focused on the feasibility of this technology, and the robustness of its design methodology. The standard of the review has been the demonstrated principles of designing large stable underground openings in rock. The conclusions that follow are based on the design methodology's adherence to these principles.

6.1 Summary and Observations of the Rock Mechanics Review

With some noted exceptions, the review documents convey the implementation of the LRC concept as a carefully planned incremental design procedure. The procedure is implemented in the two models FLRC1 and FLRC2, which use empirical relations and isotropic and homogeneous analytical models to express the basic rock-mass conditions, properties, and average mechanical response. Integrated with a probabilistic design approach, the results of these models is a probabilistic distribution of the worst-point steel-liner response in terms of maximum strain and cyclic strain range.

Independent analyses of the concept were conducted using continuum and discontinuum numerical models. These models show that a soil-anchor analogy, which is embedded in limit equilibrium models for evaluating ground uplift, greatly oversimplifies the conditions of potential uplift. The analogy and the LE models may not be well-suited to describe the relatively complex rock-mass response from a pressurized LRC. Continuum

numerical models used to evaluate the cavern-wall response and steel-liner strain for the Skallen LRC demonstration plant show results in reasonable agreement with the those expressed in the review documents using the LRC design methodology. However, the steel-liner response may be affected by the local rock-mass conditions in the vicinity of the cavern wall. This local response results from intersecting fractures occurring naturally in rock masses, creating rock wedges in the cavern wall. Thus, treating the rock mass as a continuum can oversimplify the rock mass response and potentially underestimate the steel-liner strain.

While the use of somewhat simple design analyses may be reasonable, it suggests that confirmation of the design adequacy be made at various intervals in the design process using detailed numerical models, both continuum and discontinuum, for two- and three-dimensional conditions, as appropriate. Although numerical models have been used throughout the development of the LRC design methodology, the methodology does not specify that such models be used in a design-confirmation context during the design process. This is a significant concern. However, the problem can be remedied easily by conducting detailed design evaluations at suitable intervals. Because these are independent, detailed, numerical-model evaluations, they are conducted apart from the design analyses and probabilistic procedures of the FLRC1 and FLRC2 models and, therefore, will not complicate these procedures.

The review found the finite element model of the fracture evaluation of the concrete liner to use a no-tension fracture propagation criterion. It is noted that fracture propagation depends on the material toughness (or critical energy-release rate). Unless the tensile strength of the concrete is calibrated to the toughness and the element size used in the analysis, the fracture predictions using this approach would not be appropriate. In lieu of a more sophisticated fracture mechanics analysis, the current method should use consistent values of tensile strength and fracture toughness. An example derivation of consistent values of tensile strength and material toughness is provided in Appendix B.

The LRC design methodology should be used with caution when multiple caverns are involved that have overlapping influence. In this case, detailed design evaluations will be necessary using numerical models.

The effect of seismic loads is not considered in the LRC design methodology. The potential for seismic loads should be included. The effect of such loads would require detailed evaluations using numerical models.

6.2 Judgement of the LRC Concept

The judgement of the overall LRC concept is based on the content of the review documents, the independent calculations presented, and the past development and performance of existing large underground caverns. The LRC attributes of concern are (1) cavern size, (2) cavern geometry, and (3) cavern loading.

6.2.1 Cavern Size

Although constructability issues were not part of this review, the size of the caverns necessary for LRC is not unprecedented in the development of underground openings in crystalline rock. Hamrin (1986) reports the construction of a cavern for radioactive-waste disposal that is of comparable size and shape to an LRC. Examples of very large and complex underground caverns can also be found in the development of hydroelectric power plants (e.g., Dasgupta and Sharma, 1999), hydrocarbon storage facilities (e.g., Høsøien, 1986) and civil projects such as sports arenas (e.g., Rygh, 1986, Barton et al., 1991).

6.2.2 Cavern Geometry

In relative terms, the LRC geometry can be considered simple. The domed vertical cylinder with a rounded invert is an inherently stable shape with respect to gravity loading and the in-situ horizontal stresses in the rock mass. Compared, for example, to the system of caverns in a hydroelectric power complex, the compact geometry of the LRC provides higher flexibility in placing the cavern at an optimum location for construction and operation stability.

6.2.3 Cavern Loading

When developing underground openings for civil or mining purposes, in the vast majority of cases, the concern is to maintain stability of the surrounding rock mass as it is being loaded by gravity and the in-situ rock mass stresses (i.e., the service load). Relatively large displacements in the rock mass are generally acceptable as long as the final opening remains stable.

While, obviously, the LRC must remain stable for the purpose of construction, it differs somewhat from the conventional use of large caverns by its service load (i.e., the gas pressure) and the need to minimize the tensile strain in the thin steel liner. While pressurized caverns exist (e.g., compressed-air energy storage, surge chambers associated with hydroelectric power plants), the level of the pressure relative to the rock-mass in-situ stress conditions is unique for LRC (higher by a factor of about 4 to 8). As a result, any inward deformations (elastic and plastic) of the rock mass during construction will be reversed upon cavern pressurization. The average amount of deformation associated with the cavern pressurization depends on the stiffness and the strength of the rock mass, as well as the cavern geometry (its height-to-diameter ratio and amount of roof and invert curvature). Rock-mass structural features (i.e., natural fractures) will affect the local deformations of the cavern wall and, therefore, the steel-liner strains.

6.2.4 Judgement

The successful development of the LRC concept will depend on a careful and flexible approach that incorporates established rock-mechanics principles to achieve a balanced union between a good understanding of the rock mass conditions and the mechanical response, the possible cavern size, and the maximum gas pressure. With some noted exceptions, it appears that the LRC design methodology reflects this type of approach. Central to the approach must be a thorough evaluation of the natural rock-mass structure (i.e., pre-existing fracture sets and major discontinuities, such as faults, shear zones, and weak areas of the rock), including the effects this structure might have on cavern-wall deformations. Such approaches are advocated and commonly used in the design and development of underground facilities. When considering the vast experience that already exists in large cavern development, it is reasonable to expect that stable, lined rock caverns can be constructed. With the use of a careful development approach that relies not only on continuum models, which treat the rock mass response in an average sense, but which also use models that include the discontinuum nature of rock masses, it is also reasonable to expect that an LRC can be built to maintain operation for the levels of pressures indicated in the review documents.

6.3 Recommendations

This rock mechanics review of the LRC design methodology shows that adopting the following recommendations can strengthen the current methodology.

- In lieu of a more sophisticated fracture-mechanics evaluation of the concrete liner, the current finite-element fracture model should use a tensile strength that is consistent with the fracture toughness.
- The LRC design methodology should include the use of detailed numerical models (2D, 3D, continuum and discontinuum, as appropriate) at certain stages in the LRC design process to verify the adequacy of the design provided by the relatively simple analysis procedures in the FLRC1 and FLRC2 models.
- The LRC design methodology should emphasize that its purpose is to guide the design of a single cavern. In a multiple-cavern LRC complex, potential overlapping cavern effects must be analyzed with the use of detailed three-dimensional numerical models.
- The LRC design methodology should include a seismic potential evaluation. If significant potential exists, the LRC design methodology should include an evaluation of the dynamic loads from a statistically realistic seismic event using a detailed numerical model.

- The LRC design methodology should include a verification of its probabilistic approach by evaluating the design for a set of credible lower-bound conditions using a detailed numerical model. The minimum result of the model should be a barely acceptable design.

These recommendations are associated primarily with verification of the design adequacy using detailed numerical models, and are a result of the somewhat simple design analysis methods used in the current methodology. The recommendations do not directly involve the design procedure implemented in the FLRC1 and FLRC2 models. Therefore, these recommendations can be implemented easily in the current LRC design methodology and would strengthen this methodology.

7.0 REFERENCES

Ang, A. H.-S., and W. H. Tang. (1975) ***Probability Concepts in Engineering Planning and Design***, Vol. 1, Basic Principles. New York: John Wiley & Sons.

Barton, N., L. Tunbridge, F. Løset, H. Westerdahl, J. Kristiansen, G. Vik and P. Chryssanthakis. (1991) "Norwegian Olympic Ice Hockey Cavern of 60 m Span," in ***Proceedings of the 7th International Congress on Rock Mechanics (Aachen, Germany, September 1991)***, Vol. 2, pp. 1073-1081. Rotterdam: A. A. Balkema.

Bishop, A. W. (1955) "The Use of the Slip Circle in the Stability Analysis of Slopes," *Géotechnique*, ***5***(1), 7-17.

Brady, B.H.G., and E. T. Brown. (1993) ***Rock Mechanics for Underground Mining***, 2nd Ed. London: Chapman & Hall.

Cundall, P. A. (1971) "A Computer Model for Simulating Progressive Large Scale Movements in Blocky Rock Systems," in ***Proceedings of the Symposium of the International Society for Rock Mechanics (Nancy, France, 1971)***, Vol. 1, Paper No. II-8.

Dasgupta, B., and V. M. Sharma. (1999) "Numerical Modelling of Underground Power Houses in India," in ***Distinct Element Modeling in Geomechanics***, pp. 187-217. V. M. Sharma et al., Eds. New Delhi, Oxford & IBH Publishing Co.

Detournay, E., H. Huang and B. Damjanac. (2001) "Material Scaling Laws for a Discrete Particle Assembly," submitted for publication to *Mechanics of Materials*.

Donald, I. B., and S. K. Giam. (1988) "Application of the Nodal Displacement Method to Slope Stability Analysis," in ***Proceedings of the Fifth Australia-New Zealand Conference on Geomechanics (Sydney)***, pp. 456-460.

Ghaly, A., and A. Hanna. (1994) "Ultimate Pullout Resistance of Single Vertical Anchors," *Can. Geotech. J.*, ***31***, 661-672.

Goodman, R. E. (1980) ***Introduction to Rock Mechanics***. New York: John Wiley & Sons.

Hamrin, H. (1986) "Experiences from Excavation of Large Rock Caverns for Storage of Nuclear Waste," in ***Large Rock Caverns (Proceedings of the International Symposium, Helsinki, August 1986)***, Vol. 2, pp. 1481-1488. K. Saari, K., Ed. London: Pergamon Press, 1986.

Harrison, J. P., and J. A. Hudson. (2000) ***Engineering Rock Mechanics: Part 2, Illustrative Worked Example***. Oxford: Elsevier Science Ltd.

Hoek, E., and J. W. Bray. (1977) ***Rock Slope Engineering***, Revised 2nd Ed. London: IMM Publications, 1977.

Hoek, E., and E. T. Brown. (1980) ***Underground Excavations in Rock***. London: The Institution of Mining and Metallurgy.

Høsøien, N. (1986**)** "Crude Oil Caverns at Mongstad, Norway," in ***Large Rock Caverns (Proceedings of the International Symposium, Helsinki, August 1986)***, Vol. 1, pp. 109-120. K. Saari, K., Ed. London: Pergamon Press, 1986.

Hudson, J. A., and J. P. Harrison. (1997) ***Engineering Rock Mechanics: An Introduction to the Principles***. Oxford: Elsevier Science Ltd.

Iman,, R. L., J. M. Davenport and D. K. Zeigler. (1980) ***Latin Hypercube Sampling (A Program User's Guide)***. Sandia National Laboratories, Technical Report, SAND79-1473.

Itasca Consulting Group, Inc. (1999) ***UDEC (Universal Distinct Element Code)***, Version 3.1. Minneapolis: ICG.

Itasca Consulting Group, Inc. (2000) ***FLAC (Fast Lagrangian Analysis of Continua)***, Version 4.0. Minneapolis: ICG.

Johansson, J., R. Sturk and H. Stille. (1994) "Storage of Gas in Shallow Rock Caverns — Conclusions Based on Results from the Grängesberg Test Plant," Czech Gas and Oil Association, September 14.

Larsson, H., R. Glamheden and G. Ahrling. (1989) "Storage of Natural Gas at High Pressure in Lined Rock Caverns — Rock Mechanics Analysis," in ***Storage of Gases in Rock Caverns***, pp. 177-184. Rotterdam: A. A. Balkema.

Littlejohn, G. S., and D. A. Bruce. (1975) "Rock Anchors — State of the Art, Part 1: Design (1)," *Ground Eng.*, ***8***(3), 25-32 (1975); "Rock Anchors — State of the Art, Part 1: Design (2)," *Ground Eng.*, ***8***(4), 41-48 (1975).

Mahtab, M. A., and P. Grasso. (1992) ***Geomechanics Principles in the Design of Tunnels and Caverns in Rock***, Developments in Geotechnical Engineering, 72. Amsterdam: Elsevier Science.

Mandl, G. (1988) ***Mechanics of Tectonic Faulting, Models and Basic Concepts***, Developments in Structural Geology, 1. Amsterdam: Elsevier Science.

Matsui, T., and K. C. San. (1992) "Finite Element Slope Stability Analysis by Shear Strength Reduction Technique," *Soils & Found.*, ***32***(1), 59-70.

Mueller, B., J. Reinecker, O. Heidbach and K. Fuchs. (2000) ***The 2000 Release of the World Stress Map.*** The World Stress Map Project — A Service For Earth System Management, A Research Group of the Heidelberg Academy of Sciences and Humanities. http://www-wsm.physik.uni-karlsruhe.de/pub/images/headline2.gif

Naylor, D. J. (1982) "Finite Elements and Slope Stability," in ***Proceedings of the Conference on Numerical Methods in Geomechanics (NATO Advanced Study Institute, Lisbon, Portugal, 1981)***, pp. 229-244.

Rosenblueth, E. (1981) "Two-Point Estimates in Probabilities," *J. Appl. Math. Modelling*, ***5***, 329-335 (October).

Rygh, J. A. (1986) "Holmlia Sporthall and Swimming Pool in Rock Planning, Construction, Use," in ***Large Rock Caverns (Proceedings of the International Symposium, Helsinki, August 1986)***, Vol. 1, 219-230. K. Saari, K., Ed. London: Pergamon Press.

Stagg, K. G., and O. C. Zienkiewicz. (1968) ***Rock Mechanics in Engineering Practice***. London: John Wiley & Sons.

Stille, H., J. Johansson and R. Sturk. (1994) "High Pressure Storage of Gas in Lined Shallow Rock Caverns — Results from Field Tests," in ***Rock Mechanics in Petroleum Engineering (Proceedings of EUROCK 94***. H. Roest and C. Kenter, Eds. Rotterdam: A. A. Balkema.

Sturk, R., J. Johansson, L. Olsson and H. Stille. (1996) "Probabilistic Rock Mass Characterization and Deformation Analysis," in *Prediction and Performance in Rock Mechanics & Rock Engineering (Proceedings of ISRM International Symposium EUROCK '96, Turin, September 1996)*, Vol. 1, pp. 319-325. Barla, Ed. Rotterdam: A. A. Balkema, 1996.

Tengborg, P. (1989) "Storage of Natural Gas in Lined Rock Caverns — Studies for a Future Project in Southern Sweden," in ***Storage of Gasses in Rock Caverns***, pp. 151-157. Rotterdam: A. A. Balkema.

U.S. Department of Energy (USDOE). (2000) ***Advanced Gas Storage Concepts: Technologies for the Future***. Morgantown, West Virginia: National Technology Laboratory, 2000.

Ugai, K. (1989) "A Method of Calculation of Total Factor of Safety of Slopes by Elasto-Plastic FEM (in Japanese)," *Soils & Found*, ***29***(2), 190-195.

Ugai, K., and D. Leshchinsky. (1995) "Three-Dimensional Limit Equilibrium and Finite Element Analyses: A Comparison of Results," *Soils & Found.*, ***35***(4), 1-7.

Vesi• , A. S. (1971) "Breakout Resistance of Objects Embedded in Ocean Bottom," *J. Soil Mech. & Fdn. Div., Proc. ASCE*, ***98***(SM9), 1183-1205.

Wirsching, P. H., and Y.-T. Wu. (1987) "Advanced Reliability Methods for Structural Evaluation," *J. Engr. Ind.*, ***109***, 19-23.

Zienkiewicz, O.C., C. Humpheson and R. W. Lewis. (1975) "Associated and Non-Associated Visco-Plasticity and Plasticity in Soil Mechanics," *Géotechnique*, ***25***(4), 671-689.

Appendix A

Selected LRC Review Documents

Appendix A

Selected LRC Review Documents

Storage of gas in shallow rock caverns - Conclusions based on results from the Grängesberg test plant

STORAGE OF GAS IN LINED SHALLOW ROCK CAVERNS - CONCLUSIONS BASED ON RESULTS FROM THE GRÄNGESBERG TEST PLANT

Jan Johansson
Naturgasteknik AB, Stockholm, Sweden

Robert Sturk
Skanska Teknik AB/Royal Institute of Technology, Stockholm, Sweden

Håkan Stille
Royal Institute of Technology, Stockholm, Sweden

1 THE CONCEPT OF LINED ROCK CAVERNS FOR GAS STORAGE

1.1 Background

Rock caverns has during several decades been used as storage facilities for a wide range of products. In Scandinavia a large amount of unlined oil storage facilities were built during the 60s and 70s. Some unlined storages for gas have also been constructed. The internal pressure in these storages has not exceeded 1 MPa. The main principle of the storage concepts used hitherto is to let the ground water confine the stored products by using the natural ground water pressure or water curtains.

Internationally, however, a large number of gas storages operated with high pressure exist. These storages, for example depleted or operating oil and gas fields, aquifers and salt caverns, are restricted to areas with geological conditions and formations unavailable in Sweden where proterozoic basement rock is dominating.

As alternatives to the traditional high pressure storages were needed in Scandinavia, two concepts have been subjected to practical and theoretical studies, lined shallow storages and water tightened storages at large depths (for example Calminder & Hahn 1982 and Lindblom 1986).

This paper describes the present status of the lined rock cavern gas storage concept, based on the comprehensive test results from Grängesberg.

1.2 Concept Principles

In short, the lined rock cavern concept, also shown in Figure 1, is based on the interaction between the following elements:

- an impermeable lining, with no pressure absorbing function, enclosing the gas in the cavern.
- a concrete layer, serving as a base for the lining, to transfer the pressure forces to the rock and to distribute and absorb the deformation.
- the surrounding rock mass, absorbing the pressure forces and thus acting as the pressure vessel.
- a drainage system, taking care of groundwater inflow as well as potential gas leakages.

It should be noted that the groundwater pressure has no influence on the storage concept in respect of pressure levels and gas containment. The gas sealing is done by the liner only.

A lined gas storage must fulfil two general criteria related to the ability of absorbing the pressure forces:

1. The rock cover above the facility must provide sufficient resistance against up-lift.
2. The deformations in the rock mass and the concrete layer must be limited so that the deformation capacity of the liner is not exceeded.

The main objective with the research work carried out within the field of lined gas storages is to determine whether these demands can be fulfilled or not.

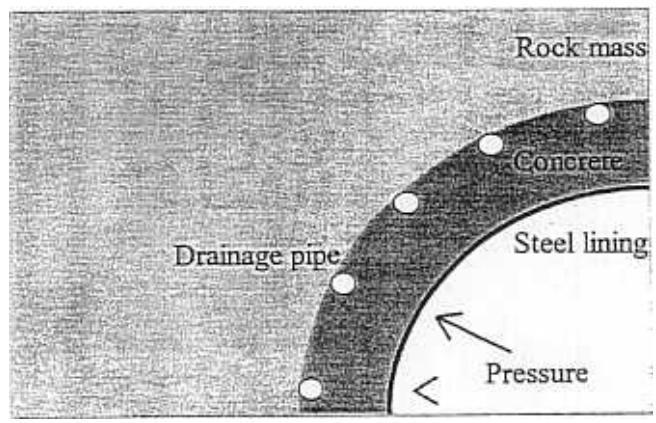

Figure 1. Horizontal section of the lined rock cavern concept.

1.3 Technical and Economical Advantages

When comparing the concept of lined shallow rock caverns with the traditional gas storages concepts (depleted reservoirs, aquifers and salt caverns) and water tightened unlined caverns at large depths, several technical and economical advantages can be identified (Särkkä, 1994). The main advantage is the flexibility that characterise the lined concept. The parameters that influence the total economy for a storage project, for example pressure, temperature and geometry, may to a large extent be varied.

The technical flexibility, i.e. the possibility to construct and locate lined storages of different sizes in a wide range of geological environments, is important mainly considering the possibility to satisfy the regional and local storage demands. Storage facilities of desired volume and capacity may be constructed close to distribution nets and gas customers. A lined storage is suitable both to cover seasonal load balancing and daily or weekly peak demands. The shallow location also implies short construction time.

Another important advantage with lined storages is that the gas is fully contained, thus never coming in contact with water or rock/soil. This implies that contamination of the stored gas is avoided and special treatment before distribution to the net is not needed. As the gas is dry and clean and the storage is structurally stable, the withdrawal rate might be held at a high level determined only on an economic basis. Furthermore, practically the whole stored volume can be utilised as working gas and no cushion gas is needed.

2 THE GRÄNGESBERG TEST PLANT

To increase the knowledge about the concept a pilot plant was constructed during 1988. The project started as a joint venture including a number of Scandinavian companies interested in developing new techniques for storing natural gas. The pilot plant is located in Grängesberg in central Sweden 250 km west of Stockholm and comprises three test rooms.

Outlines of the concept and the objectives of the pilot tests have previously been presented by Lindbo et al. 1989 and Tengborg 1989. Results from the tests have previously been presented by Isander 1994 and Stille et al. 1994.

2.1 Geological conditions

The predominant type of rock in the area is a medium-grained granite (Uniaxial Compressive Strength = 340 MPa and Young's modulus = 56 GPa). An 8-9 m thick metabasite dyke traverses the granite in the area in which the pilot plant is located. One contact zone (width 0,5 m) is altered and forms a weakness zone in the rock mass.

The initial stresses of the granite are low according to the rock stress measurements, i.e. 1-4 MPa. The largest horizontal stress has a mean value of 2.5 MPa and a north-west orientation. The smallest horizontal stress has a mean value of 1.3 MPa. The mean value of the vertical stress is 1.4 MPa.

A classification of the rock mass was done using both the Q method and the RMR method. The mechanical properties of the rock mass, the deformation modulus and the compressive strength, were evaluated based on RMR and Q values and results from laboratory tests. The values of the above parameters are shown in Table 1.

Table 1. Rock mass properties.

Rock mass section	RMR value	Q value	Young's modulus (GPa)	Compressive strength (MPa)
Granite	75	20	30	9
Metabasite	80	22	40	15
Weakness zone	52	8	2	5

2.2 Design of the test rooms

The three test rooms are excavated as vertical cylinders, the principle layout is shown in Figure 2. The rooms are lined on the inside with concrete and steel. The rock overburden above the rooms is 50 m.

Room 1 was designed specifically for the purpose of testing a 0.4 mm thick lining of austenitic stainless steel (SS 2343). The concrete lining is about 0.4 m thick (the measured uniaxial compressive strength after 28 days was approximately 45 MPa) and conventionally reinforced (Ø10-c150mm in a square pattern, yield point 590 MPa minimum).

Room 2 is equipped with a lining of 6 mm plates of micro-alloyed steel (yield point 350 MPa minimum). The concrete lining is about 0.6 m thick (the measured uniaxial compressive strength after 28 days was approximately 39 MPa) and unreinforced.

Room 3 has a 0.5 mm thick lining of stainless steel. The concrete lining is 0.3 m thick (the measured uniaxial compressive strength after 28 days was approximately 36 MPa) and conventionally

reinforced (Ø16-c150mm in a square pattern, yield point 590 MPa minimum).

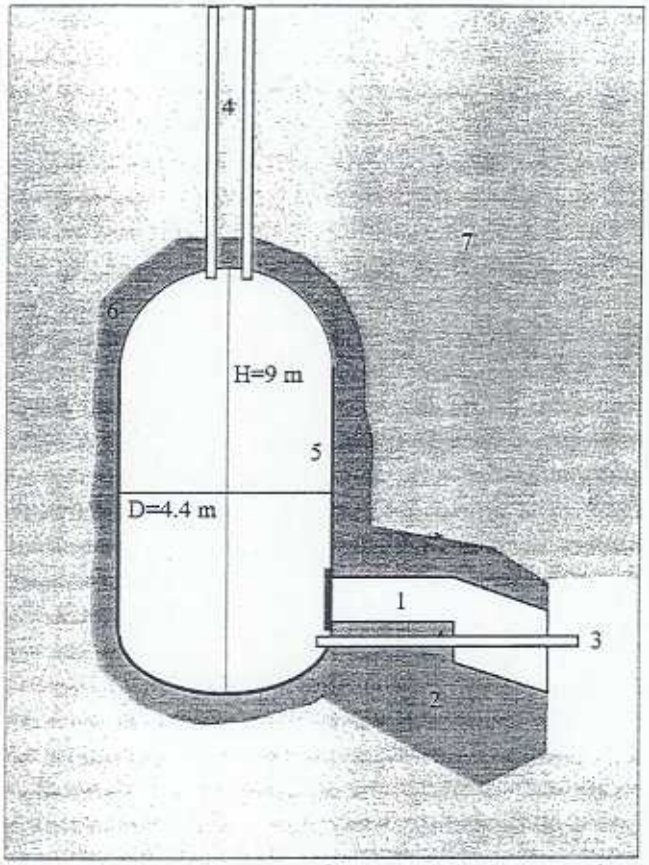

Figure 2. General layout of Room 2. 1. Access tube, 2. Concrete plug, 3. Water fill, 4. Gas fill, 5. Steel lining (6 mm), 6. Concrete lining (0.6 m), 7. Rock mass.

2.3 Monitoring system

The radial expansion of the rooms and the deformations in the rock and concrete are continuously registered during pressure testing. Extra measuring devices are installed in the rock in Room 3 for the purpose of studying the movements in the nearby weakness zone. Strains in the steel lining in Room 2 have also been measured continually.

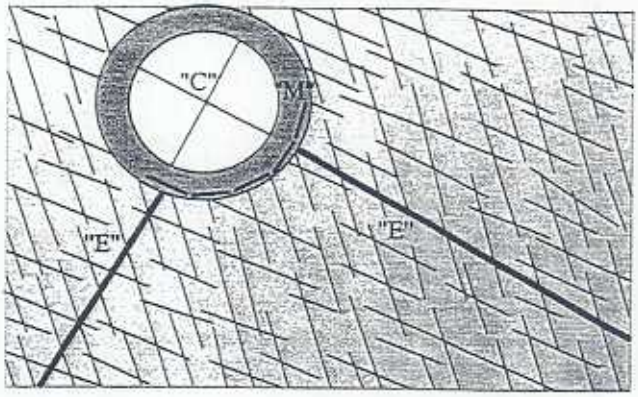

Figure 3. Measuring installations in the test rooms, schematic horizontal section.

The radial rock mass deformations are measured by multiple extensometers, labelled "E" in Figure 3. Mini-extensometers "M" are installed in the concrete to measure tangential strains in the concrete. The expansion of the whole system, i.e. the total radial deformation, is measured by convergence lines, "C", inside the test rooms. The measuring installations are somewhat different in the three rooms, due to geological variations and different lining material. All sensors are continuously monitored by data-loggers during the test periods.

Figure 4 shows the monitoring system in the cavern wall. This set-up facilitates evaluation of the deformation of the single construction elements and their contribution to the total deformation.

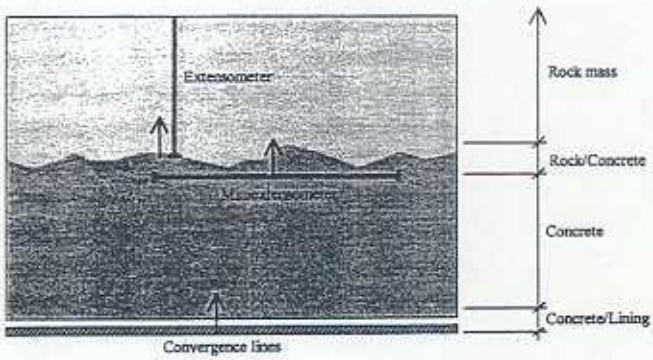

Figure 4. Detail of the monitoring system in the cavern wall.

2.4 Tests performed

Tests have been carried out in four phases during 1989-1993. Only limited tests have been carried out in Room 1 with a maximum pressure of 14 MPa. In Room 2, comprehensive pressure tests and trials have been carried out including more than 200 cyclic loads, see Figure 5. The maximum pressure achieved is 52 MPa.

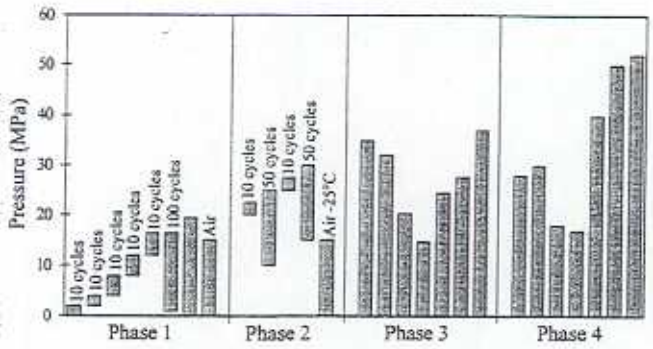

Figure 5. Pressure tests performed in Room 2.

Room 3 has been subjected to a great number of loads, 28 MPa at most, including 91 cyclic loads, see Figure 6.

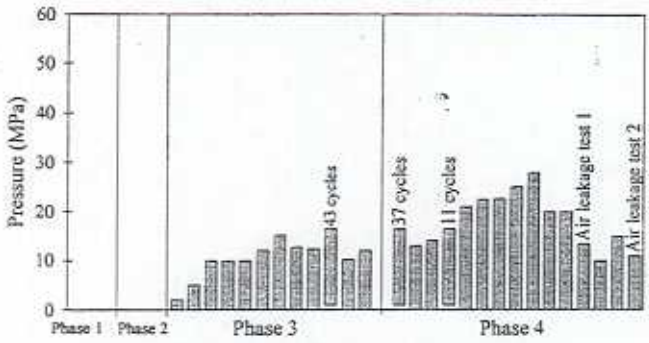

Figure 6. Pressure tests performed in Room 3.

2.5 Results

Rock mass behaviour

The deformations in the rock mass in all three rooms have been recorded by a total of 64 sensors divided between 24 extensometers. To simulate the long-term deformations in the rock, hundreds of load cycles have been performed. Figure 7 shows the additional deformation in the two horizontal extensometers in Room 2 as a result of 100 loads between 1 and 16.5 MPa. The total deformation for all horizontal extensometers is shown in Figure 9. The largest deformation measured in Room 2 is 5.65 mm at 52 MPa.

There are 10 special joint-meters (0.25 m long extensometers) installed in Room 3 in the concrete lining above definite joints in the rock surface. The largest deformation measured is 0.79 mm at the maximum pressure of 28 MPa. The deformations recorded in all the joint-meters are shown in Figure 8. Both opening and closure of rock joints have occurred.

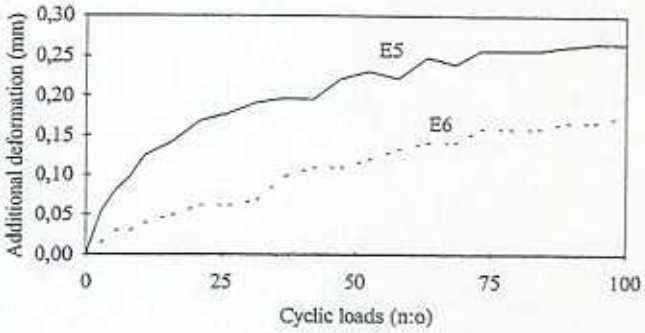

Figure 7. Additional deformations in Room 2 due to 100 cyclic loads between 1 and 16.5 MPa.

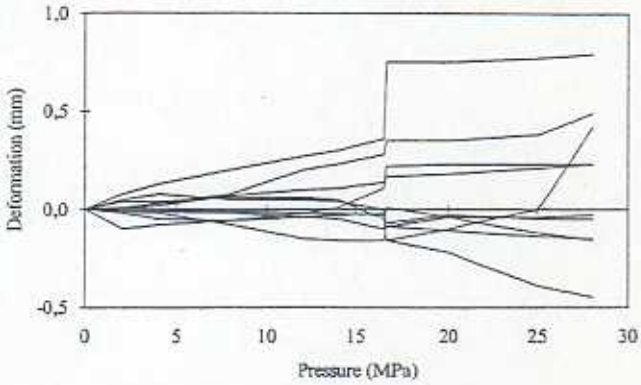

Figure 8. Rock joint movements in Room 3.

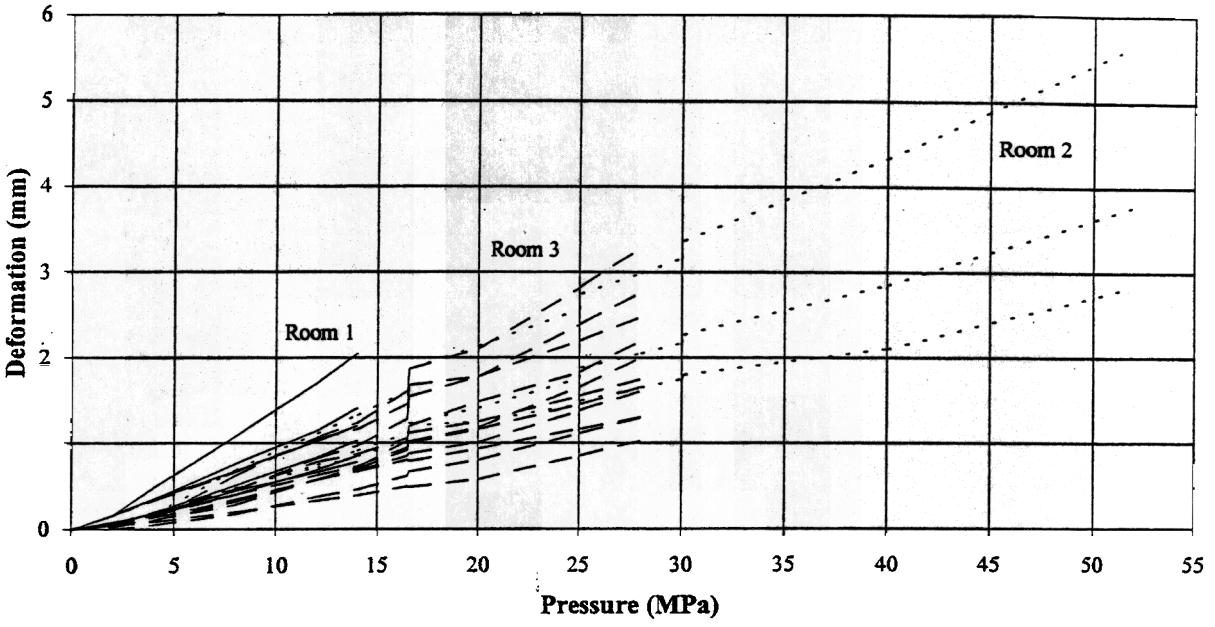

Figure 9. Deformations measured in all horizontally installed extensometers in all three test rooms.

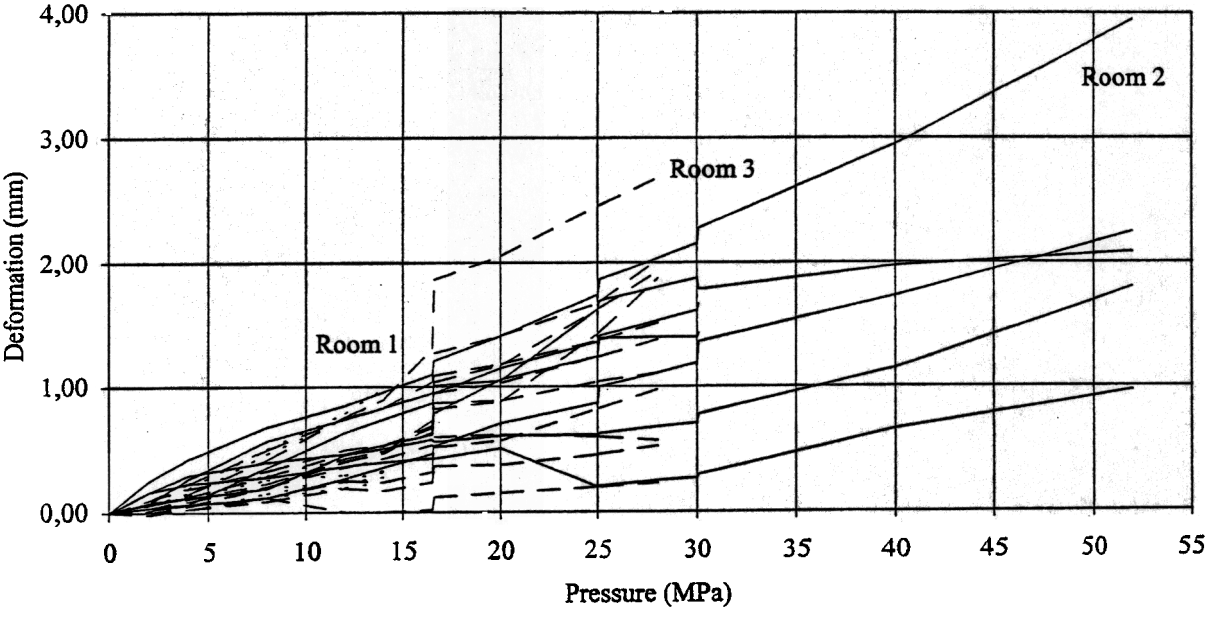

Figure 10. Deformations in all horizontal mini-extensometers.

Concrete lining behaviour

The test rooms are equipped with a total of 69 mini-extensometers which have recorded both horizontal and vertical movements in the concrete. The extensometers are located in the inner part of the concrete lining relatively close to the rock surface (see Figures 3 and 4). The deformation in all the horizontal mini-extensometers is shown in Figure 10, which gives an indication of the size and variation of the deformations. The deformations shown are the tangential deformations that occur in the concrete along a stretch of 1m.

Some parts of the steel lining have been dismantled in Room 2 for the purpose of studying the condition of the concrete behind it. The concrete lining is relatively intact considering the large loads to which it has been subjected. Cracks and crack zones have formed at reciprocal intervals varying between 0.25 m and 1 m. No large, loose pieces of concrete or crush zones have been found. These

observations are confirmed by the compressive strength measurements performed on drilled concrete cores. The result shows that the concrete has a compressive strength of 49-53 MPa after four years compared with 42 MPa at the time of casting (April 1989), i.e. an increase of 17-26%.

Steel lining behaviour

As the project proceeded, it gradually became easier to measure the strain in the lining of Room 2 due to the installation of six micro-extensometers in all. These sensors continuously measure the strain in the steel lining over a measured length of 150 mm. Figure 11 shows the strains in the lining during Phase 4 in the micro-extensometer showing the largest strain.

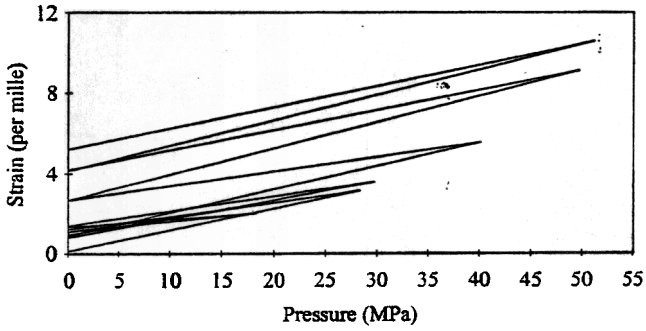

Figure 11. Strains in the steel lining in Room 2 during Phase 4 in the micro-extensometer showing the largest strain.

The average maximum strain in the steel lining is 4.5‰, thus exceeding the yield point of the steel (1.7‰). Locally, much higher strains (up to 11‰) have been measured due to local deformations in connection with crack zones in the concrete. The resulting permanent strains in the steel lining amount to 5‰.

Samples from the steel have been subjected to laboratory analysis. This metallurgic analysis implies that the structure of the steel has not been affected by the high pressures and that the properties of the steel after the loadings are unchanged in relation to the original properties.

Total behaviour

The deformations in the structure as a whole (rock-concrete-steel) have been measured with the aid of convergence lines. An example of diameter changes in Room 2 during Phase 4 is shown in Figure 12.

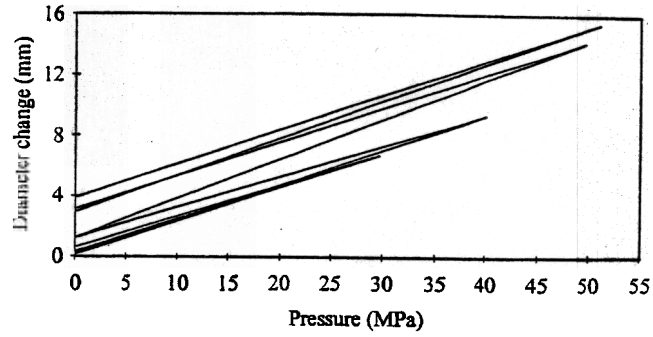

Figure 12. Diameter changes in Room 2 during Phase 4.

The total deformations at 25 MPa, and the distribution of the deformations have been summarised in Table 2. The rock mass contributes 50% of the total radial deformations. The remaining part is related to deformations in the concrete lining and its transition zones. Local rock deformations play an important role with regard to the total behaviour in the pilot scale, causing a variation of 25%. The total radial deformation implies an average tangential strain in the steel lining of 1.8‰.

Table 2. Size and distribution of radial deformation at 25 MPa in the pilot scale (diameter 4.4 m).

Element	Radial deformation (mm)
Steel lining	0
Transition steel-concrete	0,5
Concrete lining	1
Transition concrete-rock	0,5
Average rock deformation	2
Local rock deformation	±1
Total deformation	3-5

3 GUIDELINES FOR DESIGN OF A LINED GAS STORAGE

3.1 Criterias for Localisation

As outlined in Chapter 1 the concept is characterised by a high degree of flexibility regarding for example localisation. Though the concept has been primarily developed and demonstrated to function well in competent basement rock (Grängesberg), locations within geological formations of lower quality are not ruled out.

The minimum geological requirements are connected with the possibility to excavate a large scale rock cavern (diameter of 20-40 m). If this basic criteria is fulfilled a lined gas storage may be constructed. However, to make the storage economically feasible the storage pressure must of course be relatively high. The highest possible storage pressure is dictated by the chosen lining material and the geological conditions, i.e. the deformations must not exceed the maximum strain capacity of the lining. This leads to a design loop (see Figure 13) where the design parameters are optimised in relation to each other within the frames of the geological conditions.

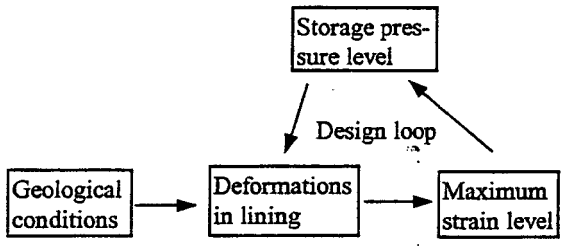

Figure 13. Design loop for technical and economical optimisation of a lined gas storage.

Obviously it is difficult to determine the minimum geological requirements as the economical feasibility depend on both site specific conditions and the value of the storage facility in the specific gas system. However, conclusions from the research work carried out imply that a wide range of geological formations all over the world may be suitable for lined gas storage. Rock masses comparable to the competent Scandinavian bedrock are found for example in North-America, Scotland and parts of Africa and Asia. Other useful geological formations, i.e. some sedimentary and metamorphosed rock masses, are found in for example Central Europe and the British Isles.

3.2 Pressure Levels

General

Several types of storage demands may generally be identified, for example seasonal storage, peak-shaving storage, storage to secure delivery and strategic storage. These different storage types imply different facility sizes and variations in pressure and load cycles. In a seasonal storage the pressure varies on a yearly basis, whereas in a peak-shaving storage the pressure varies on a daily or weekly basis. Both these demands are often met with by the same storage facility so that the short term pressure variation caused by peak demand is superimposed on the long term variation caused by seasonal storage.

In Sweden a maximum pressure of 20-25 MPa is anticipated for commercial lined gas storage. Technically these pressure levels are definitely realistic, which also has been demonstrated in Grängesberg. According to the test results considerably higher pressure levels might come into question as the rock mass has shown a good pressure absorbing ability. The observed linear deformation behaviour up to 52 MPa, see Figure 9, support this statement.

Required Depth

The only real limitation of the rock mass ability to withstand the inner pressure, considering a reasonable competent rock mass, is the resistance against vertical up-lift. This can be determined either by calculating the weight of a cone shaped rock overburden, or by using a the analogy of anchor plates in a material with friction and cohesion. These methods can be combined using numerical analysis.

By using these methods to calculate the resistance against up-lift it has been concluded that a 35 m diameter storage located in granitic rock requires a rock cover of approximately 150 m at 25 MPa inner pressure (Factor of Safety = 3). The required rock cover for a similar storage located in sedimentary rock is somewhat larger, approximately 180 m.

The calculations made are consistent and therefore considered adequate. However, it has not been possible to calibrate the methods as no practical tests to failure have been performed.

3.3 Expected Deformations

General deformation

To simplify the description, the deformations are divided into general and local deformations. The general deformation represents the evenly distributed radial "mean" deformation caused by the inner pressure.

These deformations can be calculated using numerical calculation models and/or analytical solutions. In the Grängesberg case a Finite Element Model (JOBFEM) have been used to calculate deformations in the concrete and the rock. The research work carried out has shown that this type or modelling may be used to accurately predict the general behaviour of a lined rock cavern when pressurised to levels of 20-30 MPa.

Local deformations

The local variations in radial deformation and tangential strain are ruled by the local geological

conditions and by the cracking pattern in the concrete wall. Local variations are a result of for example movements in single rock joints or isolated larger deformations due to weakness zones in the rock mass. The local variations are added to the general deformation and thus important for the strain levels in the liner. The complex nature of the rock mass imply that the local variations can be difficult to predict. However, experience from Grängesberg and other conventional underground projects indicate that they may be estimated by experience or by using for example discrete computer models. Deformations in single rock joints, leading to increased cracking of the concrete, influence the strain levels arising in the liner.

During loading the rock mass behaves according to an elasto-plastic model. At low pressures this means a mainly elastic behaviour. At higher pressures (in the Grängesberg case approximately 5-10 MPa) tensile stresses occur in the rock surface. When the strength of the rock mass is exceeded, shearing and compression take place in the joints leading to plastic deformations.

Cracks in the concrete, causing a local increase of the strain in the liner, develop when the tangential tensile strain exceeds approximately 0.2‰ which in the Grängesberg case happened at low pressures 0-5 MPa. At these low pressures single cracks open locally with an uneven distribution around the circumference of the concrete lining. The local behaviour in the concrete and steel lining is illustrated by the test results from Grängesberg in Figures 14 and 15.

It is interesting to note that the general deformation continuously increases with the pressure. Single stretches with deformation peaks represents a local behaviour. The local deformations are probably very much governed by movements in single rock joints and concrete cracks.

The influence of a local weakness zone has been studied in Grängesberg. The zone, which is about 0.5 m wide and at its closest about 2.5 m from Room 3, has a noticeable effect on the deformations, see Figure 16. In absolute figures, however, the effects are minor, the additional radial deformation in the room at 28 MPa being in the order of 0.8 mm.

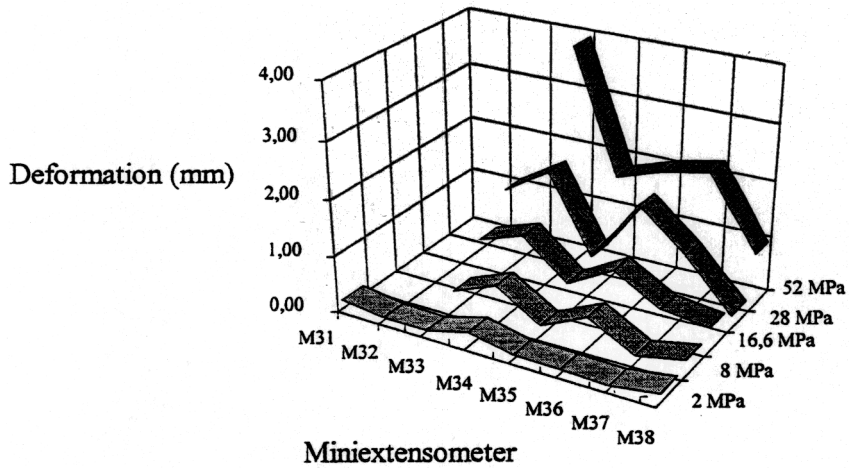

Figure 14. Deformations in a horizontal row of mini-extensometers installed in the concrete wall of Room 2, Grängesberg.

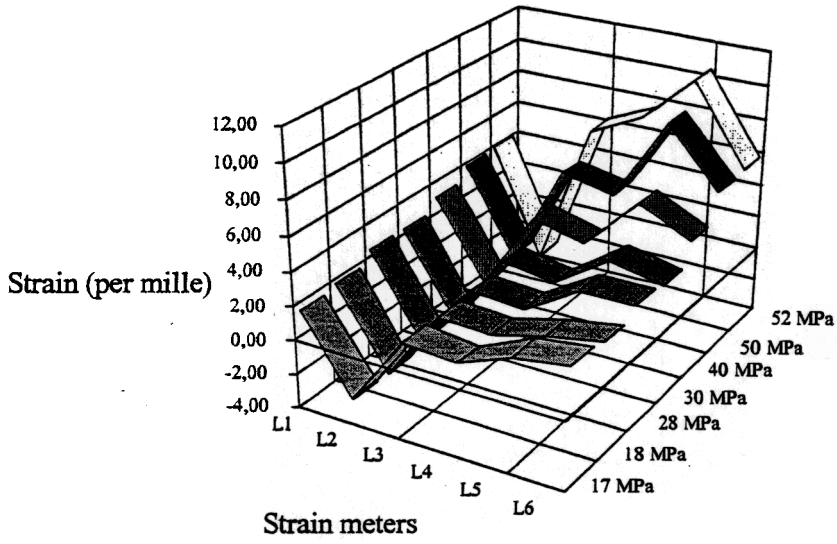

Figure 15. Strains measured in six strain-meters (measuring length 150 mm) installed on the steel lining in Room 2, Grängesberg.

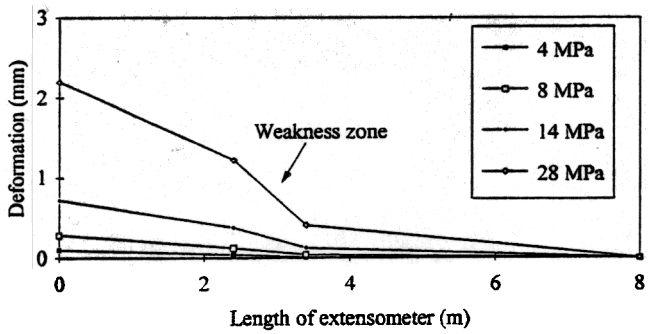

Figure 16. Distribution of deformations in an extensometer through a 0.5 m wide weakness zone.

Long-Term Behaviour

Knowledge about the long-term behaviour is essential when designing a storage subjected to high pressures and cyclic loads.

In order to simulate the expected life time load of a storage, several hundreds of cyclic loads to high pressure levels have been performed in the Grängesberg test rooms.

The general conclusion is that no accelerating deformations have occurred, on the contrary a hardening behaviour has been recorded, see Figure 7. This is explained by the fact that the rock mass closest to the caverns is compacted as rock joints are closed and sheared.

The influence of the weakness zones on the deformations also appears as an effect during cyclic loading. Figure 17 shows the increase in diameter measured in four convergence lines inside Room 3 during 91 cyclic loads between 1 and 16.5 MPa. Two of these, C2 and C3 located in a direction parallel to the weakness zones, show a decreasing rate of deformation growth. However, C4 and C5 oriented perpendicularly to the weakness zone show both a larger deformation and a slower decrease in the deformation growth rate.

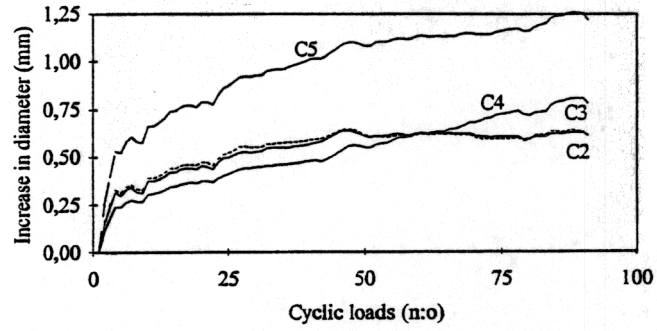

Figure 17. Increase in diameter in Room 3 as a result of 91 cyclic loads between 1 and 16.5 MPa.

Calculation examples, total deformation

It should be emphasised that the model of function used in Grängesberg, describing the behaviour of a lined rock cavern, is applicable to predict deformations in any rock mass.

In order to illustrate the flexibility of the concept, two calculation examples have been made for a commercial storage facility (maximum pressure = 25 MPa and diameter 40 m) using a simple analytical model. One example describes a location in a geological environment comparable with Grängesberg (Rock Mass E-modulus = 40 GPa), see

Table 3, the other a location in sedimentary rock (Rock Mass E-modulus = 10 GPa), see Table 4.

Table 3. Estimated size and distribution of radial deformation at 25 MPa in commercial scale for a competent granitic rock mass with E-modulus = 40 GPa.

Element	Radial deformation (mm)
Steel lining	0
Transition steel-concrete	0.5
Concrete lining	1
Transition concrete-rock	0.5
Average rock deformation	19
Local rock deformation	±1
Total deformation	20-22

The average strain in the steel lining will in this case be 1.0‰ (1.8‰ in Grängesberg) which means that the yield point (1.7‰) will not be exceeded. Locally in connections with cracks in the concrete the steel will yield but the strains in the lining will be smaller than in the pilot scale in Grängesberg.

Table 4. Estimated size and distribution of radial deformation at 25 MPa in commercial scale for a sedimentary rock mass of fair quality with E-modulus = 10 GPa.

Element	Radial deformation (mm)
Steel lining	0
Transition steel-concrete	0.5
Concrete lining	1
Transition concrete-rock	0.5
Average rock deformation	88
Local rock deformation	±1
Total deformation	89-91

The average strain in the steel lining will in this case be 4.5‰, much higher than in the first example. However, the steel lining in Room 2 in Grängesberg has been subjected to average strains of 4-5‰ and local strains of at least 11‰ at the maximum pressure of 52 MPa. Hence, the larger deformation associated with the weaker rock mass does not imply a problem in respect of too large strains in a steel lining material comparable to that used in Grängesberg. However, by reducing the internal pressure to 10-15 MPa the strains will be considerably smaller.

A consequence of this is that a wide range of geological environments or rock masses with lower quality than found in areas with basement rock may host a lined gas storage facility.

4 CONCLUDING REMARKS

The most important conclusion from the Grängesberg tests was that the tested concept fulfilled its main purpose to confine the gas at very high pressure levels and after a vast number of cyclic loads. The rock mass has proven its function as pressure vessel at pressure levels far above those intended for a commercial storage plant (20-25 MPa). Generally after several years of research it can be concluded that no main technical questions related to the concept remain and the concept is ready for demonstration in a larger scale.

The lined storage concept is considered to be the most suitable underground gas storage method at present conditions in Sweden. A demonstration plant, as a continuation of the Grängesberg pilot unit, could be located in the vast majority of natural gas consuming countries.

It should be emphasised that the concept under certain circumstances provide an attractive alternative to traditional gas storages. To sum up, the following advantages with lined gas storages, compared to traditional storages, may be identified.

- The size of the facility may to a large extent be varied. A facility may be constructed and expanded in phases. Each storage module may have a working gas volume of up to 30 MNm^3.
- The possibility to locate the storage facility close to gas customers and existing gas distribution nets is good, as it is not restricted to certain geological formations.
- The possibility to control the stored gas is good. This implies minimum impact on the environment.
- The contained gas is never in direct contact with ground water and/or rock or soil. This implies that the gas is not contaminated during storage and separation of water and particles before distribution is not needed.
- The storage is structurally stable and the need for cushion gas is minimal.
- The maximum withdrawal rate is high, limited only by the dimensions of the pipes and temperature restrictions.

REFERENCES

Calminder, Å., Hahn, T., 1982: "Recent Developments in Underground Storage Techniques," Rock Mechanics: Caverns and Pressure Shafts, ISRM Symposium, Aachen, pp. 893-901.

Isander, A., 1994: "Research Facilities in Grängesberg - Rock Mechanical Results, Phase 1-4, " Proc. of 1994 ISRM International Symposium, Santiago, Chile.

Lindblom, U. E., 1986: "Compressed Natural Gas Storage in Rock Caverns," Internal Report, Hagconsult, Sweden.

Lindbo, T., Sandstedt, H., Karlsson, P-O., 1989: "Storage of Natural Gas in Lined Rock Caverns - Pilot Plant, " Proc. of Storage of Gases in Rock Caverns, Nilsen & Olsen (eds.), Balkema, Rotterdam, pp. 367-370.

Stille, H., Johansson, J., Sturk, R., 1994: "High Pressure Storage of Gas in Lined Shallow Rock Caverns - Results from Field Tests, " Proc. of EUROCK 94, Rock Mechanics in Petroleum Engineering, Balkema, to be published.

Särkkä, P., 1994: "Natural Gas Storage in Mined Caverns, " Proc. of the 19th World Gas Conference. IGU/A-94, Groningen, pp 77-98.

Tengborg, P., 1989: "Storage of natural gas in lined rock caverns - Studies for a future project in southern Sweden, " Proc. of Storage of Gases in Rock Caverns, Nilsen & Olsen (eds.), Balkema, Rotterdam, pp. 151-157.

High pressure storage of gas in lined shallow rock caverns- Results from field tests

HIGH PRESSURE STORAGE OF GAS IN LINED SHALLOW ROCK CAVERNS - RESULTS FROM FIELD TESTS

H. Stille
Royal Institute of Technology, Stockholm, Sweden

J. Johansson
Naturgasteknik AB, Stockholm, Sweden

R. Sturk
Skanska Teknik AB, Stockholm, Sweden

ABSTRACT: At the Grängesberg Research Plant field tests have been performed regarding storage of gas at very high pressures in lined shallow rock caverns. The surrounding rock mass (granite) has proven to be very capable of withstanding loads at levels far above the initial rock stresses. No tendency of vertical uplift has been recorded. At an internal pressure of 52 MPa the maximum registered radial deformation in the rock was 5.65 mm, corresponding to a tangential strain of 2 per mille. The combined construction element liner-concrete-rock has fulfilled its main purpose, i.e. to confine the gas, throughout a tough load history. Leakage tests at high pressures have indicated that even a large failure in the liner can be controlled without any severe consequences.

1 INTRODUCTION

The pilot plant for lined gas storage facilities, located in central Sweden 250 km west of Stockholm, comprises three test rooms and was built during 1988 as a joint project by a number of Scandinavian companies interested in developing new techniques for storing natural gas in lined rock caverns. Tests have been carried out in four phases during 1989-1993.

Outlines of the concept and the objectives of the pilot tests have been presented earlier by Lindbo et al., 1989 and Tengborg, 1989. Early results have been presented by Rosendal et al., 1992. After the completion of the field tests the results have been subjected to a comprehensive theoretical analysis by Stille et al., 1994.

The three test rooms are excavated as vertical cylinders 5 m in diameter and 10 m high. The rooms are lined on the inside with concrete and steel. The rock overburden above the rooms is 50 m.

In short, the lined rock cavern concept, shown in Figure 1, is based on the interaction between the following elements:

- a lining, enclosing the gas in the cavern
- a concrete layer, serving as a base for the lining, to transfer the pressure forces to the rock and to distribute developing cracks
- the surrounding rock mass, absorbing the pressure forces and thus acting as the pressure vessel.
- a drainage system, taking care of groundwater inflow as well as potential gas leakages.

Water curtains have been used to ensure constant groundwater conditions. 15 vertical holes have been drilled around each room at a distance of 2-4 m. It should be noted that the groundwater pressure has no influence on the storage concept in respect of pressure levels and gas containment.

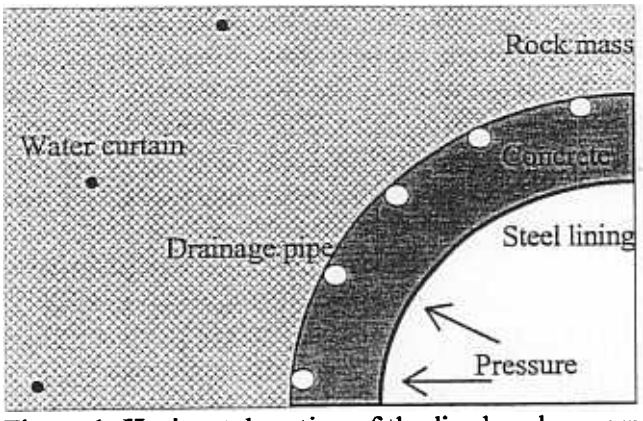

Figure 1. Horizontal section of the lined rock cavern concept.

2 GEOLOGICAL CONDITIONS

The predominant type of rock in the area is a medium-grained granite (Uniaxial Compressive Strength = 340 MPa and Young's modulus = 56 GPa). An 8-9 m thick metabasite dyke traverses the granite in the area in which the pilot plant is located. One contact zone (width 0,5 m) is altered and forms a weakness zone in the rock mass.

Steep joints are found in the area. These are mainly divided into three major joint directions, two of which lie within the section N40-70°W and the third in the sector N0-10°E. Flat joints occur only sparsely. The joints are essentially tight with openings of less than 1 mm. Chlorite and calcite occur on some of the mainly raw and planar joint surfaces.

The initial stresses of the granite are low according to the rock stress measurements, i.e. 1-4 MPa. The largest horizontal stress has a mean value of 2.5 MPa and a north-west orientation. The smallest horizontal stress has a mean value of 1.3 MPa. The mean value of the vertical stress is 1.4 MPa.

A classification of the rock mass was done using both the Q method and the RMR method. The mechanical properties of the rock mass, the deformation modulus and the compressive strength, were evaluated based on RMR and Q values and results from laboratory tests. The values of the above parameters are shown in Table 1.

Table 1. Rock mass properties.

Rock mass section	RMR value	Q value	Young's modulus (GPa)	Compressive strength (MPa)
Granite	75	20	30	9
Metabasite	80	22	40	15
Weakness zone	52	8	2	5

3 TESTS PERFORMED

3.1 *Test room 1*

Room 1 was designed specifically for the purpose of testing a 0.4 mm thick lining of austenitic stainless steel (SS 2343). The concrete lining is about 0.4 m thick and conventionally reinforced. Limited tests have been carried out in Room 1 with a maximum pressure of 14 MPa. In principle the design of the room corresponds with that of Room 2.

3.2 *Test room 2*

Room 2 is equipped with a lining of 6 mm plates of micro-alloyed steel (SS 2134). The concrete lining is about 0.6 m thick and unreinforced. The test room is cylindrical in form with a rounded bottom and a semi-spherical roof, see Figure 2. Comprehensive pressure tests and trials have been carried out in this room including more than 200 cyclic loads, see Figure 3. The maximum pressure achieved is 52 MPa. The tests also comprises loading after long-term cooling of the room and freezing of the surrounding rock mass, but results from these tests are not included in this paper.

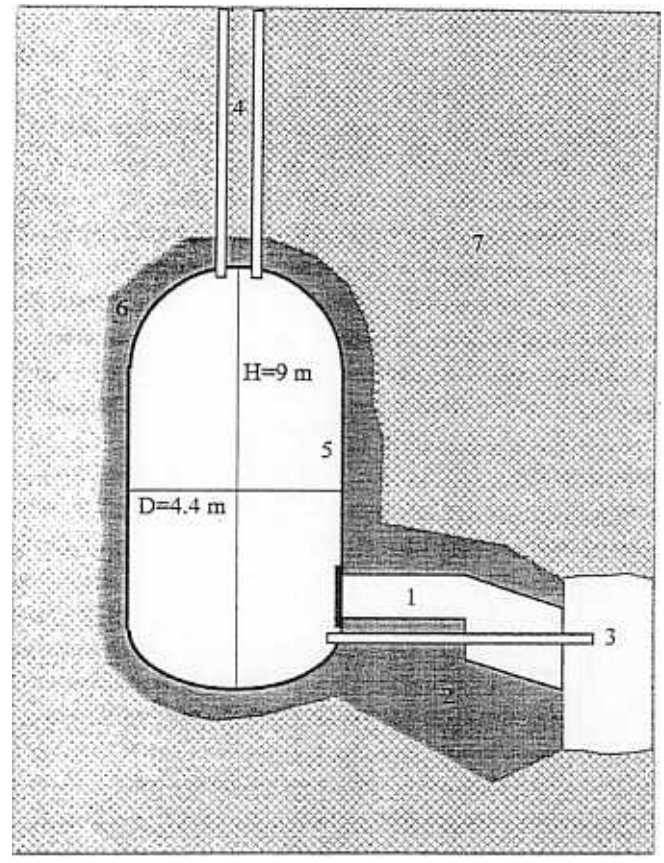

Figure 2. General layout of Room 2. 1. Access tube, 2. Concrete plug, 3. Water fill, 4. Gas fill, 5. Steel lining (6 mm), 6. Concrete lining (0.6 m), 7. Rock mass.

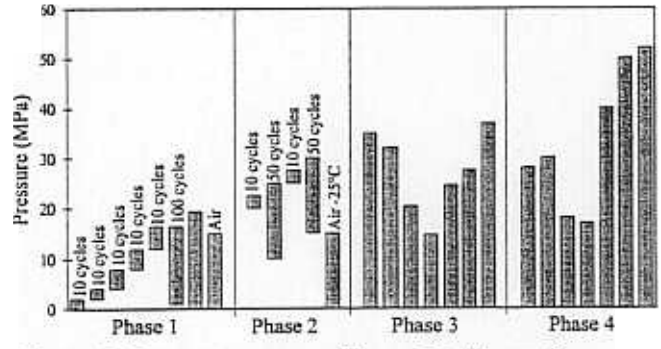

Figure 3. Pressure tests performed in Room 2.

3.3 *Test room 3*

Room 3 has a 0.5 mm thick lining of stainless steel. The concrete lining is 0.3 m thick and conventionally reinforced. The room has been subjected to a great number of loads, 28 MPa at most, including 91 cyclic loads, see Figure 4. In principle the design of the room corresponds with that of Room 2.

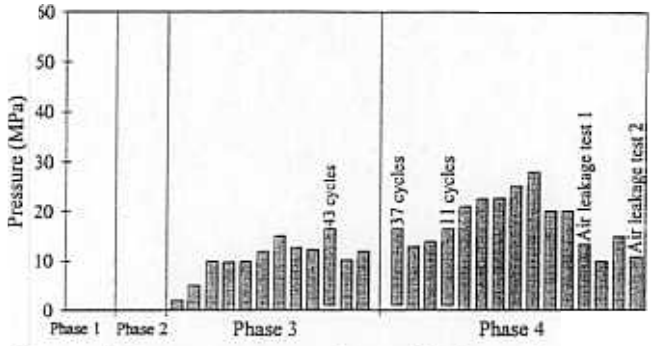

Figure 4. Pressure tests performed in Room 3.

3.4 *Monitoring system*

The radial expansion in the rooms and the deformations in the rock and concrete are continuously registered during pressure testing. Extra measuring devices are installed in the rock in Room 3 for the purpose of studying the movements in the nearby weakness zone. Strains in the steel lining in Room 2 have also been measured continually. The radial rock mass deformations are measured by multiple extensometers, labelled "E" in Figure 5. Mini-extensometers "M" are installed in the concrete to measure tangential strains in the concrete. The expansion of the whole system, i.e. the total radial deformation, is measured by convergence lines, "C", inside the test rooms. The measuring installations are somewhat different in the three rooms, due to geological variations and different lining material. All sensors are continuously monitored by data-loggers during the test periods.

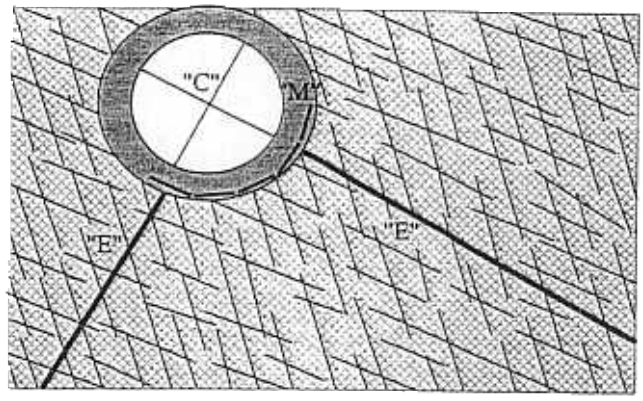

Figure 5. Measuring installations in the test rooms, schematic horizontal section.

4 RESULTS

4.1 *Rock mass behaviour*

The deformations in the rock mass in all three rooms have been recorded by a total of 64 sensors divided between 24 extensometers. Table 2 shows measured deformations for 20 extensometers at five different pressure levels. The total deformation for all horizontal extensometers is shown in Figure 6. The largest deformation measured in Room 2 is 5.65 mm at 52 MPa. At pressures higher than 40 MPa there were distinct sound phenomena in the form of bangs and popping noises in the rock mass. The sounds were heard att irregular intervals and continued to be audible during depressurizing right down to low pressure levels.

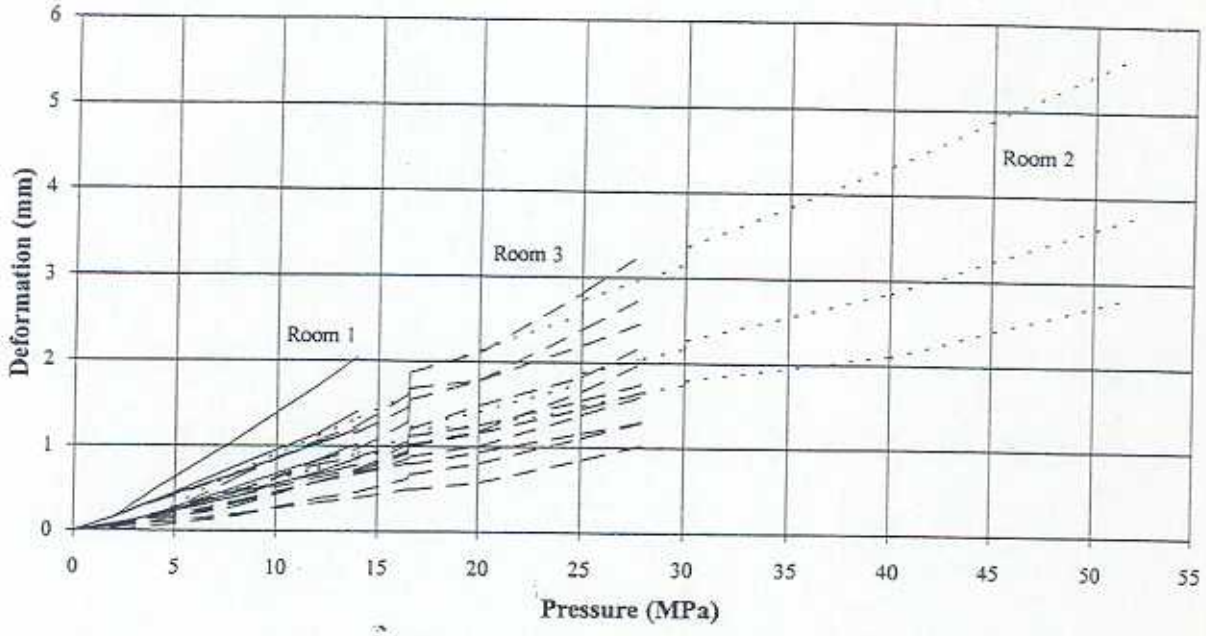

Figure 6. Deformations measured in all horizontally installed extensometers in all three test rooms.

Table 2. Deformations in the rock mass at different pressure levels (deformations in mm).

Extensometer	Direction	Pressure (MPa)				
		8	14	28	40	52
Room1						
E2	Horizontal	0.76	1.41	-	-	-
E3	Horizontal	0.51	1.03	-	-	-
E4	Vertical	0.45	0.78	-	-	-
E14	Horizontal	0.41	0.85	-	-	-
E15	Horizontal	1.08	2.05	-	-	-
E16	Horizontal	0.68	1.20	-	-	-
Room 2						
E5	Horizontal	0.69	1.33	2.99	4.33	5.65
E6	Horizontal	0.48	0.85	1.65	2.10	2.84
E7	Vertical	0.48	0.91	2.05	2.85	3.78
Room 3						
E21	Vertical	0.47	0.87	1.75	-	-
E22	Horizontal	0.45	0.97	2.77	-	-
E23	Horizontal	0.35	0.67	1.31	-	-
E24	Inclined	0.28	0.72	2.20	-	-
E25	Inclined	0.17	0.46	1.30	-	-
E26	Inclined	0.33	0.68	1.61	-	-
E27	Inclined	0.32	0.70	2.00	-	-
E28	Inclined	0.66	1.16	2.48	-	-
E29	Inclined	0.40	0.73	1.66	-	-
E30	Inclined	0.20	0.39	1.03	-	-
E31	Horizontal	0.62	1.24	3.29	-	-

During loading the rock mass behaves according to an elasto-plastic model. At low pressures this means a mainly elastic behaviour. At higher pressures (in this case approximately 5-10 MPa) tensile stresses occur in the rock surface. When the strength of the rock mass is exceeded, shearing and compression take place in the joints and plastic deformations occur. If the permanent deformations are subtracted from the total deformations (Figure 6) the remaining part of the deformations reflects the elastic behaviour of the rock mass ruled by a deformation modulus, see Figure 7. This modulus might be slightly different in different directions in the rock mass due to local geological conditions.

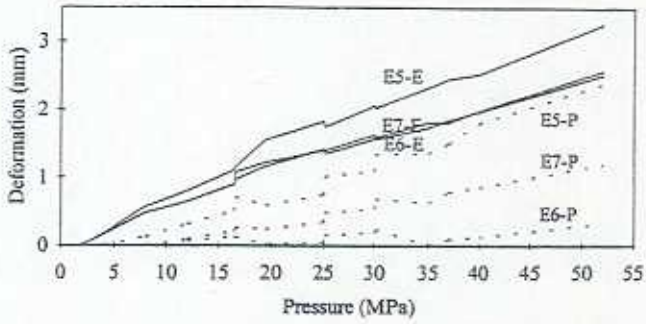

Figure 7. Elastic and plastic (permanent) deformations measured in three extensometers in Room 2.

To simulate the long-term deformations in the rock, hundreds of load cycles have been performed. Figure 8 shows the additional deformation that has occurred in the two horizontal extensometers in Room 2 as a result of 100 loads between 1 and 16.5 MPa. The rate of deformation growth is decreasing and the main part of the additional deformations are taken out during the first 50 cycles. The 100 cycles have caused a 17% increase in the total deformation.

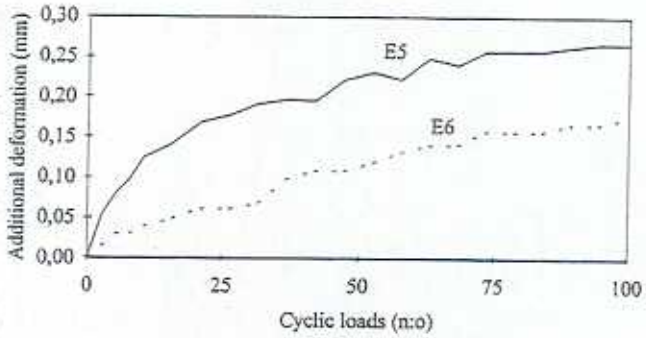

Figure 8. Additional deformations in Room 2 due to 100 cyclic loads between 1 and 16.5 MPa.

It is especially interesting to study the effect of two nearby weakness zones on the deformations in Room 3. The west zone, which is about 0.5 m wide and at its closest is about 2.5 m from the room, has an noticeable effect on the deformations, see Figure 9. In absolute figures, however, the effects are minor, the additional radial deformation in the room at 28 MPa being in the order of 0.8 mm. The east zone, which is 0.1-0.2 m wide and located about 1.2 m from the room, has not shown any effect in the installed extensometers.

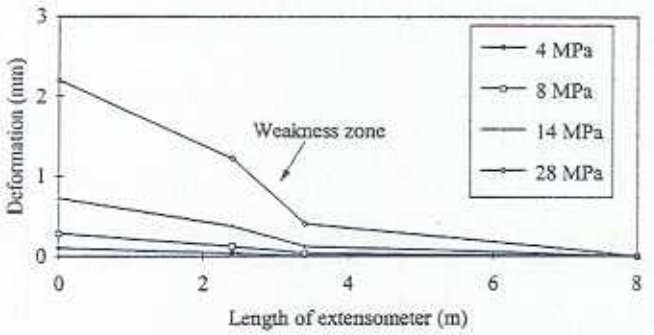

Figure 9. Distribution of deformations in an extensometer through a 0.5 m wide weakness zone.

The influence of the weakness zones on the deformations also appears as an effect during cyclic loading. Figure 10 shows the increase in diameter measured in four convergence lines inside Room 3 during 91 cyclic loads between 1 and 16.5 MPa. Two of these, C2 and C3, are located in a direction parallel to the weakness zones. These meters show a similar behaviour to that of the extensometers in Room 2, i.e. a decreasing rate of deformation growth. However, C4 and C5 oriented perpendiculary to the weakness zones show both a larger deformation and a slower decrease in the deformation growth rate.

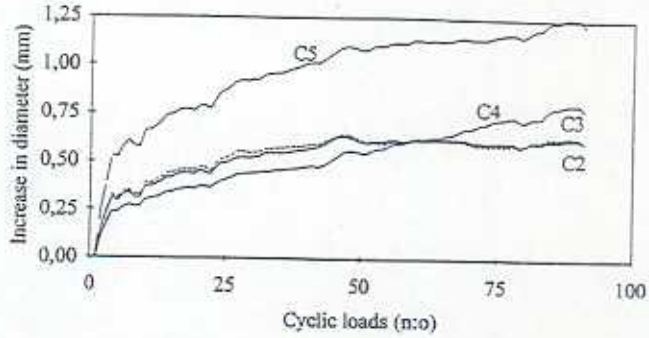

Figure 10. Increase in diameter in Room 3 as a result of 91 cyclic loads between 1 and 16.5 MPa.

During test loading of Room 2, injected and drained volumes of water in the surrounding rock mass were carefully measured. The aim was to study possible joint and block movements in the rock. Block movements in the rock mass cause an alteration of the joint areas in different sections of the rock. By measuring variations in the flow in the water curtain and drainage system these block movements can be indirectly verified.

Tests have been performed at a curtain presure of about 0.1 MPa overpressure relative to the groundwater pressure. The total injected and drained flow is shown in Figure 11. Initially the injected and the drained flows are constant. At a pressure of 3 MPa the water bearing fractures starts to widen. Both the injected flow and the drained flow thereafter increase proportionally to the pressure. As an effect of the cyclic loads, a decrease in flows can be observed, this is probably due to shearing and compression of rock joints. After the cyclic loads the difference between injected and drained flows has increased. The rock mass between the water curtain and the room is at this stage less permeable.

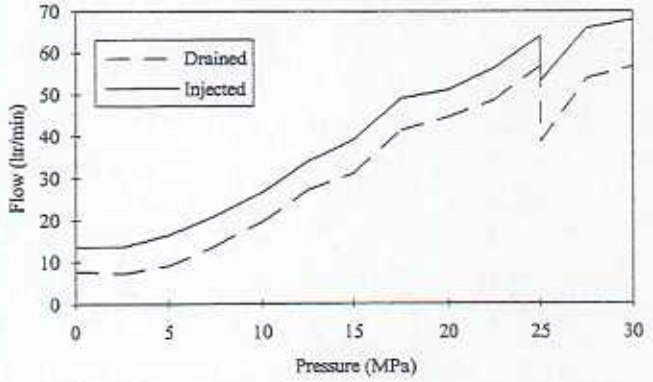

Figure 11. Total injected and drained flow measured in Room 2 at loads of up to 25 MPa, 50 cyclic loads between 10 and 25 MPa and a further pressure increase to 30 MPa.

4.2 *Concrete lining behaviour*

The test rooms are equipped with a total of 69 mini-extensometers which have recorded both horizontal and vertical movements in the concrete. The extensometers are located in the inner part of the concrete lining relatively close to the rock surface (see Figure 5). The deformation in all the horizontal mini-extensometers is shown in Figure 12, which gives an indication of the size and variation of the deformations. The deformations shown are the tangential deformations that occur in the concrete along a stretch of 1m. Cracks in the concrete develop when the tangential tensile strain exceeds approximately 0.02% which in this case happens at low pressures, approximately 0-5 MPa. At these low pressures single cracks open locally with an uneven distribution around the circumference of the concrete lining. At higher pressures cracks continue to develop and open. At this stage the cracking evens out, implying a larger number of cracks per metre and that the cracks widen more uniformly.

Some parts of the steel lining have been dismantled in Room 2 and Room 3 for the purpose of studying the condition of the concrete behind it. The sections selected for dismantling were in areas where large movements in the concrete had been measured and thus where fracturing was expected to be greatest. To investigate the concrete lining in Room 2 more thoroughly, four concrete cores (dia. 100 mm) were drilled. The cores, which have been drilled right down to the rock, are 0.6-1.1 m long.

The concrete lining in Room 2 is relatively intact considering the large loads to which it has been subjected. Cracks and crack zones have formed at reciprocal intervals varying between 0.25 m and 1 m. No large, loose pieces of concrete or crush zones have been found. Nor does the surface layer appear to be particularly affected or crumbled, but is still hard. These observations are confirmed by the compressive strength measurements performed on one of the drilled concrete cores. The result shows that the concrete has a compressive strength of 49-53 MPa after four years compared with 42 MPa at the time of casting (April 1989), i.e. an increase of 17-26%).

The mapping of the concrete surface in Room 2 also showed that the crack frequency varies somewhat in different directions, from 1-2 cracks/m to 2-4 cracks/m. Two crack zones have been mapped in the area in which the greatest deformation (3.95 mm/m) has been recorded. These zones contain several minor cracks and are probably the result of shear failure in the concrete adjacent to a major crack. The results of the deformation measurements and the inspection imply that the crack openings of

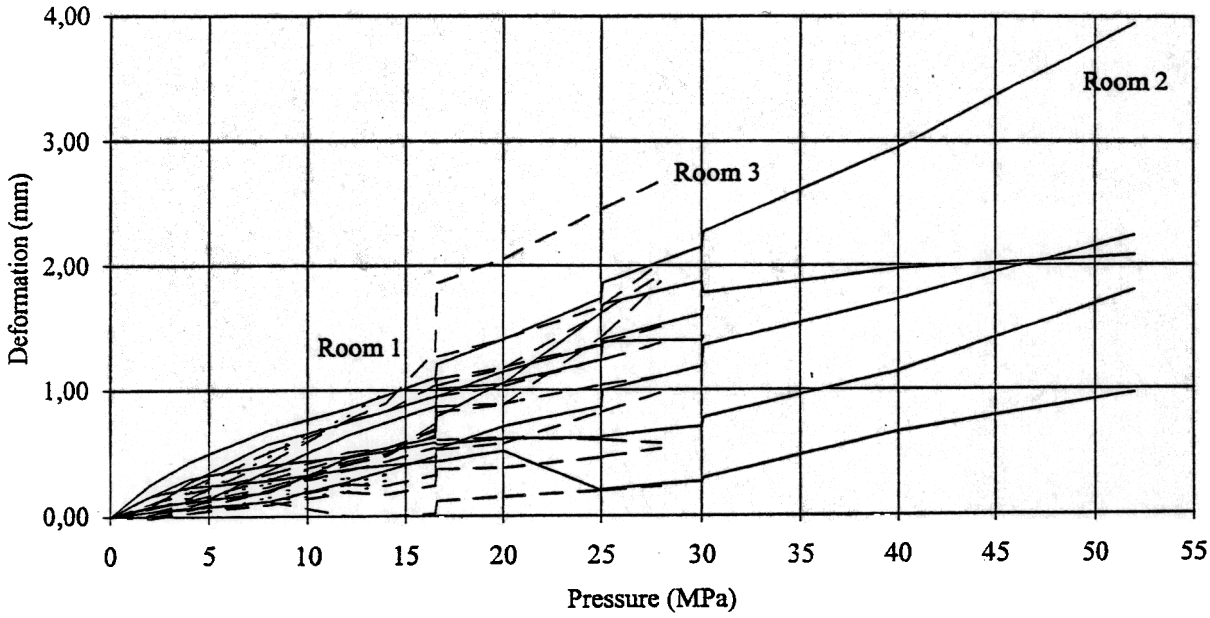

Figure 12. Deformations in all horizontal mini-extensometers.

single cracks are limited in size and do not exceed 1 mm at a pressure of 52 MPa. Most of the cracks are vertical. Some inclined cracks have been observed. In the dome the cracks are chiefly horizontal.

The concrete surface in Room 3 seems to be unaffected and no cracks have been observed. This is either due to the fact that the cracks are too narrow to be observed by the human eye or that no

cracks have developed despite a tangential strain by far exceeding 0.02% (0.1% strain measured).

There are 10 special joint-meters (0.25 m long extensometers) installed in Room 3 in the concrete lining above definite joints in the rock surface. The largest deformation measured is 0.79 mm at the maximum pressure of 28 MPa. The deformations recorded in all the joint-meters are shown in Figure 13. Both opening and closure of rock joints have occurred.

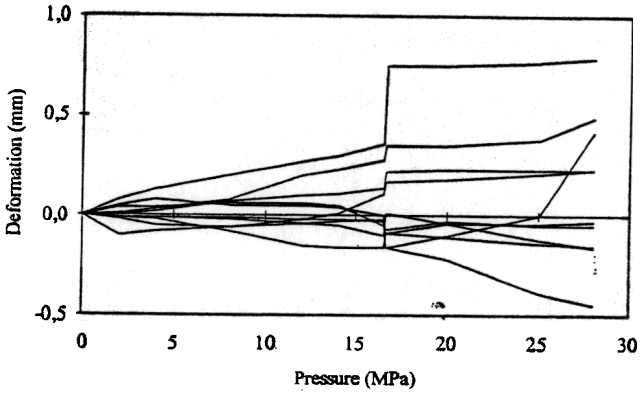

Figure 13. Rock joint movements in Room 3.

4.3 *Steel lining behaviour*

As the project proceeded, it gradually became easier to measure the strain in the lining of Room 2 due to the installation of six micro-extensometers in all. These sensors continuously measure the strain in the steel lining over a measured length of 150 mm. Figure 14 shows the strains in the lining during Phase 4 in the micro-extensometer showing the largest strain.

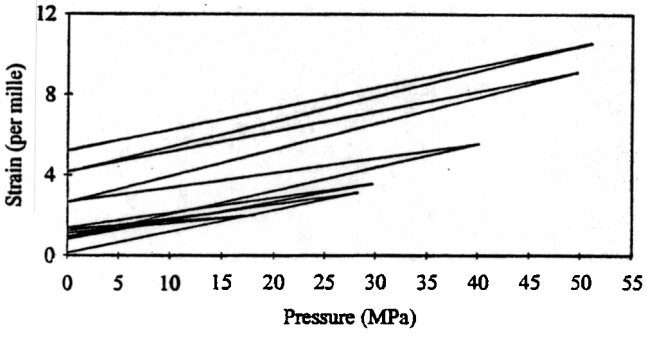

Figure 14. Strains in the steel lining in Room 2 during Phase 4 in the micro-extensometer showing the largest strain.

The average maximum strain in the steel lining is 0.45%, thus exceeding the yield point of the steel (0.17%). Locally, much higher strains (up to 1.1%) have been measured due to local deformations in connection with crack zones in the concrete. The resulting permanent strains in the steel lining amount to 0.5%.

Samples from the steel have been subjected to laboratory analysis. This metallurgic analysis implies that the structure of the steel has not been affected by the high pressures and that the properties of the steel after the loadings are unchanged in relation to the original properties.

4.4 *Total behaviour*

The deformations in the structure as a whole (rock-concrete-steel) have been measured with the aid of convergence lines. An example of diameter changes in Room 2 during Phase 4 is shown in Figure 15.

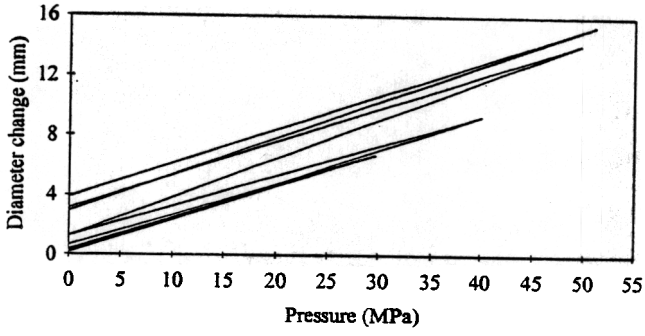

Figure 15. Diameter changes in Room 2 during Phase 4.

The total deformations at 25 MPa (expected maximum pressure in a commercial storage plant), and the distribution of the deformations have been summarised in Table 3. The rock mass contributes 50% of the total radial deformations. The remaining part is related to deformations in the concrete lining and its transition zones. Local rock deformations play an important role with regard to the total behaviour in the pilot scale, causing a variation of 25%. The total radial deformation implies an average tangential strain in the steel lining of 0.18%.

Table 3. Size and distribution of radial deformation at 25 MPa in pilot scale (diameter 4.4 m).

Element	Radial deformation (mm)	Share of deformation (%)
Steel lining	0	0
Transition steel-concrete	0,5	12,5
Concrete lining	1	25
Transition concrete-rock	0,5	12,5
Average rock deformation	2	50

Local rock deformation	±1	±25
Total deformation	3-5	100 ±25

4.5 *Air leakage tests*

Air leakage tests with artificially created leaks have been done on two occasions for the purpose of studying the drainage system's ability to perform its three main tasks, i.e. detection, localisation and collection. On the first occasion the test was performed in Room 2 at an air pressure of 1.6 MPa. The leakage was created by placing nozzles in holes drilled through the steel lining before the room was pressurized. The test result showed that the leakage was clearly detectable and could be localised by flow measurements in the drainage system. As regards collection, the capacity achieved was about 75-80% of the leaked air.

On the second occasion, two air leakage tests were performed in Room 3 at high pressures (11-13 MPa). The leaks were created by two axes triggered by remote control to fall and make holes through the 0.5 mm thick steel lining at the same time as the room was pressurized. Figure 16 shows the pressure fall during the first leakage test when two axes were triggered.

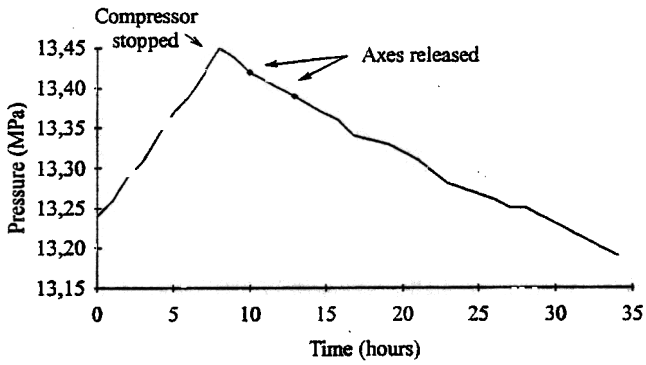

Figure 16. Pressure fall during air leakage test in Room 3. The diamond symbols mark the times at which the axes were released.

No increase in the existing initial leakage (due to minor defects in the welds) is detectable despite two new large defects (1 x 100 mm^2 each) created by the axes. The volume of air leaking out during the holding time has been estimated at 11-15 m^3/hr. The efficiency of the drainage system when collecting leaking gas has been evaluated at about 80%. An inspection of the concrete surface behind the axe blows has not revealed any cracks or other effects. During a second leakage test only one axe was successfully triggered. The collection efficiency of the drainage system was estimated at about 94-100%.

5 CONCLUSIONS

Comprehensive field tests have been carried out successfully during four years in the Grängesberg Pilot Plant. The most important conclusion is that the tested concept can fulfill its main purpose to confine the gas during a tough load history. Leakage tests at high pressures have indicated that even a large failure in the liner can be controlled without any severe consequences.

The rock mass has proven its function as pressure vessel at pressure levels far above those intended for a commercial natural gas storage plant (20-25 MPa). Experience gained in Grängesberg will improve possibilities of predicting rock mass behaviour in connection with high pressure rock storage. No accelerated deformations have occurred and the behaviour is linear. The radial deformations and joint openings have proved to be approximately half the size calculated by Larsson et al., 1989. No tendencies of vertical uplift have been recorded. Over 85% of the radial deformations take place within a distance of approximately 2 room diameters (from the periphery).

In the pilot tests the rock mass accounted for half of the radial deformations. For a commercial plant (ten times the geometrical scale), on the other hand, the rock deformation is expected to increase proportionally to the scale while the deformations in the concrete lining and the transition zones are expected to be the same as in the pilot plant. Thus, the rock will account for a dominant share of the deformation, see Table 4, and the share of the total deformation attributed to the concrete and the transitional areas is expected to be marginal. Furthermore it should be pointed out that the average strains in the steel lining will decrease from 0.18% in the pilot scale to 0.10% in the full scale

Table 4. Estimated size and distribution of radial deformation at 25 MPa in commercial scale (diameter 44 m).

Element	Radial deformation (mm)	Share of deformation (%)
Steel lining	0	0
Transition steel-concrete	0,5	2,3

Concrete lining	1	4,5
Transition concrete-rock	0,5	2,3
Average rock deformation	20	90,9
Local rock deformation	±1	±4,5
Total deformation	21-23	100 ±4,5

ACKNOWLEDGEMENTS

Thanks are extended to Sydkraft AB's Stiftelse för Forskning for the financial support that has made publication of this paper possible. We would also like to express our gratitude to Sydgas AB and the other joint owners of the project for supporting the tests in Grängesberg.

REFERENCES

Larsson, H., Glamheden, R., Åhrling, G., 1989: "Storage of natural gas at high pressure in lined rock caverns - Rock mechanics analysis," Proc. of the Int. Conf. on Storage of Gases in Rock Caverns, Nilsen & Olsen (eds), Balkema, Rotterdam, pp. 177-184.

Lindbo, T. Sandstedt, H., Karlsson, P-O., 1989: "Storage of natural gas in lined rock caverns - pilot plant," Proc. of Storage of Gases in Rock Caverns, Nilsen & Olsen (eds), Balkema, Rotterdam, pp. 367-370.

Tengborg, P., 1989: "Storage of natural gas in lined rock caverns - Studies for a future project in southern Sweden," Proc. of Storage of Gases in Rock Caverns, Nilsen & Olsen (eds), Balkema, Rotterdam, pp. 151-157.

Rosendal, T., Tengborg, P., Särkkä, P., 1992: "Scandinavian Concept For Storing of Gas in Lined Rock Caverns," Proc. of 1992 Int. Gas Research Conference, V. III, pp. 1-8, Gas Research Institute, Chicago.

Stille, H., Johansson, J., Sturk, R., Särkkä, P., 1994: "Gaslagring i Inklädda Bergrum - Teori och Praktik." Royal Institute of Technology, Stockholm. To be published.

Probabilistic Rock Mass Characterization and Deformation Analysis (Conference paper)

PROBABILISTIC ROCK MASS CHARACTERIZATION AND DEFORMATION ANALYSIS
CARACTERISATION DES MASSES ROCHEUSES ET ANALYSE DES DEFORMATIONS PAR LA METHODE DES PROBABILITÉS
WAHRSCHEINLICHKEITSANALYSE DER GEBIRGSEIGENSCHAFTEN UND DESSEM DEFORMATIONSVERHALTEN

Robert Sturk
Royal Institute of Technology/Skanska AB, Sweden
Jan Johansson
Royal Institute of Technology/Naturgasteknik AB, Sweden
Lars Olsson
Geostatistik AB, Sweden
Håkan Stille
Royal Institute of Technology, Sweden

ABSTRACT: Predicting the behaviour of an inhomogeneous rock mass is a difficult but necessary task in underground construction. Deformation analyses are based on estimated mechanical properties that in turn often are directly or indirectly empirically derived from rock mass classification. The classification systems consist of series of rock parameters determined from field investigations and laboratory tests. Obviously, there are large uncertainties involved in the process of making a deformation prognosis. This paper describes a methodology of quantifying these uncertainties. The main idea is to treat each parameter in the classification systems as stochastic variables and describe them with probability distributions. The consequence of this is that both the intermediate results, the mechanical properties of the rock mass, and the end results, the deformation prognosis, are expressed as probability distributions with statistical parameters such as mean and variance. A similar approach may be used for describing the properties and behaviour of tunnel support systems. Altogether, this helps the rock engineer in making better decisions.

RESUMÉ: Cet article présente une méthode permettant d'évaluer les incertitudes rencontrées dans la caractérisation de la masse rocheuse et l'analyse des déformations des ouvrages souterrains. L'idée maitresse étant de considérer les paramètres empiriques des systèmes de classification des roches comme des variables aléatoires et de les décrire avec la répartition des probabilités. Par ce moyen, aussi bien les résultat intermédiaires, propriétés mécaniques issues de la classification des masses de roches, que les résultats finaux, prévision des déformations, sont exprimés selon une fonction statistique de répartition avec des paramètres comme la moyenne et la variance. Une approche similaire pourra-être utilisée pour décrire les propriétés et le comportement des systèmes de support des tunnels. En définitive l'ingénieur pourra, à l'aide de cette méthode, prendre de meilleures décisions. L'utilisation pratique de la méthode des probabilités est présentée dans un exemple hypothétique.

ZUSAMMENFASSUNG: In diesem Bericht wird ein Verfahren um Unsicherheiten, die im Untertagbau bei der Schätzung der Gebirgseigenschaften und dessen Deformationsverhalten vorhanden sind zu quantifizieren, beschrieben. Die Hauptidee ist, Kennverte der empirischen Gebirgsklassifikation als stochastische Variable zu verwenden und mit Wahrscheinlichkeitsverteilungen zu versehen. Der Konsequenz von diesem ist dass das Teilresultat, die durch Klassifikation erhaltene mechanische Eigenschaften des Gebirges, sowohl wie das Endresultat, die Verformungsprognose, asl Wahrscheinlichkeitsverteilungen angesehen werden, mit statistische Kennwerte so wie Durchschnisttswert und Standardabweichung. Bei der Beschreibung der Eigenschaften und des Verhaltens der Sicherungsmassnahmen im Tunnelbau, kann ein Ähnlicher Ansatz verwendet werden. Das Ganze unterstützt dem Ingenieur damit er bessere Entscheidungen treffen kann. Die Nutzbarkeit der Wahrscheinlichkeitsmethodik ist durch ein hypotetisches Beispiel dargestellt.

INTRODUCTION

Underground projects often includes decision situations in which one must consider very complex series of events and interaction between several systems. The rock mass as a construction material and the engineering design of underground structures also involve different types of uncertainties. It is also known that geological hazards play an important role

in underground projects both for clients and contractors.

All this implies that predictions concerning the rock mass and decision making for underground projects is difficult. By applying decision and risk analysis together with a probabilistic design philosophy these difficulties and uncertainties can be structured and hopefully quantified, thus providing a base for better predictions and eventually better decisions.

When performing analytical deformation analysis, for example in order to design a support system for a tunnel, the rock mass parameters, i.e. Young's modulus and rock mass strength, are very important. As these parameters are subjected to large uncertainties, mainly in the form of spatial variability, a probabilistic model approach will improve the assessment of parameters and the deformation analysis.

In this paper the practical use of characterizing the rock mass and of calculating the ground response in tunnels with a probabilistic methodology is described and exemplified by a hypothetical case.

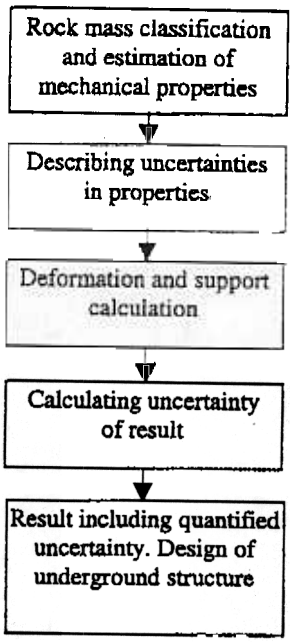

Figure Flow chart describing the process of carrying out rock mass characterization and deformation analysis for underground structures. Steps including probabilistic aspects are framed with a dotted line.

2 PROBABILISTIC METHODOLOGY

2.1 *General overview*

The methodology introduced in this paper comprises several steps illustrated in Figure 1. This logic sequence of carrying out a deformation analysis is commonly used in underground projects. However, the new ideas in the methodology are related to the fact that uncertainties in input data is quantified. In the following description of the different steps, those including probabilistic aspects are focused upon.

2.2 *Rock mass classification and estimation of mechanical properties*

Deformation analysis where the rock mass is regarded as an elasto-plastic material, described by cohesion, friction and Young's modulus, obviously necessitates accurate assessments of the rock mass properties. Normally, the input parameters are based on rock mass classification and empirical relations for assessing mechanical properties.

The rock classification should be based on field investigations and laboratory testing. Different systems are available, the most widely spread are Rock Mass Rating (RMR) and the Q-system.

Several useful empirical relations to estimate mechanical properties of the rock mass has been presented in the literature; for example by Barton et al. (1980), Stille et al. (1982), Serafim & Pereira (1983), Hoek et al. (1995) and Palmstrøm (1995). Some of these relations are based on the classification system RMR and Q, while others are independent of those systems.

The use of the probabilistic methodology for classification and estimation of properties (c.f. Section 3) is transparent, which imply that anyone of the above methods may be used.

2.3 *Describing uncertainties in rock mass quality and properties*

In order to describe the uncertainty present in the evaluation of rock mass properties, a suitable scale of expressing that uncertainty is needed. Often, probability is a suitable measure, especially if one adopts the subjective interpretation of probability (bayesian statistics).

In order to assess the probabilities correctly, several precautions must be taken so that the assessment

does not degenerate into a rough guessing. The subject of assessing subjective probabilities has been treated in the literature, especially on decision analysis, see for instance Stael von Holstein & Matheson (1978), Lourens (1984) and Veneziano (1994). With a subjective approach one can use engineering judgement in a stringent manner and also incorporate measurements into the assessment through the application of Bayes' theorem, Benjamin & Cornell (1970) and Ang & Tang (1975). It must be pointed, in this context, that subjective probabilities are not a replacement for measurements in a frequentist analysis.

The assessments of uncertainty are usually given in the form of a Probability Density Function (PDF) or a Probability Mass Function (PMF), for discrete distributions. In some cases it is sufficient or necessary to characterize the stochastic variable only through suitable measures, usually the mean and variance without specifying the distribution.

Often one has an estimate of the rock properties of small rock elements (units) but what is needed, in order to describe the actual load case, is the value for a larger volume. This problem is simplified if the overall behaviour is governed by the sum (or the mean) of the elements, which is often the case for failure mechanisms in ductile materials (e.g. elasto-plastic materials). It should be observed that the mean of several samples has a smaller variance (spread) that have the samples themselves, Vanmarcke (1977). The calculation of the variance of the mean can be done using the method described by Vanmarcke (1977), (1977a), (1983) or by using a simulation procedure where a sample of suitable size is drawn from the distribution of point values and the mean is calculated. If this is repeated many times the variance of the mean can be estimated. When doing this, one should give some thought to the possible correlation between points close to each other. If there is no correlation the mean value will have a smaller variance than if there is a strong correlation.

2.4 *Deformation and support calculation using numerical and analytical solutions*

Deformation analysis as a tool for design of tunnels and rock caverns has been widely used within underground construction. Principally, one may distinguish two calculation methods; numerical and analytical calculations. Various numerical calculation methods has been developed and refined during the last decades as computer capacity constantly increases. Numerical methods are not treated further in this paper.

Analytical solutions in the form of ground response curves has been presented by Brown et al. (1983), among others. Ground response curves in combination with support reaction for different support systems has been described by for example Stille et al. (1989) and Chang (1994). In this paper the GRC concept is used as a base for the deformation analysis.

2.5 *Calculating uncertainty of result*

To get the uncertainty of the calculated deformation a method must be used that can solve expressions containing stochastic variables. Different methods are available and the choice of method depends on whether an analytical or numerical method is used to calculated the deformation and on the amount of accessible information.

If a numerical method is used one can use a stochastic finite element calculation to find the expected value (mean) and the variance of the calculated deformation at different points, Ishii et al. (1989). For analytical solutions the calculation of uncertainties, in practical work, can be done using different methods. Among the more useful are the Point Estimate Method, Rosenbluth (1975) and Harr (1987), and Monte Carlo simulation, Ang & Tang (1984). The authors prefer the Monte Carlo method as it gives a picture of the stochastic distribution of the result and not just its mean and variance.

3 CALCULATION EXAMPLE

In order to illustrate the practical use of the probabilistic methodology a hypothetical example is presented below.

3.1 *Simulation of rock properties*

The probabilistic rock mass characterization and deformation analysis has been done for a 4.5 diameter tunnel at a depth of 50 m. The rock mass consists of highly weathered gneiss with a quality corresponding to Poor - Very poor rock according to RMR.

Given a pre-investigation programme comprising geophysics, core drilling and laboratory testing the

RMR-system may be used to classify the rock mass. The parameters in the RMR-system have been described as stochastic variables using probability density functions.

Several different statistical distributions have been used. The choice of specific distributions is difficult as limited information on how geological parameters are distributed is available in the literature. Therefore, subjective assessment of PDF's is a good tool in this application. Two examples is presented in Figure 2 and 3 respectively.

Figure 2 PDF (triangular distribution) for the parameter "RQD" within the RMR-system.

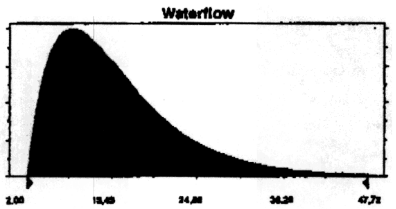

Figure 3 PDF (gamma distribution) for the parameter "inflow of water" (litre/min, 10 m tunnel) within the RMR-system.

Young's modulus is determined using a combined relationship based on methods presented by Serafim & Pereira (1983) for the lower range values and Barton et al. (1980) for the upper range values. This combined relationship have, according to the author's experience, proven to be suitable for granitic and gneissic rock masses.

Rock mass compressive strength is described using the Rock Mass index concept (RMi), see Palmstrøm (1995), where the RMi value equals the rock mass strength (σ_{cm}), c.f. Figure 4.

The rock mass properties are simulated using Monte Carlo simulation. The input parameters in the empirical relationships are consequently given as stochastic variables.

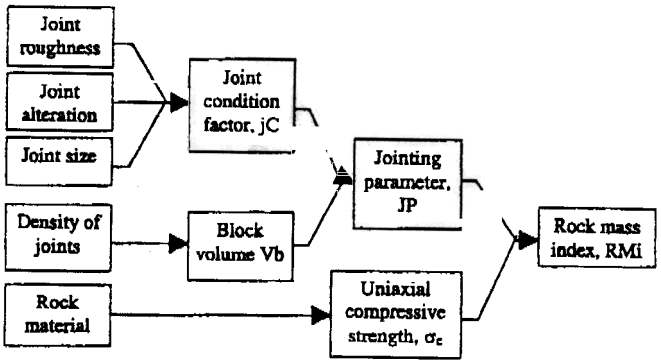

Figure 4 The principle of RMi, after Palmstrøm 1995.

3.2 *Reduction of variance*

Given accurate input data Young's modulus within the studied rock mass might be considered to follow the simulated distribution. This implies a relatively large spread with high and low values representing different parts of the rock mass. An important issue in this context is, as described above, the variance of the mean and its relevance for the actual load case.

For the current load case the overall Young's modulus along a string consisting of several units is more relevant for the deformation analysis than the single values, see Figure 5. For the assumed geology the rock mechanical properties are considered to be uncorrelated.

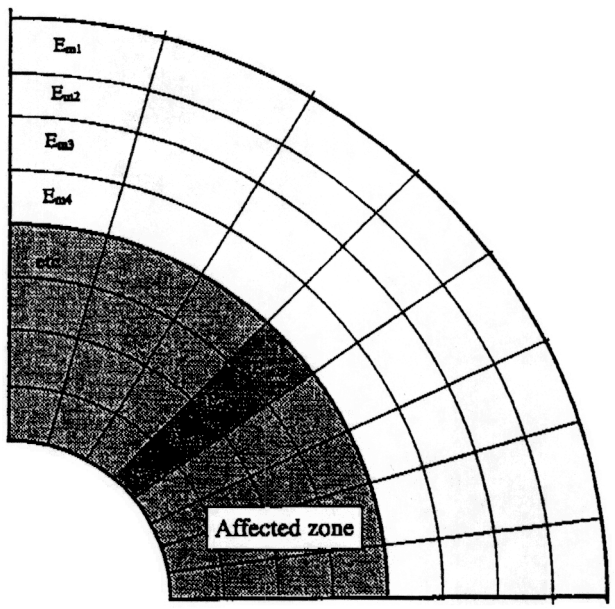

Figure 5 Schematic illustration of a string consisting of several units. This principle is adopted in order to simulate a representative Young's modulus for the rock mass in the actual load case around a tunnel.

As the deformation of the rock mass is proportional to the rock stress, the units closest to the tunnel will have larger influence on the overall deformation than units further out. The weights put on each unit should correspond to the stress distribution in the affected zone (i.e. the zone in which deformations will take place). The size of the affected zone depend on the load case and the rock mass strength. In this case the affected zone is estimated to have a length of two tunnel radii.

Similar to the Young's modulus the reduction of variance for rock mass compressive strength must be considered. The spatial variability of the rock mass strength can be substantial, i.e. one volume of the rock mass may be stronger or weaker than its neighbour. This reflects reality as the rock mass often is inhomogeneous and very complex from a structural point of view.

The load case in a tunnel will imply that adjacent block volumes in the tunnel periphery will mutually carry the load. A weaker volume will in this respect be compensated by a stronger volume. This imply that the overall characteristic rock mass strength consists of the mean strength of a suitable number of volumes.

3.3 *Deformation analysis*

Deformation analysis is done analytically using the GRC-concept. The analytical solutions and input parameters has been implemented in a Excel spread sheet and calculation has been done using Monte Carlo simulation (software package = Crystal Ball).

The deformation is calculated at the initial pressure (p_0), which is a fixed parameter, and at ten other proportionally decreasing pressure levels. At each pressure level the deformation is given in the form of a stochastic distribution with statistical parameters. This information, more specifically the median and the percentiles, is subsequently used to plot the probabilistic ground response curve.

In order to illustrate the principle the support reaction of a 100 mm shotcrete lining, Chang (1994), has also been simulated. The uncertainty in this case is given by the variability of the strength parameters of the shotcrete (compressive strength and Young's modulus) and the variability in thickness. It should be emphasized that these uncertainties are smaller than the spatial variability of parameters related to the rock mass.

4 RESULTS

The simulated RMR-value, from the example, is presented in Figure 6. As can be seen from the chart the variability of the rock quality within this particular rock mass is quantified. Given results like this it is possible to estimate probabilities of exceeding or falling below interesting limits.

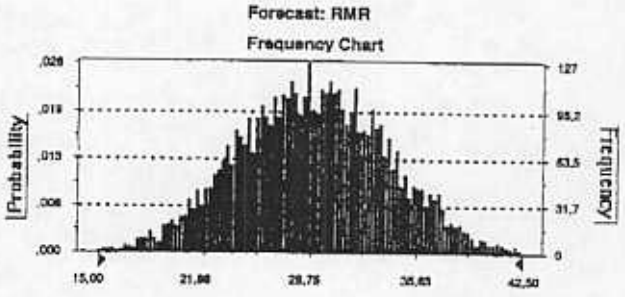

Figure 6 Probability distribution of RMR-value within the exemplified rock mass.

In Figure 7 and 8 the simulation results, after reduction of variance, for Young's modulus and rock mass strength are presented. These distributions have been used as input in the deformation analysis.

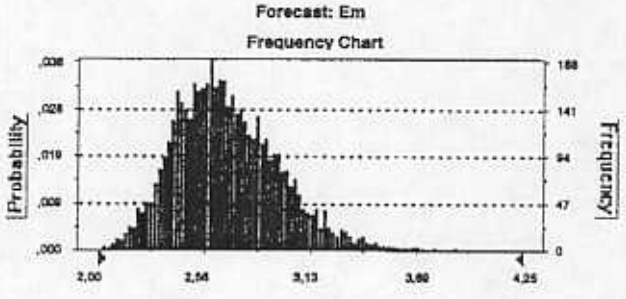

Figure 7 Probability distribution for rock mass Young's modulus (GPa) of the weathered gneiss.

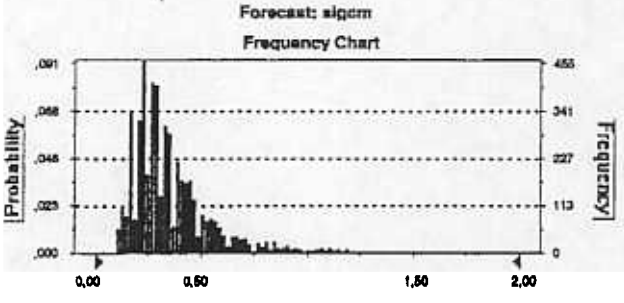

Figure 8 Probability distribution for rock mass strength (MPa) of the weathered gneiss.

The effects of the reduction of variance of Young's modulus and the rock mass strength is shown in Table 1. As can be seen the mean values are quite similar before and after reduction, the range, however, are considerably narrower after the reduction. This is, for normal load cases, a more accurate modelling of the confined rock mass.

Table 1 Reduction of variance for Young's modulus and rock mass compressive strength.

Parameter	Mean value	Range
E_m(GPa) before red.	2.81	1.13 - 7.90
E_m(GPa) after red.	2.69	1.89 - 4.19
σ_{cm} (MPa) before red.	0.36	0.01 - 6.60
σ_{cm} (MPa) after red.	0.36	0.10 - 1.84

The probabilistic deformation analysis is presented as a ground reaction curve, see Figure 9. The GRC shows expected radial deformations in the tunnel. Given the statistical parameters from the simulated distributions the reaction curves may be drawn in different ways according to specific demands. In this case the 50% percentile (median) and the 5%, 95% and 100% percentiles have been presented. The median and 5% and 95% percentiles for the shotcrete lining have also been drawn.

In Figure 10 the probability distribution of radial deformations at zero pressure (largest deformation) is presented.

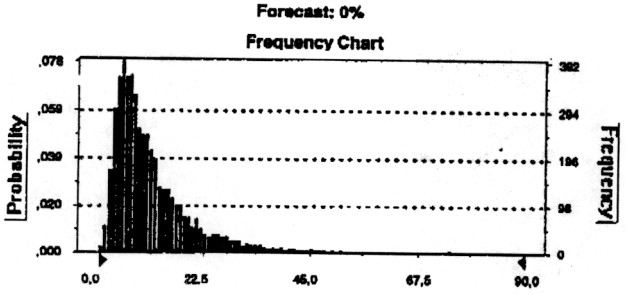

Figure 10 Probability distribution of radial deformation (mm) at zero pressure.

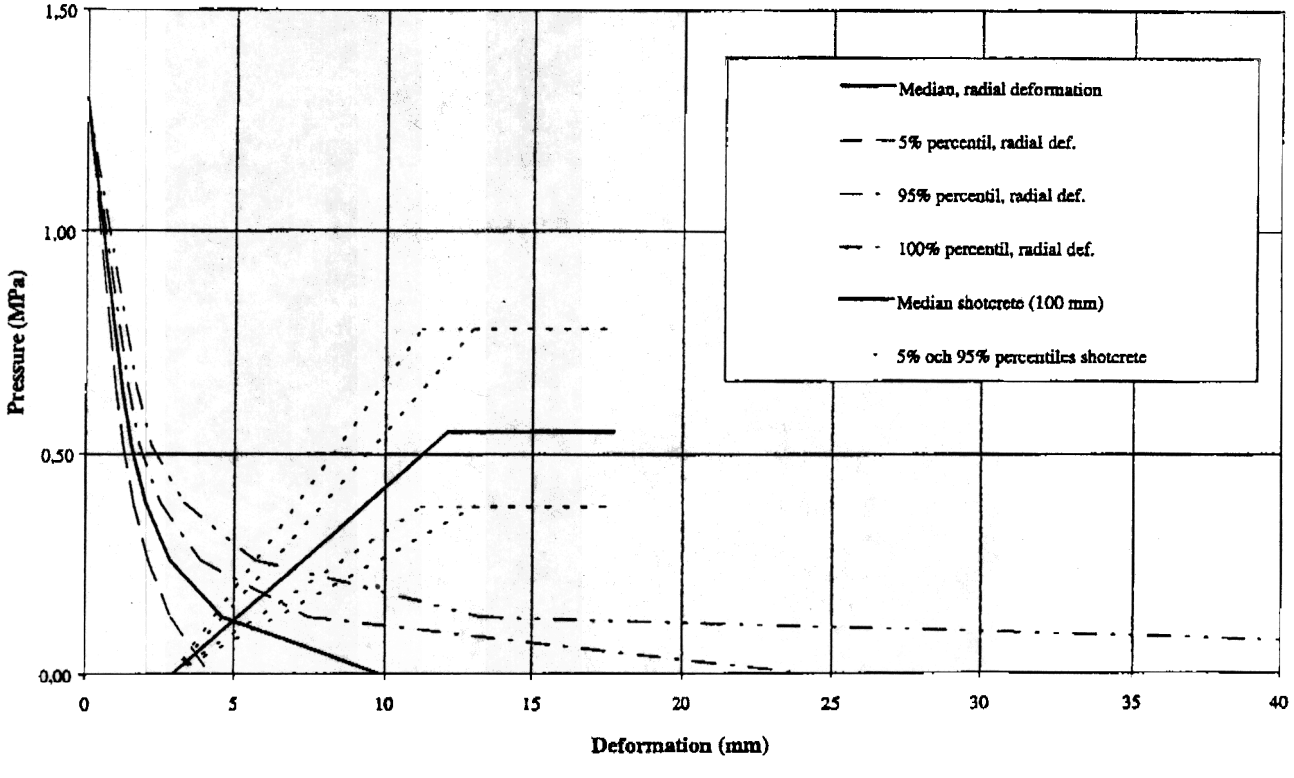

Figure 9 Probabilistic Ground Reaction Curve for weathered gneiss and the response curve for a 100 mm shotcrete lining.

5 DISCUSSION AND CONCLUSIONS

In the paper it has been shown that the application of probabilistic methods to practical rock mechanics problems is feasible using personal computers and commercially available software. In the example the Ground Reaction Curve-concept was used, the methodology, however, is applicable to other analytical calculation methods.

Although there are several methods to do the probabilistic calculations the authors advocate using the Monte Carlo simulation method on the grounds that it is easy to apply and gives a picture of the resulting probability distribution. This is a good help when judging the risks involved.

It is important to take into consideration the spatial variability of the rock mass, furthermore this variability should be reduced under certain circumstances. Otherwise one will end up with a conservative design.

For design purposes the methodology can be used to design a support system with a prescribed safety level. This is done by choosing the support in such way that the probability of the simultaneous occurrence of a large load and weak support is sufficiently small.

The use of the probabilistic rock mass characterization and deformation analysis is one of many tools available when performing stringent decision and risk analysis for underground projects. Such analyses will be of increasing interest when projects constantly become larger and more complex.

REFERENCES

Ang, A. H-S., Tang, W. H., 1975: "*Probability Concepts in Engineering Planning and Design, Volume I - Basic Principles*". John Wiley & Sons, New York.

Ang, A. H-S., Tang, W. H., 1984: "*Probability Concepts in Engineering Planning and Design, Volume II - Decision, Risk and Reliability*". John Wiley & Sons, New York.

Barton, N., Løset, F., Lien, R., Lunde, J., 1980: "Application of the Q-system in design decisions". Subsurface space 2, Bergman (ed.), pp. 553-561, New York, Pergamon.

Benjamin, R. J., Cornell A. C., 1970: "*Probability, Statistics and Decision for Civil Engineers*". McGraw-Hill, New York.

Brown, E. T., Bray, J. W., Ladanyi, B., Hoek, E., 1983: "Ground Response Curves for Rock Tunnels". *J. of Geotech. Eng.*, ASCE, 109, pp. 15-39.

Chang, Y., 1994: "Tunnel Support with Shotcrete in Weak Rock - A Rock Mechanics Study". Dr. Thesis, Division of Soil and Rock Mechanics, Royal Inst. of Techn., Stockholm.

Harr, M. E., 1987: "*Reliability-Based Design in Civil Engineering*". McGraw-Hill.

Hoek, E., Kaiser, P. K., Bawden, B. F., 1995: "*Support of Underground Excavations in Hard Rock*". A. A. Balkema, Rotterdam.

Ishii, K., Suzuki, M., Yamazaki, F., 1989: "Applications of probabilistic methods in construction industry". Proc. of ICOSSAR '89, Ang, Shinozuka & Schueller (eds.).

Lourens, P. F., 1984: "The formalization of knowledge by specification of subjective probability distributions". Univ. of Groningen, Groningen.

Palmstrøm, A., 1995: "RMi - a rock mass characterization system for rock engineering purposes". Dr. Thesis, Dep. of Geology, Univ. of Oslo, Oslo.

Rosenbleuth, E., 1975: "Point Estimates for Probability Moments". Proc. Nat. Acad. Sci. USA, Vol. 72, No. 10, pp. 3812-3814.

Serafim, J. L., Pereira, J. P., 1983: "Consideration of the geomechanical classification of Bieniawski". Proc. Int. Symp. on Engineering Geology and Underground Constr., Lisbon 1 (II), pp. 33-44.

Stael von Holstein, C-A., Matheson, J. E., 1978: "A manual for encoding probability distributions". SRI, Project 7078.

Stille, H., Fredriksson, A., Groth, T., 1982: "FEM-analysis of rock mechanical problems with JOB-FEM. BeFo report No. 307:1/82, Swedish Rock Engineering Research Foundation. (In Swedish)

Stille, H., Holmberg, M., Nord, G., 1989: "Support of Weak Rock with Grouted Bolts and Shotcrete". *Int. J. Rock Mech. Min. Sci. & Geomech. Abstr.*, Vol. 26, No. 1, pp. 99-113.

Vanmarcke, E., 1977: "Probabilistic modelling of soil profiles". *Journal of the Geotechnical Engineering Division*, ASCE, Vol. 103, No GT11.

Vanmarcke, E., 1977a: "Reliability of earth slopes". *Journal of the Geotechnical Engineering Division*, ASCE, Vol. 103, No GT11.

Vanmarcke, E., 1983: "Random fields". *Analysis and synthesis*, MIT Press, Cambridge, Mass..

Veneziano, D., 1994: "Uncertainty and Expert Opinion in Geological Hazards". Whitman Symp., MIT, Oct. 7-8, Cambridge, Mass..

Appendix B

Derivation of Consistent Values of Tensile Strength and Material Toughness

The following derivation provides a material tensile strength that is consistent with the critical fracture toughness of the material.

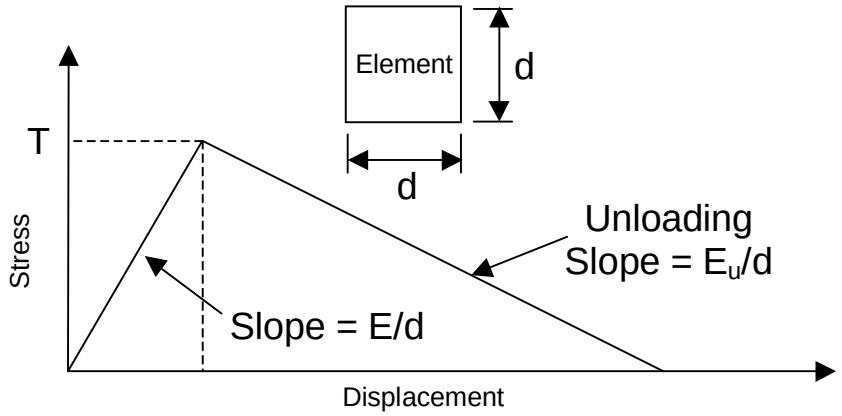

$$G_{IC} = \frac{1}{2}\left(\frac{T^2}{\frac{E}{d}}\right) + \frac{1}{2}\left(\frac{T^2}{\frac{E_u}{d}}\right) \qquad \text{(B-1)}$$

$$= \frac{1}{2}\left(\frac{T^2 d}{E}\right)\left(1 + \frac{E}{E_u}\right)$$

$$G_{IC} = \frac{K_{IC}^2}{E} \qquad \text{(B-2)}$$

$$K_{IC} = T\sqrt{\frac{d}{2}\left(1 + \frac{E}{E_u}\right)} \qquad \text{(B-3)}$$

$$T = \frac{K_{IC}}{\sqrt{\frac{d}{2}\left(1+\frac{E}{E_u}\right)}} \qquad \text{(B-4)}$$

where T = tensile strength,

d = zone size,

E = loading stiffness

E_u = unloading stiffness,

G_{IC} = critical energy release rate, and

K_{IC} = critical toughness.

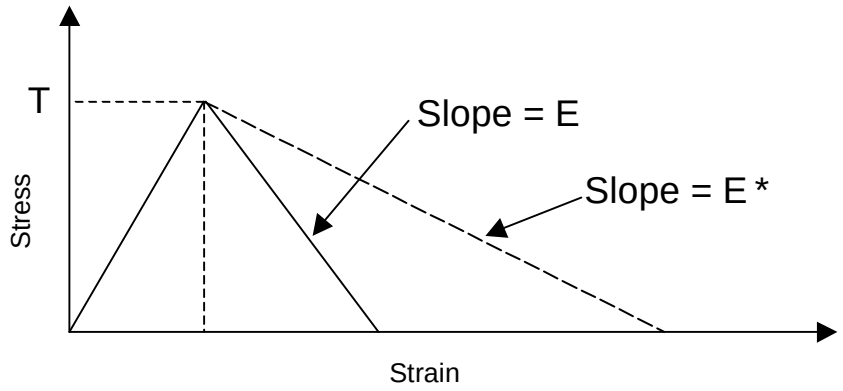

where E^* = unloading stiffness of the surrounding material,

E_l = local (material) unloading stiffness; $E_l = \infty$ in the case of infinitely brittle material, and

$$E_u = \begin{cases} E^* & \text{if } E_l > E^* \\ E_l & \text{if } E^* > E_l \end{cases} .$$